RECONSTITUTION OF REGULATED EUKARYOTIC DNA REPLICATION WITH PURIFIED BUDDING YEAST PROTEINS

A Dissertation

Presented to the Faculty of the Weill Cornell Graduate School

of Medical Sciences

in Partial Fulfillment of the Requirements for the Degree of

Doctor of Philosophy

by

Sujan Devbhandari

December 2018

RECONSTITUTION OF REGULATED EUKARYOTIC DNA REPLICATION WITH PURIFIED BUDDING YEAST PROTEINS

Sujan Devbhandari, Ph.D.

Cornell University 2018

DNA replication is a fundamental process by which organisms copy their DNA. Biochemical reconstitution approaches in bacteria and viral systems have been instrumental in enhancing our mechanistic understanding of this process. However, a reconstituted system to study eukaryotic chromosomal DNA replication has been lacking. My thesis work focused on overcoming this deficiency by aiming to reconstitute eukaryotic DNA replication with purified budding yeast proteins, as chromosome replication is highly conserved from yeast to humans but best understood in budding yeast, *Saccharomyces cerevisiae*.

Eukaryotic DNA replication initiates via a conserved two-step mechanism from multiple origin sites distributed along the length of each chromosome. In the first step, which is restricted to G1 phase, the core of the replicative helicase complex, Mcm2-7, is loaded in an inactive form at origins of replication, forming a pre-replicative complex (pre-RC). Subsequent activation of the Mcm2-7 helicase in the second step occurs exclusively in S-phase. Mcm2-7 loading has been previously reconstituted with purified proteins. However, the unusual double hexameric configuration of the Mcm2-7 complex bound around double stranded DNA observed in this reaction, while providing a molecular rationale for bi-directional origin activation, raised the question whether this structure is a true replication intermediate. Here, I show

that reconstituted pre-RCs indeed support regulated replication of plasmid DNA in yeast cell extracts exhibiting the hallmarks of cellular replication initiation.

Expanding on this observation, I have subsequently reconstituted DNA replication free in solution with purified budding yeast proteins in order to generate a system that allows for the biochemical study of all steps of eukaryotic DNA replication. The system recapitulates regulated bidirectional origin activation; synthesis of leading and lagging strands by the three replicative DNA polymerases Pol α, Pol δ and Pol ε, and canonical maturation of Okazaki fragments into continuous daughter strands. A dual regulatory role for chromatin was uncovered during the replication of chromatinized templates: i) promoting origin dependence and ii) determining Okazaki fragment length by restricting Pol δ progression. Hence, this system provides a functional platform for the detailed mechanistic analysis of eukaryotic chromosome replication.

BIOGRAPHICAL SKETCH

Sujan Devbhandari was born and raised in Kathmandu, Nepal and completed his high school studies there. From 2007 to 2011, he attended Loras College in Dubuque, Iowa and graduated with a Bachelor of Science degree in Biological Research. In 2011, he started his Ph.D. studies at Weill Cornell Graduate School of Biological Sciences. He joined the lab of Dr. Dirk Remus in 2012 where he conducted his thesis work.

मम्मी र दाई प्रति समर्पित

For my parents

ACKNOWLEDGEMENTS

With all my heart, I would like to thank my ever-inspiring and ever-supportive mentor Dr. Dirk Remus. The infectious passion he has for seeking the truth has guided me immensely during my thesis work in his lab. I would also like to thank Dr. Iestyn Whitehouse and Dr. Scott Keeney for being on my thesis committee and providing valuable guidance and constructive criticisms. I am grateful to Dr. Jessica Tyler for chairing my thesis examination committee.

I would also like to thank the members Remus lab, past and present whom I had the privilege of working with. I am indebted to Dr. Julien Gros and Dr. Charanya Kumar for their collaborations in our projects together. Also, thanks to Dr. Melissa Chan, Dr. Gerard Lynch and Syafiq Abd-Wahab for all their help in the lab. I would also like to acknowledge Dr. Jeiqing Jiang, former graduate student from Whitehouse for her collaboration during my thesis work.

Finally, I am highly indebted to all my friends and family for all their love and support during my time in the Graduate School.

TABLE OF CONTENTS

Page

LIST OF FIGURES

Page

Chapter One

Chapter Two

Chapter Three

LIST OF TABLES

Page

LIST OF ABBREVIATIONS

ACS: ARS consensus sequence

ARS: Autonomously replicating sequence

CDK: Cyclin-dependent kinase

CMG: Cdc45-Mcm2-7-GINS

DDK: Dbf4-dependent kinase

DH: Double hexamer

dsDNA : Double-stranded DNA

NTD: N-terminal domain

ORC: Origin recognition complex

Pre-RC: Pre-replicative complex

Pre-IC: Pre-initiation complex

Pre-LC: Pre-loading complex

RPC: Replisome progression complex

ssDNA: single-stranded DNA

CHAPTER ONE

INTRODUCTION

Overview

DNA replication is a fundamental process by which a cell copies its genome and passes it on to the next generation. Accurate duplication of the genetic material is essential in all domains of life. This is accomplished by multiprotein machine termed ‘replisome’ that coordinates multiple enzymatic activities (e.g. DNA helicase, DNA polymerase, primase etc.). In eukaryotes replication of DNA is regulated via multiple mechanisms to ensure genomic integrity (Diffley, 2004; Siddiqui et al., 2013) as its misregulation can cause under- or over-replication of the genome resulting in genome instability, tumorigenesis and cell death (Blow and Gillespie, 2008; Vassilev and DePamphilis, 2017).

In general, DNA replication occurs in three phases: initiation, elongation and termination. Firstly, during the initiation step, the double helical DNA is untwisted and unwound into its component single strands by the replicative DNA helicase to form a replication fork (Dewar and Walter, 2017). The unwinding of the parental DNA duplex provides the single-stranded DNA (ssDNA) template for synthesis of the daughter DNA strands by DNA polymerases during the elongation phase. As DNA polymerases synthesize the nascent DNA only in 5′ to 3′ direction, the anti-parallel configuration of the two strands of the template DNA dictates that they be copied in opposite direction from each other as the replication fork progresses along parental DNA (Marians, 1992). One strand can be copied continuously in the direction of the replication fork and is called the leading strand while the other strand,

the lagging strand, is synthesized discontinuously in the form of short Okazaki fragments (Okazaki et al., 1968). Finally, termination occurs when replication forks moving in opposite direction converge. During termination, the daughter strands synthesized by the opposing forks are ligated and the replisomes are disassembled (Dewar and Walter, 2017).

Studies in bacteriophages (reviewed in (Alberts, 1987)), bacteria (reviewed in (Marians, 1992)) and eukaryotic viruses (reviewed in (Kelly, 2017)) were vital in formulating basic principles of DNA replication. In particular, biochemical reconstitution approaches were instrumental in identifying and characterizing replication factors by allowing the purification of the respective activities from crude cell extracts that recapitulated the replication of origin-containing plasmid DNA templates. Extract fractionation and the genetic characterization of mutants exhibiting conditional defects in cellular DNA replication ultimately led identification of the complete complement of factors required for the replication of bacteriophage, *E. coli*, and SV40 genomes (Barry and Alberts, 1972; Hinkle and Richardson, 1975; Schekman et al., 1975; Wickner and Hurwitz, 1974) , culminating in the complete reconstitution of the respective replication systems with purified proteins (Bramhill and Kornberg, 1988; Funnell et al., 1986; Kelly, 2017; Marians, 1992; Tsurimoto et al., 1990; Waga et al., 1994; Waga and Stillman, 1994). This approach of reductionist biology, perhaps more appropriately called constructionist biology, created an opportunity to study the components in a minimalistic environment avoiding interference from the cellular milieu (Liu and Fletcher, 2009).

Characterization of the cell-free SV40 DNA replication reaction was essential for the identification of many basic eukaryotic replisome components,

such as replicative DNA polymerases, the single-stranded DNA binding protein, RPA, the polymerase processivity clamp, PCNA, and its loader, the RFC complex, as well as basic chromatin replication factors such CAF-1, as this virus depends on cellular replication proteins for its genome duplication in addition to the virus-encoded large T antigen DNA helicase(Li and Kelly, 1984; Smith and Stillman, 1989; Tsurimoto et al., 1990; Tsurimoto and Stillman, 1989; Wold et al., 1989). However, as the activities of SV40 large T antigen bypass the virus' dependence on the cellular initiation machinery as well as the cellular replicative DNA helicase, many aspects of SV40 replication appear fundamentally different from cellular chromosomal DNA replication (Borowiec and Hurwitz, 1988; Dodson et al., 1987). Reconstitution of chromosomal origin-dependent DNA replication is thus essential for our ability to study the mechanism of cellular genome replication.

This thesis focuses on the reconstitution of eukaryotic DNA replication with purified budding yeast proteins, which allowed us to define the minimal complement of proteins required for budding yeast DNA replication. Almost all of the proteins involved in the duplication of the budding yeast genome have a single ortholog in other eukaryotic species including humans (Table 1.1) and chromosome replication is one of the most highly conserved areas of eukaryotic cell biology (Bell and Labib, 2016). In this introduction, I review our current understanding of the various phases of eukaryotic DNA replication and the roles individual replication proteins play in this process. I will also discuss how the additional level of complexity in eukaryotes brought about by the cell cycle regulation of DNA replication and chromatinization of the genome fundamentally affects the process of genome duplication.

Table 1.1 List of proteins involved in budding yeast DNA replication and their human orthologs. (Adapted from Bell and Labib, 2016)

Protein or Complex	Derivation of Name	Human Ortholog
ORC	Origin Recognition Complex	ORC
Cdc6	Cell division cycle	CDC6
Cdt1	Cdc10 dependent transcription	CDT1
MCM	Minichromosome maintenance	MCM
DDK	Dbf4-dependent kinase	DDK
CDK	Cyclin-dependent kinase	CDK
Sld3	Synthetic lethal with Dpb11	Treslin
Cdc45	Cell division cycle	CDC45
Sld2	Synthetic lethal with Dpb11	RECQL4
Dpb11	DNA polymerase B interacting	TOPBP1
GINS	Go-Ichi-Ni-San in Japanese for 5-1-3-2 for subunits (see text)	GINS
Pol ε	Polymerase	Pol ε
Mcm10	Minichromosome maintenance	MCM 10
RPA	Replication protein A	RPA
Pol α	Polymerase	Pol α
Ctf4	Chromosome transmission frequency	AND-1
Pol δ	Polymerase	Pol δ
Fen1	Flap endonuclease	FEN1
Cdc9	Cell division cycle	LIG1
RFC	Replication Factor C	RFC
PCNA	Proliferating cell nuclear antigen	PCNA
Top1	Topoisomerase	Topo I
Top2	Topoisomerase	Topo II

Initiation

In 1963, Jacob, Brenner and Cuzin proposed the replicon model for DNA replication initiation, which postulates that the binding of a trans-acting factor (the initiator) to a specific cis-acting sequence in the genome (the replicator) defines an origin of DNA replication (replication start site) (Jacob et al., 1963). The basic premise of this model has been confirmed in DNA replication initiation across all domains of life. Many bacterial genomes comprise a single circular chromosomal DNA on which DNA replication initiates from a single origin. On the other hand, eukaryotic genomes generally consist of multiple linear chromosomes that are replicated from many origins distributed along the length of each chromosome (Leonard and Mechali, 2013). The multiplicity of replication initiation events in eukaryotic cells ensures the timely replication of the relatively large eukaryotic chromosomes, as the time required to replicate a chromosome is essentially dependent only on interorigin distance (origin density) and not on replication fork speed as in genomes replicated from a single origin (Diffley, 2011). While the utilization of multiple replication origins thus allowed for the evolution of large eukaryotic genomes, it demands robust cellular mechanisms that ensure once-and-only-once replication in each cell cycle to ensure genome integrity across generations (Diffley, 2011). This cell cycle regulation of origin function fundamentally impacts potential strategies for the reconstitution of eukaryotic DNA replication, as will be discussed further below.

Replication Origin Structure

Among eukaryotes, replication origins are best understood in the budding yeast, *Saccharomyces cerevisiae,* where they were originally

identified by their ability to support the replication of episomes or minichromosomes, giving rise to the name autonomously replicating sequence (ARS) elements (Stinchcomb et al., 1979). A fraction of these ARS elements was subsequently shown to function as origins in their chromosomal location (Brewer and Fangman, 1987; Huberman et al., 1988). Budding yeast ARSs are around 200 base-pairs (bp) long and consist of A and B domains (Fig 1.1). The A domain contains an 11-base pair, AT rich, highly conserved sequence called ARS consensus sequence (ACS) (Broach et al., 1983) that serves as a binding site for ORC (Bell and Stillman, 1992). Mutational disruption of the ACS disrupts ARS function (Bell, 1995; Marahrens and Stillman, 1992) .The B region is less highly conserved and entails short sequence elements that contribute to origin activity (Marahrens and Stillman, 1992). For instance, in the case of ARS1, the B regions contains B1, B2 and B3 elements with B1 contributing to ORC binding and B2 contributing to helicase loading (Bell and Stillman, 1992; Lee and Bell, 1997; Rao and Stillman, 1995; Rowley et al., 1995).

Although the ACS is essential for origin activity in budding yeast, this sequence element alone is insufficient to determine an origin site, as many more ACSs than origins exist in the budding yeast genome (Breier et al., 2004; Eaton et al., 2010). In fact, chromatin structure profoundly determines origin function in vivo. Nucleosome mapping across the genome showed that ACSs that are part of replication origins are embedded within a nucleosome-free region (NFR) flanked by highly positioned nucleosomes (Berbenetz et al., 2010; Eaton et al., 2010). Budding yeast origins are particularly A/T-rich and characterized by a distinct A/T skew (Breier et al., 2004). This A/T skew may

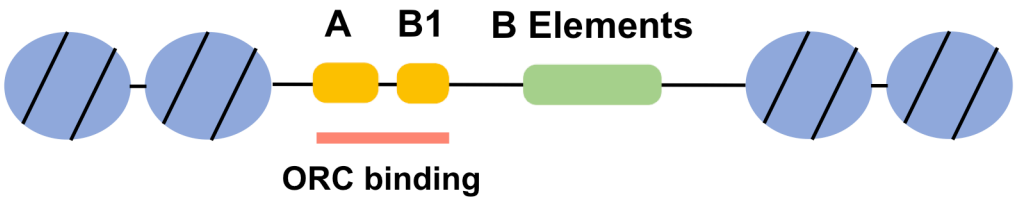

Figure 1.1 Structure of *S. cerevisiae* origin of replication. Budding yeast origins comprise A and B elements located within a nucleosome free region. B elements are further divided into the B1 element and a variable number of addition B elements. ORC binds to the region encompassing the A and B1 elements.

contribute to the inherent exclusion of nucleosomes from the origin (Segal and Widom, 2009). Nucleosome depletion from the origin is important for origin function as assembly of nucleosomes across an origin inhibit origin activity (Eaton et al., 2010; Simpson, 1990). In addition, nucleosomes are specifically positioned on either side (Fig 1.1) of the NFR at the origin, partly through the binding of ORC at the origin, and positioned origin-proximal nucleosomes appear to assist origin function by promoting pre-RC assembly (Lipford & Bell, 2001)

Intriguingly, the sequence conservation observed at budding yeast origins is not observed in higher eukaryotes and apparently random heterologous DNA sequences were for example found to support regulated replication of plasmids in Xenopus oocytes, Xenopus oocyte extracts, and mammalian tissue culture cells (Harland and Laskey, 1980; Heinzel et al.,

1991; Hyrien and Mechali, 1993; Mechali and Kearsey, 1984). Regardless, recent genome-wide studies have revealed some common patterns underlying origin activity in metazoans, including among others the formation of a NFR (Karnani et al., 2010; MacAlpine et al., 2010) and enrichment for G-rich sequences and CpG islands (Cadoret et al., 2008; Delgado et al., 1998). However, the exact function of these elements in determining replication origin function is currently an active area of research.

Two steps in eukaryotic DNA replication initiation

In eukaryotes, DNA replication initiates via a two-step mechanism to prevent repeated origin firing within one cell cycle. In the first step, which occurs exclusively at the end of mitosis and during G1 phase, origins are marked as potential sites for initiation of DNA replication in a step known as origin licensing (Blow and Laskey, 1988). This step involves the assembly of a pre-replicative complex (pre-RC) that is characterized by an extended DNase1 footprint at the origin (Diffley et al., 1994). As described below pre-RC formation involves the loading of the replicative helicase, Mcm2-7, in inactive form at the origin by the origin recognition complex, Cdc6, and Cdt1 (Labib et al., 2001). Following origin licensing in the second step, which occurs exclusively in S phase, a subset of the loaded Mcm2-7 helicase complexes is activated ultimately resulting in the formation of a pair of oppositely oriented replication forks emanating from each origin (Boos et al., 2012; Mantiero et al., 2011; Tanaka et al., 2011). The temporal separation of helicase loading and activation in the cell cycle ensures that the entire genome is replicated once and only once per cell cycle thus maintaining genome integrity (Remus and Diffley, 2009; Siddiqui et al., 2013).

Proteins involved in helicase loading

The core of the eukaryotic replicative helicase is the Mcm2-7 complex, a hetero-hexameric assembly of six distinct, yet related, AAA+ ATPases. As described above loading of the Mcm2-7 complex occurs specifically in G1 phase and results in the formation of inactive head-to-head double hexamer (DH) encircling the double stranded DNA (dsDNA) (Evrin et al., 2009; Remus et al., 2009). Mcm2-7 loading requires the coordinate activities of the origin recognition complex (ORC), Cdc6 and Cdt1 (Bell and Dutta, 2002). In the following I will briefly review the individual components of pre-RCs before describing how these factors coordinately load Mcm2-7 onto DNA.

ORC

The origin recognition complex (ORC) is the initiator protein for eukaryotic DNA replication. It was initially isolated from budding yeast cell extracts as a hetero-hexameric protein complex that specifically binds ARS DNA *in vitro* in the presence of ATP (Bell and Stillman, 1992). The binding of ORC to ARS elements *in vivo* was confirmed by *in vivo* footprinting studies (Diffley and Cocker, 1992; Diffley et al., 1994) and genome-wide chromatin immuno-precipitation (ChIP) analyses (MacAlpine and Bell, 2005), which revealed that ORC is bound at origins throughout the cell cycle. Subsequent studies found that ORC's function as the initiator is conserved throughout all the eukaryotes studied so far (Carpenter et al., 1996; Chesnokov et al., 1999; Gavin et al., 1995; Grallert and Nurse, 1996; Romanowski et al., 1996; Rowles et al., 1996; Vashee et al., 2003).

ORC consists of six subunits, Orc1-6, named in descending order of their molecular weight (Bell et al., 1993). Five of those subunits, Orc1-5, belong to the family of ATPases associated with diverse cellular activities (AAA+) (Li and Stillman, 2012), while Orc6 comprises of a conserved TFIIB like domain (Liu et al., 2011). The characteristic feature of AAA+ proteins is the formation of composite, bipartite active sites upon oligomerization with one subunit contributing the Walker A and Walker B motifs for ATP-binding and -hydrolysis and the neighboring subunit providing an arginine finger essential for ATPase activity (Neuwald et al., 1999). Orc2 and Orc3 lack essential residues for ATP binding, while Orc1, Orc4 and Orc5 can all bind ATP (Clarey et al., 2006; Klemm et al., 1997; Speck et al., 2005). Yet only Orc1 possesses ATPase activity and ATP-binding to this subunit only is required for ATP-dependent ORC binding to origins (Klemm et al., 1997). The N-terminus of Orc1 also consists of Bromo-Adjacent Homology (BAH) domain (Bell, 1995), an evolutionarily conserved chromatin associated motif (Callebaut et al., 1999). In addition to AAA+ domain, Orc1-5 also contain C-terminal winged-helix (WH) domain. Recent high-resolution structure of ORC complex bound to replication origin DNA show that the WH domains from ORC subunits make contacts with the DNA (Li et al., 2018).

Cdc6

Cdc6 was first identified during a screen for *S. cerevisiae* mutants that affect the cell divison cycle (Hartwell, 1976). It was later discovered to have a role in DNA replication initiation (Palmer et al., 1990) and to be essential prior to S-phase (Hogan and Koshland, 1992; Kelly et al., 1993). Cdc6 genetically interacts with ORC (Liang et al., 1995), which physically recruits Cdc6 to

origins (Cocker et al., 1996; Coleman et al., 1996; Liang et al., 1995; Santocanale and Diffley, 1996). Primary sequence analysis revealed that Cdc6 consists of a AAA+ domain similar to ORC, sharing homology with Orc1 in particular (Bell, 1995). Recruitment of Cdc6 to origins by ORC is ATP dependent (Coster et al., 2014; Kang et al., 2014; Kneissl et al., 2003; Perkins and Diffley, 1998) and activates the ATPase activity of Cdc6, possibly by establishing a canonical AAA+ interaction between subunits of ORC and Cdc6 (Randell et al., 2006). Structural studies show that ORC forms a crescent-shaped structure and Cdc6 bridges the gap in ORC and to form a ring like structure encircling the DNA (Chen et al., 2008; Speck et al., 2005; Yuan et al., 2017). Like Orc subunits, C-terminus of Cdc6 also contain WH domain, a domain that plays an important role in DNA binding (Liu et al., 2000).

Mcm2-7

The Mcm2-7 complex (MCM complex) is comprised of six distinct yet closely related AAA+ proteins that were originally identified in a budding yeast genetic screen aimed at identifying factors required for minichromosome maintenance and cell cycle progression (Maine et al., 1984; Moir et al., 1982). In parallel, it was also identified as a replication-licensing factor (RLF-M) in frog Xenopus laevis egg (Blow and Laskey, 1988; Madine et al., 1995; Todorov et al., 1995; Treisman et al., 1995). The MCM complex serves as the core engine of the eukaryotic replicative helicase as revealed by multiple lines of evidence: Mcm2-7 is a component of the Replisome Progression Complex (RPC), a multi-protein complex formed at replication forks in budding yeast cells specifically in S-phase (Gambus et al., 2006); depletion of Mcm2-7 subunits in S-phase acutely and irreversibly blocks the progression of

replication forks (Labib et al., 2000; Pacek and Walter, 2004); and the purified Mcm2-7 complex exhibits DNA helicase activity *in vitro* (Bochman and Schwacha, 2008).

Like ORC and Cdc6, the Mcm2-7 complex is also an assembly of AAA+ proteins, indicating a critical role for ATP metabolism in pre-RC formation. Each MCM protein consists of three core domains: A conserved N-terminal domain (NTD), AAA+ ATPase domain and C-terminal winged helix domain. Additionally, several of the Mcm subunits also consist additional N- or C-terminal tails that play important regulatory role (Frigola et al., 2013; Labib, 2010). These subunits assemble into a hexameric ring with a defined subunit order: Mcm5-Mcm3-Mcm7-Mcm4-Mcm6-Mcm2 (Davey et al., 2003). The ring displays two distinct tiers; one comprising of the NTD and other one consisting of AAA+ domains and features natural discontinuity between Mcm2-5 interface acting as a gate entry and exit of DNA (Bochman and Schwacha, 2008; Costa et al., 2011).

Cdt1

Cdt1 was first identified in fission yeast *Schizosaccharomyces pombe* as a factor essential for initiating DNA replication and as a protein inducing re-replication in the absence of cell division (Hofmann and Beach, 1994; Nishitani et al., 2000). Its budding yeast counterpart was later identified as Tah11, a gene first isolated during screen for synthetic lethality with mutant topoisomerase I allele (Fiorani and Bjornsti, 2000; Tanaka and Diffley, 2002). Although Cdt1 is conserved in all eukaryotes (Maiorano et al., 2000; Whittaker et al., 2000; Wohlschlegel et al., 2000), its primary structure has markedly diverged between yeast and metazoans. For example, while all Cdt1

homologs contain a conserved C-terminal pair of WH domain, the N-terminal region is not conserved (Lee et al., 2004). In budding yeast cells Cdt1 and MCMs are imported into the nucleus in an interdependent fashion, indicating tight complex formation between these proteins (Tanaka and Diffley, 2002; Wu et al., 2012). Indeed, budding yeast Cdt1 forms a tight complex with Mcm2-7 *in vitro* (Frigola et al., 2013; Kawasaki et al., 2006; Remus et al., 2009).

The mechanism of Mcm2-7 helicase loading

In preparation for MCM loading in G1 phase ORC recruits Cdc6 to origins, forming a complex (Cocker et al., 1996; Coleman et al., 1996) that encircles and bends double-stranded origin DNA through extensive protein-DNA interactions (Fig 1.2) (Bleichert et al., 2015; Li et al., 2018; Tocilj et al., 2017). The ORC-Cdc6 complex then recruits Cdt1-Mcm2-7 to the origin to form an unstable intermediate complex called ORC-Cdc6-Cdt1-Mcm2-7 (OCCM), which can be biochemically enriched by preventing ATP hydrolysis during the helicase loading reaction (Sun et al., 2013; Yuan et al., 2017). High-resolution cryo-EM analysis of this complex reveals that ORC-Cdc6 and Cdt1-Mcm2-7 each form a toroid structure encircling the DNA with a shared central channel (Yuan et al., 2017). Single molecule studies indicate that following the deposition of the first Mcm2-7 complex onto DNA, Cdc6 and Cdt1 are released from the complex, while ORC and MCM remain bound (Fig 1.3) (Ticau et al., 2017; Ticau et al., 2015).

Once the first Mcm2-7 complex is loaded onto the DNA, Cdc6 and a second Cdt1-Mcm2-7 complex associate with the origin-bound ORC to load the second Mcm2-7 complex around the DNA, resulting in the formation of a head-to-head Mcm2-7 DH stably bound around dsDNA (Fig 1.3) (Abid Ali et

al., 2017; Evrin et al., 2009; Li et al., 2015; Noguchi et al., 2017; Remus et al., 2009). ATP-hydrolysis by MCM appears to play an essential role during this process (Coster et al., 2014; Kang et al., 2014). The MCM hexamers in the DH are held together via interactions between the MCM N-terminal domains, while the DNA inside the central channel makes extensive contacts with specific DNA binding loops of select Mcm2-7 subunits (Noguchi et al., 2017). The head-to-head orientation of the MCM hexamers in the DH provides a structural basis for bidirectional replication fork establishment at the origin.

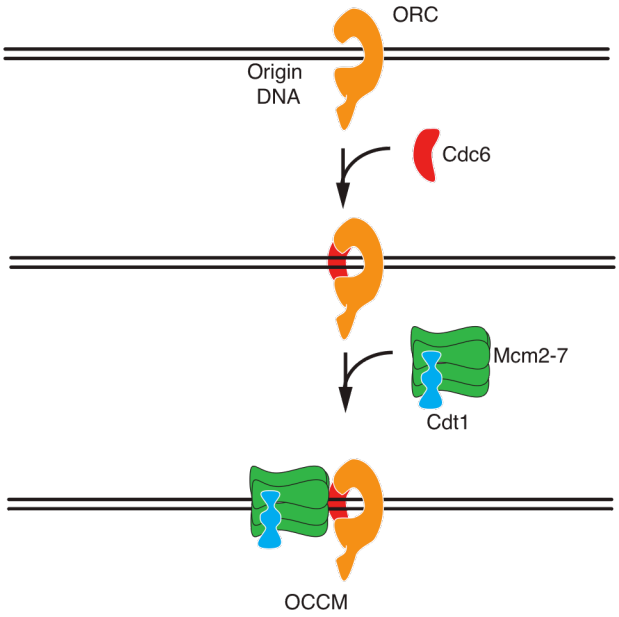

Fig 1.2 Initial recruitment of Mcm2-7 to origin DNA. Origin-bound ORC recruits Cdc6. Once Cdc6 is bound, Cdt1·Mcm2-7 is recruited to the origin to form a ORC-Cdc6-Cdt1-Mcm2-7 (OCCM) complex.

Proteins involved helicase activation

Helicase activation is the commitment step of DNA replication and occurs exclusively in S-phase. On its own, Mcm2-7 is a poor helicase but association of two helicase co-factors Cdc45 and GINS greatly stimulate its

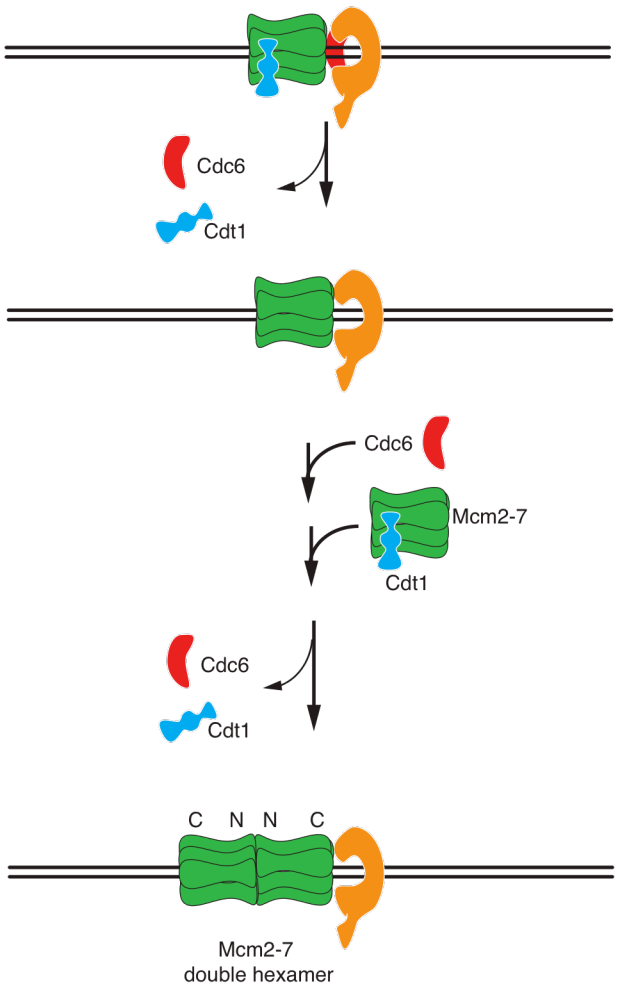

Fig 1.3 Mcm2-7 helicase loading. Origin-bound ORC recruits Cdc6. Once Cdc6 is bound, Cdt1·Mcm2-7 is recruited to the origin to form a ORC-Cdc6-Cdt1-Mcm2-7 (OCCM) complex.
.

activity via the formation of Cdc45-Mcm2-7-GINS (CMG) complex (Ilves et al., 2010). Activation of Mcm2-7 is dependent on two protein kinases: the Dbf4-dependent kinase (DDK) and the cyclin dependent kinase (CDK) with DDK activity recruiting Cdc45 and CDK activity recruiting GINS (Gambus et al., 2006; Heller et al., 2011; Labib, 2010; Yeeles et al., 2015). Additional firing factors: Dpb11, Sld2, Sld3, Pol ε and Mcm10 are also required for this process (Bell and Labib, 2016) and below I review each of these factors.

Dbf4-dependent kinase (DDK)

DDK comprises the Cdc7 catalytic kinase subunit and Dbf4, a regulatory subunit that relieves auto-inhibition of Cdc7 (Dowell et al., 1994; Jackson et al., 1993; Kitada et al., 1992). Cdc7 was first identified by Hartwell as a gene required for DNA synthesis in *S. cerevisiae* (Hartwell, 1973). Subsequently, its activity was discovered to be controlled by the cell cycle-dependent association with Dbf4, which in turn is regulated by anaphase promoting complex (APC) (Cheng et al., 1999; Oshiro et al., 1999). The essential target for DDK during DNA replication is the Mcm2-7 complex as Mcm subunit mutations bypass DDK function (Hardy et al., 1997; Sheu and Stillman, 2010). It phosphorylates multiple Mcm subunits (Lei et al., 1997; Masai et al., 2006; Sheu and Stillman, 2006). In the budding yeast, phosphorylation by DDK promotes DNA replication initiation by alleviating an auto-inhibitory activity present in Mcm4 N-terminus (Sheu and Stillman, 2010). Recruitment of essential initiation factors Sld3 and Cdc45 to the origins is also dependent on DDK activity (Masai et al., 2006; Sheu and Stillman, 2006; Yabuuchi et al., 2006).

Cyclin-dependent kinase (CDK)

In addition to DDK, CDK is also essential for DNA replication initiation in eukaryotes as established by the genetic studies in the budding yeast and the fission yeast (Hartwell, 1973; Nurse and Bissett, 1981). Similar to DDK, CDK is formed by association of a kinase and a regulatory partner, cyclin. In *S. cerevisiae*, CDK consists of a single Cdc28 kinase and its role in DNA replication involves two functionally redundant S-phase cyclins, Clb5 and Clb6 (Schwob and Nasmyth, 1993). CDK has two essential targets during DNA replication Sld2 and Sld3 and their phosphorylation leads to the recruitment of additional initiation factors to the origin (discussed below) (Tanaka et al., 2007; Zegerman and Diffley, 2007).

Helicase cofactors Cdc45 and GINS

The core of the replicative helicase Mcm2-7 is a poor helicase on its own and requires the association two essential cofactors, Cdc45 and GINS (for Go, Ichi, Ni, San, meaning 5, 1, 2, 3 in Japanese), for robust activity (Bochman and Schwacha, 2008; Ilves et al., 2010). Cdc45 was initially identified in a *S. cerevisiae* screen for temperature sensitive mutants affecting cell cycle progression (Moir et al., 1982) and was subsequently found to be required for DNA replication initiation (Zou et al., 1997). On the other hand, the GINS complex was first identified in a screen searching for interaction partner for one of its subunits Sld5. Sld5, Psf1 (partner of Sld five 1), Psf2 and Psf3 form a heterotetrameric GINS and all of these subunits are highly conserved across the species (Takayama et al., 2003). Both Cdc45 and GINS are essential component of replication fork and form a stable complex with Mcm2-

7 during S-phase (Aparicio et al., 1997; Gambus et al., 2006; Moyer et al., 2006; Pacek et al., 2006).

Other firing factors

Firing factors essential for helicase activation has been most well studied in the budding yeast. One of the key factors, Dpb11 was first identified as a high-copy suppressor of a mutation in Pol ε, an essential DNA polymerase (Araki et al., 1995). A single ortholog of Dpb11 that is essential for DNA replication initiation has been discovered across the eukaryotes, known as Rad4/Cut5 in fission yeast and TopBP1 in metazoans (Garcia et al., 2005). All of the Dpb11 orthologs consist of a series of BRCT domain, a phospho-peptide binding motif(Manke et al., 2003; Yu et al., 2003). Discovery of Dpb11 in the budding yeast paved the path for isolation of a series of SLD (synthetically lethal with Dpb11) genes that were subsequently found to be involved in MCM helicase activation (Kamimura et al., 1998). Sld2 was the first of these to be characterized and was shown to bind to C-terminal BRCT repeats of Dpb11 in CDK phosphorylation dependent fashion (Masumoto et al., 2002; Tak et al., 2006). Later, Sld3 was revealed to interact with Cdc45 and was shown to bind to the two N-terminal BRCT repeats of Dpb11 when phosphorylated by CDK (Kamimura et al., 2001; Tanaka et al., 2007; Zegerman and Diffley, 2007). In humans, two proteins known as RecQ4 and Treslin have been proposed to be the functional homologs of Sld2 and Sld3 (Marino et al., 2013; Sanchez-Pulido et al., 2010).

Pol ε complex is an essential DNA polymerase in eukaryotes and has a major role in leading strand synthesis during elongation (Morrison et al., 1990; Sugino, 1995). Surprisingly, Pol ε also has an essential role in initiation of DNA

replication that is independent of its DNA polymerase activtiy (Muramatsu et al., 2010). Pol ε comprises of four subunits: Pol2, Dpb2, Dpb3 and Dpb4 . The largest and catalytic subunit, Pol2, comprises two pairs of DNA polymerase and 3'-5' exonuclease domains, one in the N-terminal half of the protein, and the other in the C-terminal half. However, the C-terminal DNA polymerase domain lacks essential catalytic residues rendering it inactive for DNA synthesis. Intriguingly, the catalytically active N-terminal DNA polymerase domain is not essential for cell growth or DNA replication, while the catalytically inactive C-terminus of Pol2 is essential for viability (Dua et al., 1999; Kesti et al., 1999). This suggests that Pol2 has an essential structural function that is independent of its DNA polymerase activity, serving as scaffold other replication factors (Masumoto et al., 2000; Muramatsu et al., 2010). Consistent with this notion, the C-terminal region of Pol2 has been shown to genetically interact with initiation factors Dpb11 and Sld2 and helicase cofactor GINS (Muramatsu et al., 2010).

First identified in the same screen that isolated Mcm2-7 proteins in *S. cerevisiae* (Maine et al., 1984), the structurally unrelated Mcm10 protein has a strongly conserved role in DNA replication initiation across all eukaryotes (Gregan et al., 2003; Merchant et al., 1997; Wohlschlegel et al., 2002). Elimination of Mcm10 function prior to the initiation of DNA replication inhibits the recruitment of ssDNA binding protein RPA to the origin DNA but not the association of Cdc45 and GINS (Kanke et al., 2012; van Deursen et al., 2012; Watase et al., 2012), Additionally the binding of Mcm10 to the origins is dependent on both DDK and CDK suggesting a late role for Mcm10 in DNA replication initiation (Heller et al., 2011; van Deursen et al., 2012; Yeeles et al., 2015).

How the Mcm2-7 helicase is activated

Recent studies suggest that the activation of the loaded double hexamer involves two major distinct steps: first, the assembly of the CMG, and

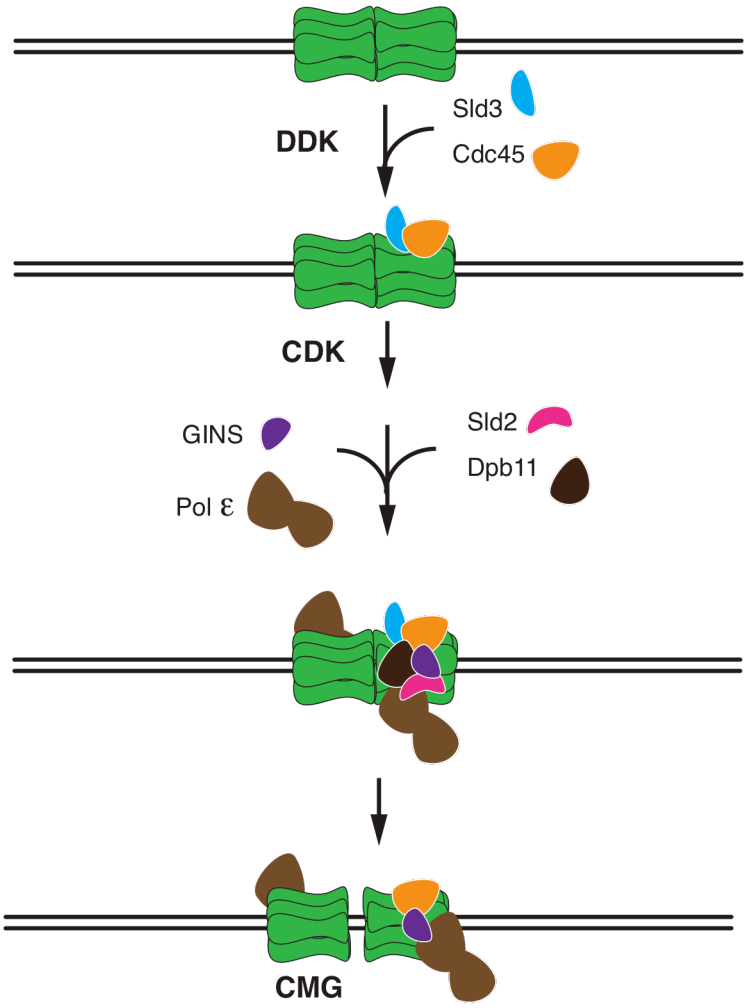

Fig 1.4 CMG formation involves the separation of the Mcm2-7 double hexamer. Combined action of DDK and CDK recruits the helicase co-factors Cdc45 and GINS to form CMG. Formation of CMG accompanies double hexamer separation. Pol ε presumably remains bound to CMG, forming a complex termed CMGE.

second the activation of the CMG helicase by Mcm10 (Figs 1.4 and 1.5) (Douglas et al., 2018; Yeeles et al., 2015). Formation of the CMG begins with the phosphorylation of the loaded Mcm2-7 DH by DDK. DDK phosphorylates

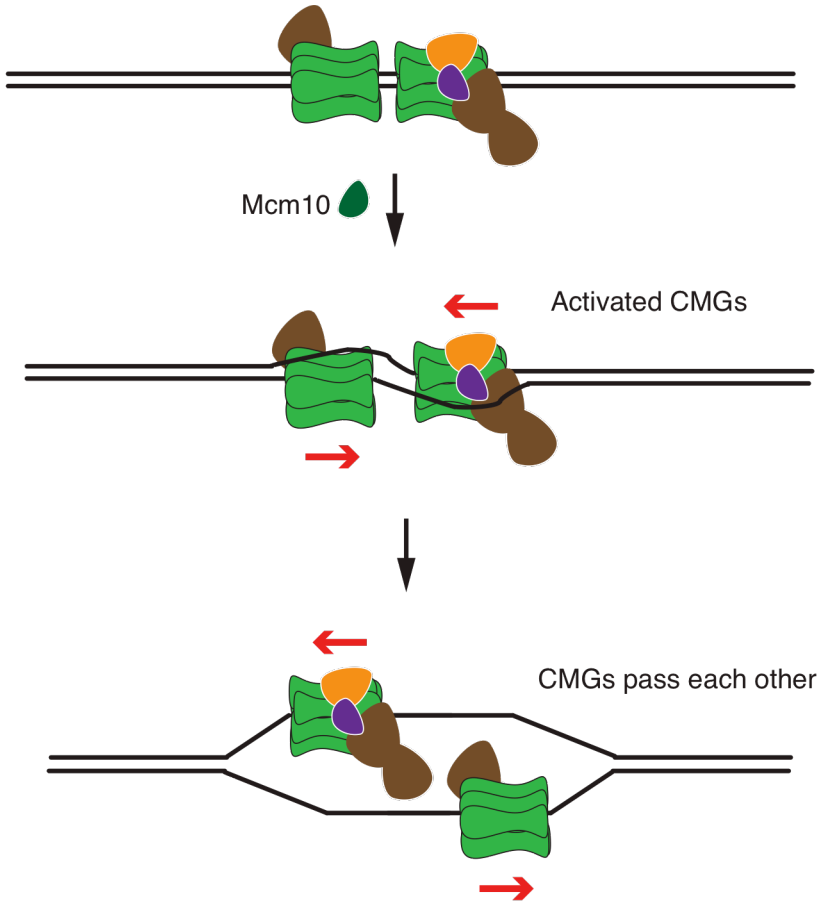

Figure 1.5 Model for CMG activation Activation of CMG helicase activity requires Mcm10. Once activated CMGs are oriented with N-terminal domain direction first thus requiring they pass each other. Red arrows by the CMGs indicate the direction of CMG translocation.

the unstructured N-terminal tails of Mcm4, Mcm6 and Mcm2 (Labib, 2010; Lei et al., 1997; Masai et al., 2006; Sheu and Stillman, 2006). This phosphorylation promotes the recruitment of two essential recruitment factors Sld3 and Cdc45 to the origin (Fig 1.4) (Deegan et al., 2016; Gros et al., 2014; Heller et al., 2011; Yeeles et al., 2015).

CDK on the other hand phosphorylates Sld2 and Sld3, which promotes the complex formation between Sld2, Sld3 and Dpb11 (Tanaka et al., 2007; Zegerman and Diffley, 2007). Activity of CDK in S-phase also promotes the interaction between Sld2, Dpb11, Pol ε and GINS to form a labile but detectable pre-loading complex (preLC) independent of Mcm2-7 loading at origins (Araki, 2010; Muramatsu et al., 2010). Thus the recruitment of Sld3 to the origin in presence of DDK activity followed by the interaction between Dpb11 and Sld3 facilitated by CDK eventually recruits the pre-LC to the origin (Labib, 2010; Muramatsu et al., 2010).

As described above, DDK and CDK recruit the helicase cofactors GINS and Cdc45 respectively and promote the formation of CMG. Formation of the CMG involves the separation of the double hexamer and accompanies initial DNA untwisting (Douglas et al., 2018). Nonetheless, the separated CMG helicases are inactive and require Mcm10 for activation. Once activated, CMG helicases translocate in 3′-5′ direction on ssDNA along the leading strand template (Fu et al., 2011; Georgescu et al., 2017; Ilves et al., 2010; Moyer et al., 2006). Activated CMGs travel N-terminal domain first, requiring the two sister CMGs to pass each other during replication initiation (Fig 1.5)(Abid Ali et al., 2017; Georgescu et al., 2017)

Elongation

Once the unwinding of the parental duplex begins and the replication forks are established, DNA polymerases and additional accessory factors necessary for genome duplication are recruited to the fork to form a multiprotein replisome (Bell and Labib, 2016; Burgers and Kunkel, 2017; Kelly, 2017). In addition to three essential DNA polymerases, Polymerase α (Pol α), Polymerase δ (Pol δ) and Polymerase ε (Pol ε), the core replisome in eukaryotes comprises the single stranded DNA binding protein RPA, the clamp loader RFC, and the clamp PCNA (Bai et al., 2017). Additionally, as half of the genome is duplicated in the form of discontinuous Okazaki fragments, factors for maturation of lagging strands play an important role during replication elongation (Smith and Whitehouse, 2012).

RPA

RPA was originally identified from human cell extracts as a component essential for replication of SV40 genome *in vitro* (Fairman and Stillman, 1988; Wobbe et al., 1987; Wold and Kelly, 1988) and was later found to be essential for cellular DNA replication (Adachi and Laemmli, 1994; Wold, 1997). In addition to replication, RPA also plays a very important role in other metabolic processes such as DNA repair and DNA recombination (Coverley et al., 1992; Coverley et al., 1991; Moore et al., 1991). It is a highly conserved protein and consists of three subunits: Rpa1, Rpa2 and Rpa3 (Wold, 1997). RPA binds single stranded DNA with high affinity and plays an important role in protecting vulnerable ssDNA exposed during the unwinding of parental duplex at the replication fork (Gomes et al., 1996; Kim et al., 1994; Oakley and Patrick, 2010).

In addition to coating ssDNA, RPA also plays an active role in DNA replication by its interaction with several other replication factors (Prakash and Borgstahl, 2012). Pol α forms a stable complex with RPA and RPA binding stimulates the primase activity of Pol α (Braun et al., 1997). RPA also directly binds with RFC as well as Pol δ and it has been reported that competition to bind RPA plays an important role in polymerase switch during DNA replication (Yuzhakov et al., 1999). Hence, RPA plays a central role at the replication fork during DNA replication elongation.

DNA polymerases

In eukaryotes, complete synthesis of daughter strands during DNA replication requires 3 DNA polymerases: Pol α, Pol δ and Pol ε (Burgers and Kunkel, 2017). Each of these polymerases has one catalytic subunit and two or three accessory subunits. DNA polymerases cannot synthesize DNA *de novo* but require a primer 3'-OH end to initiate chain synthesis. Only Pol α has the ability to synthesize the primers and thereby initiate DNA synthesis on both strands of the fork (Muzi-Falconi et al., 2003). Pol α is composed of four subunits, named Pol1, Pol12, Pri1, and Pri2 in *S. cerevisiae*. The primase subunits, Pri1 and Pri2, coordinately synthesize an 8-10 nucleotide long RNA oligo that gets extended by 10-15 nucleotides of DNA by the catalytic subunit of Pol α, Pol1 (Nunez-Ramirez et al., 2011; Pellegrini, 2012). Despite its polymerase activity, Pol α is ill suited to copy DNA extensively owing to its limited processivity and lack of proofreading exonuclease activity to correct mismatches (Perera et al., 2013).

Contrary to Pol α, both Pol δ and Pol ε are highly accurate polymerases with proofreading exonuclease activity (Morrison et al., 1991; Morrison and

Sugino, 1994). They are also highly processive enzymes when interacting with PCNA, a sliding DNA clamp that acts as a processivity factor (Burgers, 1991; Chilkova et al., 2007; Langston and O'Donnell, 2008; Lee et al., 1991). In the budding yeast Pol δ comprises of 3 subunits (Pol3, Pol31 and Pol32) (Gerik et al., 1998), whereas Pol ε comprises four subunits (Pol2, Dpb2, Dpb3 and Dpb4) (Chilkova et al., 2003; Hamatake et al., 1990). Owing to their high processivity and proofreading exonuclease activity, Pol δ and Pol ε are responsible for bulk of DNA synthesis (Burgers, 2009; Kunkel and Burgers, 2008).

Division of labor at the replication fork

The proofreading exonuclease activity of Pol δ and Pol ε has been used to explore the division of labor between these two polymerases at the replication fork. By mutating the exonuclease activity of either Pol2 or Pol3 and placing a marker gene in different orientation relative to the replication origin, it was shown that these two polymerases proofread on opposite strands (Shcherbakova and Pavlov, 1996). In a separate approach, using catalytic mutants that increase the rate of specific nucleotide misincorporations, it was determined that Pol ε extended primarily the leading strand (Pursell et al., 2007), while Pol δ was primarily involved in the synthesis of lagging strand (Nick McElhinny et al., 2008). This differential activity of the two polymerases on separate strands was further confirmed using the mutants that have higher ribonucleotide incorporation in the genome during DNA replication (Clausen et al., 2015; Daigaku et al., 2015; Koh et al., 2015).

Interaction studies *in vivo* as well as *in vitro* with purified proteins showed that Pol ε binds directly to CMG helicase (Langston et al., 2014;

Sengupta et al., 2013). Furthermore, cryo EM analysis of the complex consisting of CMG and Pol ε indicated that Pol ε consisted of two flexible lobes, with the non-catalytic lobe being anchored to the CMG and the catalytic lobe extending flexibly away from the CMG core (Sun et al., 2015; Zhou et al., 2017). CMG also interacts with Pol α indirectly through the Ctf4 protein (mammalian orthologue: AND-1 (Gambus et al., 2009; Kilkenny et al., 2017; Zhu et al., 2007). Ctf4 forms a homotrimer that can simultaneously interact with CIP (Ctf4-interacting peptide)-boxes present both GINS and Pol α. *In vitro*, Pol α can also directly associate with the CMG helicase to prime lagging strand synthesis (Georgescu et al., 2015; Sun et al., 2015). In contrast to Pol ε and Pol α, there is no evidence for direct interaction between Pol δ and CMG. Pol δ does not bind to CMG under conditions where Pol ε and Pol α bind to the replicative helicase (Sengupta et al., 2013). These genetic and biochemical data combined suggest that the lagging strand is replicated by Pol δ in an uncoupled manner from the CMG helicase, while the leading strand is synthesized by Pol ε tethered to CMG (Fig 1.6).

The strict strand assignment for Pol ε to the leading strand of the replication fork, however, is disputed (Johnson et al., 2016; Stillman, 2015). An alternative model has been suggested in which Pol δ synthesizes both leading and lagging strands and Pol ε only proofreads the errors made during leading strand synthesis, which could explain the genetic data observed with the exonuclease mutants (Johnson et al., 2015). Intriguingly, strains lacking the catalytic domain of Pol ε are viable (Dua et al., 1999; Kesti et al., 1999) indicating that Pol δ, Pol α, or both can synthesize the leading strand in the absence of Pol ε polymerase activity. Finally, a role for Pol δ in establishing leading strand synthesis has also been suggested based on studies both *in*

vitro and *in vivo* (Daigaku et al., 2015; Garbacz et al., 2018; Yeeles et al., 2017). Overall, these data suggest a degree of flexibility of polymerase usage on the leading and lagging strand during DNA replication.

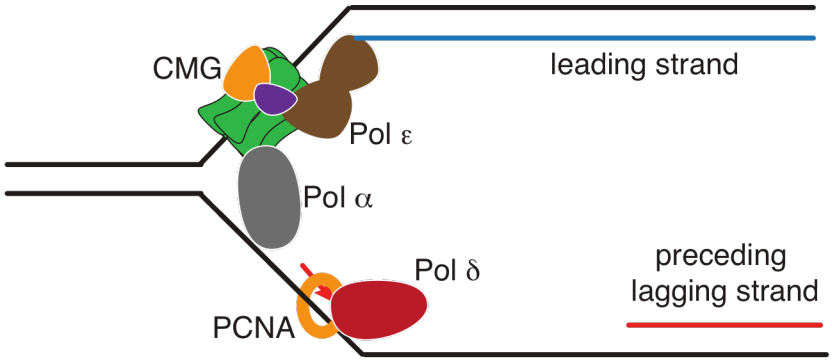

Fig 1.6 Division of Labor at eukaryotic Replication Fork. The Pol α primase harbors the primase activity required to initiate DNA synthesis. Pol ε and Pol δ synthesize the majority of the leading and lagging strand, respectively.

Okazaki fragment maturation

Regardless of the debate concerning which polymerase synthesizes the leading strand at the fork, it is now widely accepted that the bulk of the lagging strand in eukaryotes is synthesized by pol δ (Kunkel and Burgers, 2008; Stodola and Burgers, 2017). Compared to the leading strand, which can be replicated continuously, lagging strands are synthesized discontinuously and

require additional proteins for its maturation. Efficient DNA synthesis by Pol δ requires the processivity clamp PCNA, which is loaded in ATP dependent manner at the 3'-primer-template junction by the clamp loader, RFC (Podust et al., 1995; Prelich et al., 1987; Yao and O'Donnell, 2012). Like RPA, PCNA and RFC were initially identified in human cell extracts as factors necessary for replication of the SV40 genome (Prelich et al., 1987; Tsurimoto and Stillman, 1989). PCNA is a homo-trimeric ring-shaped sliding clamp that encircles DNA after loading onto DNA by RFC, thereby tethering Pol δ to the template to enhance its processivity ((Yao and O'Donnell, 2012). RFC on the other hand, consists of five subunits, RFC1-5, which are members of AAA+ superfamily of proteins (Kelch et al., 2012; Majka and Burgers, 2004). In addition to loading PCNA, RFC is also involved in polymerase switching by competing with Pol α for the primer 3' end, thereby promoting the handover of the primer 3'-end to Pol δ following PCNA loading (Schauer and O'Donnell, 2017; Waga et al., 1994; Yuzhakov et al., 1999). This phenomenon of polymerase switching promotes genome integrity by limiting DNA synthesis by the error prone Pol α.

On the lagging strand, Pol δ extends the primer until it reaches the 5′ end of the preceding Okazaki fragment. The ligation of two Okazaki fragments requires the removal of the RNA primer from the 5′ end of the preceding Okazaki fragment to generate a DNA-DNA nick that can be sealed by DNA ligase I (Cdc9 in budding yeast and Lig1 in human cells) (Barnes et al., 1990; Howes and Tomkinson, 2012; Johnston and Nasmyth, 1978). Biochemical and genetic studies indicate that a major pathway for primer removal involves the combined action of Pol δ and the structure specific flap endonuclease1 (Fen1) (Balakrishnan and Bambara, 2013; Grasby et al., 2012). In this pathway, the strand displacement activity of Pol δ displaces the 5′ end of the preceding

Okazaki fragment, generating a short flap that can be cleaved by Fen1 (Garg et al., 2004; Rossi and Bambara, 2006; Stodola and Burgers, 2016). PCNA also participates in this pathway by directly interacting with both Fen1 and DNA ligase 1 (Levin et al., 2000; Li et al., 1995; Vijayakumar et al., 2007).

Topoisomerases

Unwinding of the double helical DNA during the progression of replication forks leads to the accumulation of positive supercoils in front of the fork, which would impair replisome progression if not resolved (Schvartzman and Stasiak, 2004; Vos et al., 2011; Wang, 2002). Removal of supercoils requires topoisomerases, enzymes that change the topology of DNA molecules by transiently cleaving re-sealing the DNA (Champoux, 2001). They are classified as type I if they cleave a single DNA strand, or type II if both strands of DNA are cleaved (Vos et al., 2011). Positive supercoiling ahead of the fork can be resolved in two ways. The first way involves the relaxation of the supercoil by either type I or type II topoisomerase ahead of the fork. Alternativley, the replisomes may freely rotate clockwise relative to the direction of fork movement along the path of template DNA to dissipate the positive supercoils of the unreplicated DNA ahead of the fork to the replicated DNA behind the fork. This causes the two replicated sisters to cross over each other, leading to the formation of precatenanes, which can only be resolved by type II but not type I topoisomerase (Dewar et al., 2015; Peter et al., 1998; Schvartzman and Stasiak, 2004).

In budding yeast as well as higher eukaryotes, both Top1/Topo I (type I) and Top2/Topo II can remove positive supercoils ahead of the fork to promote fork progression (Bermejo et al., 2007; Vos et al., 2011). Top1 moves along

with the replication fork and is a component of the RPC, indicating that it is the primary topoisomerase acting at the forks during fork progression (Gambus et al., 2006). Consistent with this notion, depletion of Top2 in budding yeast cells as well as immunodepletion of Topo II from *Xenopus laevis* egg extract did not prevent the completion of DNA synthesis, suggesting that Top2/ Topo II activity is dispensible for elongation. However, Top2 is essential for the subsequent decatenation of daughter dimer molecules (Baxter and Diffley, 2008; DiNardo et al., 1984).

Termination

In eukaryotes, replication terminates when the replication forks fired from neighboring origin converge upon each other. Convergence of the forks ultimately results in the encounter of opposing replisomes, which is followed by replisome disassembly and filling of any gaps remaining in the daughter DNA strands (Dewar and Walter, 2017). Unlike initiation and elongation, termination of DNA replication in eukaryotes has not been extensively studied.

Mapping termination events in budding yeast cells synchronously released into S phase showed that around 70 of almost 300 termination events occurred in specific chromosomal locations (Fachinetti et al., 2010). However, genome-wide replication profiling of budding yeast and mammalian cells by Okazaki fragment sequencing indicates that termination events generally occur midway between the origins (McGuffee et al., 2013; Petryk et al., 2016). Indeed, the location of termination events was shown to be primarily dependent on origin location and timing of origin activation, suggesting that termination events do not occur at specific loci in eukaryotic genome (Hawkins

et al., 2013; McGuffee et al., 2013). These data suggest that termination in eukaryotes does not require specific genomic DNA sequences.

During plasmid replication in *Xenopus* egg extract, two converging replication forks can bypass each other without any detectable slowing or stalling (Dewar et al., 2015), suggesting that there is no significant steric clash during fork encounter. Following fork bypass and completion of DNA replication, CMG was shown to be removed from the DNA. Removal of CMG during termination is essential to prevent re-replication of the genome and preserve genome integrity ((Dewar and Walter, 2017). In budding yeast and frogs, removal of CMG depends on ubiquitination of Mcm7 (Maric et al., 2014; Moreno et al., 2014). Mcm7 ubiquitination requires E3 ubiquitin ligase SCF^{Dia2} and $CRL2^{LRR1}$ in budding yeast and frogs respectively (Dewar et al., 2017; Maric et al., 2014). Once ubiquitylated, CMG is removed from the chromatin by the ATPase p97 (Franz et al., 2011; Maric et al., 2014; Moreno et al., 2014).

DNA replication in the context of chromatin

The genome of eukaryotic cells is confined into the nucleus by compacting it into chromatin. Chromatin comprises a repeating structural unit, called nucleosome (Kornberg, 1977). The nucleosome consists of 147 base pairs of DNA wrapped around a histone octamer containing one centrally located H3-H4 tetramer flanked by two H2A-H2B dimers (Luger et al., 1997). The wrapping of the DNA around the histone core poses a significant challenge to replisome progression, requiring the disassembly of nucleosomes ahead of the fork to access the DNA template. DNA replication in turn thus also poses a significant challenge to chromatin structure and the preservation

of the epigenetic information (Lucchini and Sogo, 1995; McKnight and Miller, 1977; Whitehouse and Smith, 2013). How nucleosome disassembly ahead of the fork and nucleosome re-assembly behind the fork is coordinated at the replisome remains poorly understood.

Factors promoting replisome progression through chromatin

Progression of the replisome through chromatin requires the coordinated activities of histone chaperones and chromatin remodelers (MacAlpine and Almouzni, 2013). Histone chaperones are broadly defined as non-catalytic proteins that sequester non-nucleosomal histones to prevent or reverse incorrect histone-DNA interactions and to mediate in turn the orderly assembly of canonical nucleosomes (Laskey et al., 1978; Ransom et al., 2010). Chromatin remodelers on the other hand are large multi-protein complexes that catalytically change the structure, position and histone composition of nucleosomes.

A key histone chaperone involved in promoting DNA transactions within a chromatin template is FACT, a heterodimer of Spt16 and Pob3 (SSRP1 in humans) (Orphanides et al., 1999). FACT binds to H3-H4 tetramers (Tsunaka et al., 2016) as well as H2A-H2B dimers (Belotserkovskaya et al., 2003) and plays an important role during transcription by disrupting and restoring nucleosomes ahead of and behind RNA polymerase, respectively (Jamai et al., 2009; Voth et al., 2014). FACT is also involved in changing chromatin structure during DNA replication as it promotes replication initiation *in vivo* and promotes fork progression on nucleosomal templates *in vitro* (Kurat et al., 2017; Tan et al., 2006). Another histone chaperone with a potential role in regulating access to nucleosomal DNA is Nap1. Nap1 binds to H2A/H2B in co-

immunoprecipitation studies and has the ability to assemble nucleosomes *in vitro* (Ito et al., 1996). It can also remove nucleosomes from DNA *in vitro* (Lorch et al., 2006).

In addition to histone chaperones, chromatin remodelers have also been implicated in the disassembly of the nucleosomes ahead of the fork (Alabert et al., 2017). In budding yeast, chromatin remodeling enzymes Ino80 and Isw2 both promote efficient replication fork progression (Iida and Araki, 2004; Kurat et al., 2017; Vincent et al., 2008). Along the same lines, members of Iswl family (WICH and ACF) and Ino80 complex also promote fork progression in mammalian cell lines (Collins et al., 2002; Lee et al., 2014; Poot et al., 2004).

Nucleosome assembly behind the fork

The newly synthesized DNA must be packaged into chromatin immediately to preserve epigenetic histone modifications and to maintain the normal nucleosome density (Alabert et al., 2017; Bell and Labib, 2016). The former is thought to be achieved by the transfer of parental histones locally to both daughter strands (Radman-Livaja et al., 2011). The latter requires the assembly of new nucleosomes behind the fork. The deposition of both parental and newly synthesized histones requires specific chaperones and remodelers, as discussed below.

Parental histone transfer

Parental nucleosomal H3-H4 tetramers carry the majority of epigenetic information and appear to remain intact during DNA replication, suggesting that parental histone H3-H4 tetramers are transferred as a unit during DNA

replication (Katan-Khaykovich and Struhl, 2011; Prior et al., 1980; Vestner et al., 2000; Yamasu and Senshu, 1990). Mcm2, a subunit of the replicative helicase, has H3-H4 binding activity and possesses chaperone activity (Groth et al., 2007; Ishimi et al., 2001). The histone-binding domain in Mcm2 binds to H3-H4 tetramer by mimicking DNA in the nucleosome thus providing a potential binding site in the replisome for the recycling of parental histones (Huang et al., 2015). Consistent with this, human Mcm2 has been shown to be important for the symmetric segregation of parental nucleosomes into both leading and lagging strands, as histone binding mutations in human Mcm2 result in a marked increase of parental nucleosome partitioning to the leading strand (Petryk et al., 2018). Interestingly, the Pol ε subunits, Dpb3 and Dpb4, also seem to be important for symmetrical histone segregation at the fork as their absence in budding yeast cells results in H3-H4 tetramer being deposited disproportionately to lagging strand (Yu et al., 2018).

Assembly of new nucleosomes

Electron microscopy (EM) studies analyzing nucleosome density at replication forks indicated that newly synthesized daughter strands at replication forks exhibit a similar nucleosome density as the parental duplex indicating that nucleosome re-assembly after DNA replication is fast (Lucchini and Sogo, 1995; Sogo et al., 2002). During S-phase there is a burst of histone synthesis to accommodate the high demand for new nucleosome assembly. For instance, 33 million new nucleosomes have to be deposited in human cells per replication cycle (Alabert et al., 2017). As with nucleosome disassembly, appropriate deposition of nascent histones onto daughter strand involves the

activities of histone chaperones and chromatin remodelers (Yadav and Whitehouse, 2016).

Asf1 is a key chaperone involved in the deposition of nascent chromatin. It binds to a newly synthesized H3-H4 dimers and helps maintain the dimeric nature of the complex (English et al., 2006; Natsume et al., 2007). In *S. cerevisiae,* Asf1-bound histone H3 is subject to acetylation by Rtt109 on residue lysine 56 (Driscoll et al., 2007; Han et al., 2007; Tsubota et al., 2007). Acetylation of H3 K56 promotes the handover of the modified H3-H4 dimer from Asf1 to the downstream chaperones CAF-1 and RTT106 (Burgess et al., 2010; Li et al., 2008). CAF-1 is recruited to the replication fork by its interaction with PCNA and plays a prominent role in the assembly of new H3-H4 tetramers behind the fork (Hoek and Stillman, 2003; Li et al., 2008; Zhang et al., 2000). Biophysical studies of CAF-1 function show that two CAF-1 complexes may cooperate to deposit an H3-H4 tetramer onto nascent DNA (Mattiroli et al., 2017; Sauer et al., 2017) prior to the recruitment of H2A and H2B. Nap1 is the major chaperone for H2A-H2B stabilizing the H2A-H2B dimer and facilitating its nuclear import (D'Arcy et al., 2013; Straube et al., 2010). Nap1 also prevents nonproductive accumulation of H2A-H2B onto DNA (Andrews et al., 2010; D'Arcy et al., 2013) and is a prime candidate to deliver H2A-H2B to H3-H4 tetramer and complete the nucleosome assembly.

Coordination between fork progression and nucleosome assembly

In mammalian cells, inhibition of histone synthesis rapidly slows the replication fork and blocks replisome progression (Mejlvang et al., 2014; Seale and Simpson, 1975; Weintraub, 1972), indicating the necessity to coordinate DNA replication and nucleosome assembly. In budding yeast, although

replication fork progression is not strictly dependent on nucleosome assembly, the integrity of the progressing fork appears to be affected by replication coupled chromatin assembly. Mutations in budding yeast cells that impair replication-coupled chromatin assembly display elevated sister chromatid exchange, loss of fork integrity and large chromosomal rearrangements (Clemente-Ruiz et al., 2011; Clemente-Ruiz and Prado, 2009; Myung et al., 2003).

Nucleosome assembly on newly replicated DNA has been shown to be coupled with lagging strand synthesis. Genome-wide mapping of Okazaki fragment in *S. cerevisiae* showed that ligation sites between the Okazaki fragments occur near the nucleosome midpoint and that Okazaki fragment length and distribution depend on chromatin assembly (Smith and Whitehouse, 2012) . Consistent with this, lagging strand maturation proteins, Fen1 and DNA ligase I, can efficiently operate on a nucleosome (Chafin et al., 2000; Huggins et al., 2002).

Thesis summary

As described above, we now seem to know the majority of essential proteins involved in eukaryotic DNA replication. Before my thesis work, the biochemical reconstitution of steps involved in eukaryotic DNA replication was only partially achieved. Pre-RCs had been reconstituted with purified proteins, which allowed the demonstration that Mcm2-7 are loaded as inactive DHs around DNA. At the time, however, it was not known if the inactive DH configuration of Mcm2-7 was a functional intermediate during DNA replication. This question is being addressed in the first part of my thesis, Chapter two,

which describes the development of a partially reconstituted cell-free budding yeast DNA replication system.

In the second part of my thesis work, reported in Chapter three, I purified 24 different budding yeast proteins that were known to be important for DNA replication *in vivo*. Using these proteins, I developed a system that can activate reconstituted pre-RCs in an orderly and stepwise manner to form canonical budding yeast replication forks. I characterized this system to reveal functional roles of the clamp loading reaction, topoisomerases, and the role of chromatin during DNA replication.

CHAPTER TWO

RECONSTITUTED PRE-REPLICATIVE COMPLEX SUPPORT REGULATED DNA REPLICATION *

Introduction

DNA replication in eukaryotes initiates from many origin sites distributed along the length of each chromosome in a two-step mechanism (Masai et al., 2010). In the first step, the sites of DNA replication initiation, termed as origins of replication are “licensed” in G1 phase. Origin licensing involves the assembly of a pre-replicative complex (pre-RC) containing the DNA helicase, Mcm2-7, in an inactive form. Pre-RC formation requires the coordinate activities of the six-subunit origin recognition complex (ORC), Cdc6 and Cdt1, which load the Mcm2-7 complex in a head to head double-hexameric form around double-stranded DNA (Evrin et al., 2009; Gambus et al., 2011; Remus et al., 2009). In the second step called origin activation, the inactive double-hexameric Mcm2-7 helicase is activated during S phase ultimately resulting in the formation of a pair of oppositely oriented replication forks with a single Mcm2-7 helicase hexamer at the apex of each fork (Boos et al., 2012).

Activation of the Mcm2-7 helicase depends on the formation of pre-initiation complex (pre-IC) to recruit the essential helicase cofactors Cdc45 and GINS to form CMG (for Cdc45, Mcm2-7, and GINS), the replicative DNA helicase that encircles the single stranded DNA. This step requires the activity of two protein kinases, Dbf4-dependent kinase (DDK) and cyclin dependent

** Gros, J., Devbhandari, S., and Remus, D. (2014). Origin plasticity during budding yeast DNA replication in vitro. The EMBO journal 33, 621-636.*

kinase (CDK), and involves essential initiation factors, Sld3-Sld7 complex, Dpb11, Sld2, DNA polymerase ε and Mcm10 (Araki, 2010; Labib, 2010). The essential phosphorylation target for DDK is Mcm2-7 helicase whereas the CDK substrates are Sld3 and Sld2. In addition to promoting activation of helicase during S-phase, CDK also plays a crucial role in inhibiting pre-RC assembly from the onset of S phase, through G2 and M phases until the next G1 phase. This dual role for CDK ensures that origins are fired only once per cell cycle and prevents DNA re-replication by temporally separating the origin licensing and origin activation steps during DNA replication.

While the insight into the requirement of factors for replication initiation and their relative order of assembly at eukaryotic replication origins have advanced over time, comparatively little is known about the mechanism of Mcm2-7 helicase activation. It is imperative that biochemical reconstitution of DNA replication with purified proteins would provide a powerful means to investigate this process. In this regard, a cell free system to study budding yeast *Saccharomyces cerevisia* DNA replication has been reported where origin licensing and origin activation steps are mimicked by using two different cell cycle extracts. In this system, pre-RCs are first assembled on bead coupled DNA templates using an extract from G1-arrested budding yeast and then transferred to S-phase extract and activated (Heller et al., 2011). This approach has provided information regarding the sequence of replication factor recruitment to pre-RC. In other studies, pre-RC assembly has also been reconstituted *in vitro* with purified budding yeast proteins (Evrin et al., 2009; Remus et al., 2009). Nonetheless, it is not yet known if these pre-RCs reconstituted with purified proteins are able to support DNA replication. This

chapter of the thesis focuses on investigating if the reconstituted pre-RCs using purified budding yeast proteins can undergo regulated DNA replication in the presence of S phase-arrested yeast extract; taking us a step closer to reconstitute complete eukaryotic DNA replication using only purified proteins.

Results

Reconstituted pre-RCs can license DNA for cell-free replication

We first sought to determine if the pre-RCs reconstituted with purified proteins could substitute for G1-phase extracts in a previously described *in vitro* replication system where the immobilized DNA template is licensed in G1 phase extract and activated by subsequent transfer of the template to S phase extract (Heller et al., 2011). The DNA template used was pARS/WTA (Marahrens and Stillman, 1992), a 5.9 kb ARS1-containing plasmid referred to here as pARS1, coupled to paramagnetic beads. Pre-RCs were assembled using the purified budding yeast ORC, Cdc6 and Cdt1 proteins (Fig 2.1A) as previously described (Remus et al., 2009). Following assembly, pre-RCs were isolated and phosphorylated with purified DDK (Fig 2.1A). Phosphorylated pre-RCs were then recovered and incubated with S-phase extract prepared from yeast cells with the *cdc7-4* temperature sensitive mutation arresting the cells at non-permissive temperature. This strain also conditionally overexpressed limiting replication initiation factors Sld3, Cdc45, Sld2 and Dpb11. DNA synthesis was assessed by monitoring the incorporation of [α-^{32}P]dCTP into purified DNA using alkaline agarose gel electrophoresis and autoradiography. As shown in Fig 2.1B, robust DNA synthesis was observed following this approach and this DNA synthesis was dependent on both purified ORC as well as Cdc6. The observed DNA synthesis also required DDK as well as CDK

Figure 2.1 Reconstituted pre-RCs support DNA replication *in vitro*

(A) Purified ORC, Cdc6, Cdt1•Mcm2-7, DDK and Sic1 used in current study. Proteins were separated by SDS-PAGE and stained with Coomassie. Size markers (kDa) are indicated on left of each gel picture and position of respective protein on the right. λPPase = protein phosphatase (see Materials and Methods for DDK purification).

(B) Left: Reaction scheme; blue circle indicates plasmid, gray sphere indicates magnetic bead. Reaction products were analyzed in lanes 1-6 by autoradiography after alkaline agarose gel electrophoresis.

(C) Left: Reaction scheme; Lanes 1-3: Autoradiogram of replication products fractionated by alkaline agarose gel electrophoresis. Lanes 4-6: Western blot analysis of proteins associated with DNA after wash step. Pre-RCs were washed after DDK phosphorylation as indicated on top, prior to S-phase extract addition. Low-salt wash: 0.3 M K-glutamate buffer; high salt wash:0.5 NaCl buffer.

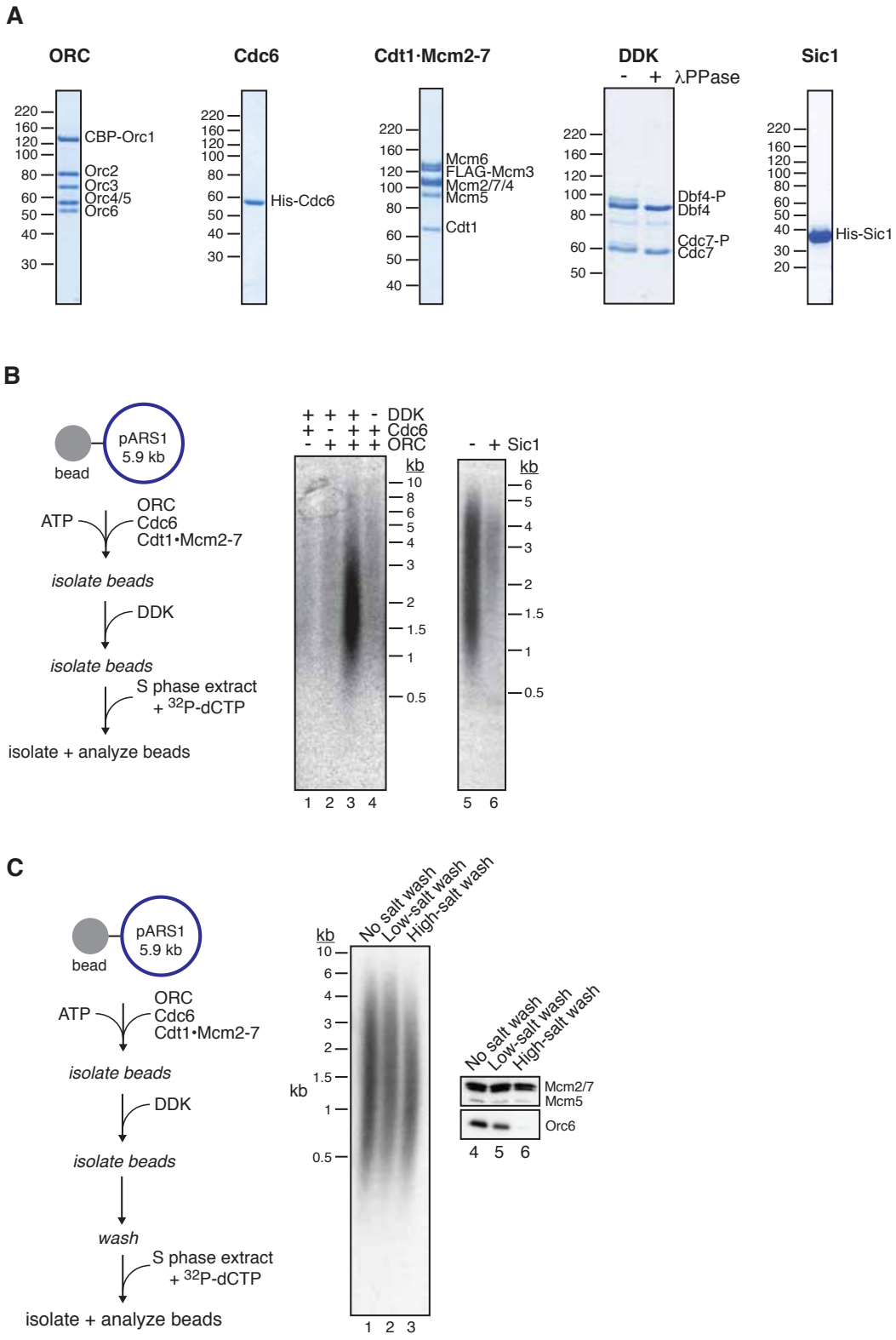
A
ORC
Cdc6
Cdt1·Mcm2-7
DDK
- + λPPase
Sic1
220
160
120
100
80
60
50
40
30
CBP-Orc1
Orc2
Orc3
Orc4/5
Orc6
His-Cdc6
Mcm6
FLAG-Mcm3
Mcm2/7/4
Mcm5
Cdt1
Dbf4-P
Dbf4
Cdc7-P
Cdc7
His-Sic1
B
pARS1
5.9 kb
bead
ATP
ORC
Cdc6
Cdt1•Mcm2-7
isolate beads
DDK
isolate beads
S phase extract
+ 32P-dCTP
isolate + analyze beads
+ + + - DDK
+ - + + Cdc6
- + + + ORC
kb
10
8
6
5
4
3
2
1.5
1
0.5
1 2 3 4
- + Sic1
kb
6
5
4
3
2
1.5
1
0.5
5 6
C
pARS1
5.9 kb
bead
ATP
ORC
Cdc6
Cdt1•Mcm2-7
isolate beads
DDK
isolate beads
wash
S phase extract
+ 32P-dCTP
isolate + analyze beads
No salt wash
Low-salt wash
High-salt wash
kb
10
6
4
3
2
1.5
1
0.5
1 2 3
No salt wash
Low-salt wash
High-salt wash
Mcm2/7
Mcm5
Orc6
4 5 6

activity since the absence of DDK in the reaction and supplementation of CDK inhibitor Sic1 in the S-phase extract both resulted in inhibition of the signal (Fig 2.1B). Taken together, these data demonstrate that reconstituted pre-RCs can license DNA for regulated replication *in vitro* that bears hallmarks of cellular DNA replication initiation.

During the pre-RC assembly, unlike Cdc6 and Cdt1, ORC remains bound at origins even after Mcm2-7 has been loaded (Bowers et al., 2004; Diffley et al., 1994; Remus et al., 2009). Studies in *Saccharomyces cerevisiae* suggest that ORC is required for both the establishment and maintenance of pre-RCs in G1 phase (Chen et al., 2007). However, elution of ORC from licensed chromatin in *Xenopus* does not disrupt the replication competence (Hua and Newport, 1998; Rowles et al., 1999). Yeast ORC can be eluted from DNA by salt wash without disrupting the loaded Mcm2-7. Nonetheless, in high-salt conditions, sliding of Mcm2-7 double hexamer along the length of DNA has been observed (Evrin et al., 2009; Remus et al., 2009). Hence, we asked if high-salt wash affects the ability of reconstituted pre-RCs to support DNA replication *in vitro*. While ORC is efficiently removed from DNA following high-salt wash, loaded Mcm2-7 are resistant to elution from the closed circular plasmid as expected (Fig 2.1C, lanes 4-6). Notably, Mcm2-7 complexes largely retained their ability to support DNA replication even after the high-salt treatment (Fig 2.1C, lanes 1-3) indicating that ORC does not have to remain bound to DNA for replication initiation following pre-RC assembly. This data also suggests that Mcm2-7 double hexamers retain their ability to initiate DNA replication after diffusion along DNA.

Figure 2.2 Assembly of initiation factors to the reconstituted pre-RCs

(A) Left: Reaction Scheme. Lanes 1-10: Western blot analysis of indicated proteins associating with DNA beads after 40-min incubation in S-phase extract. Pre-ICs were assembled in S-phase extract prepared from YDR89 (lanes 1-5) or YSD8 (lanes 6-10) strains.

(B) Mcm10 is not required for pre-IC assembly. Western blot analysis of S-phase whole cell extract (WCE) prepared from YSD8 cells in which Mcm10-myc was immunodepleted (lane2, Mcm10Δ) or mock-depleted (lane1). Lanes 3-6: Western blot of indicated proteins associated with DNA beads 40 min after addition of S-phase extract of Mcm10Δ or mock-depleted extract.

(C) Autoradiograph of replication products obtained following reaction scheme as in (A). Purified DNA was isolated after the reaction and analyzed by alkaline agarose gel electrophoresis.

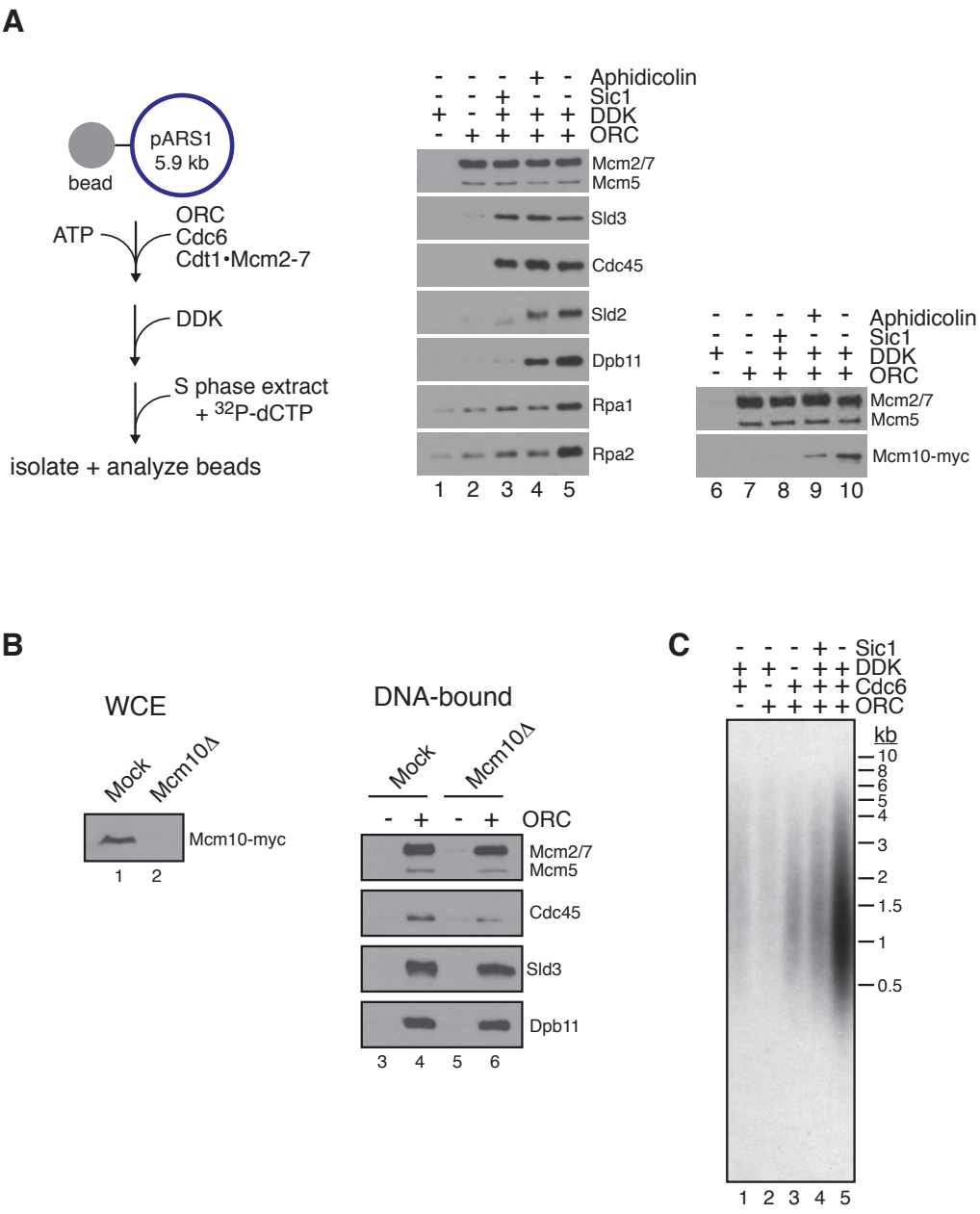
A
pARS1
5.9 kb
bead
ATP
ORC
Cdc6
Cdt1•Mcm2-7
DDK
S phase extract
+ 32P-dCTP
isolate + analyze beads
Aphidicolin
Sic1
DDK
ORC
Mcm2/7
Mcm5
Sld3
Cdc45
Sld2
Dpb11
Rpa1
Rpa2
1 2 3 4 5
Mcm10-myc
6 7 8 9 10
B
WCE
Mock
Mcm10Δ
Mcm10-myc
1 2
DNA-bound
3 4 5 6
C
kb
10
8
6
5
4
3
2
1.5
1
0.5
1 2 3 4 5

Ordered assembly of replication initiation factors to the reconstituted pre-RCs

G1- and S-phases of cell cycle are incompatible for origin activation and licensing, respectively, requiring temporal and spatial separation of the two reaction conditions to initiate DNA replication *in vitro* using cell cycle extracts. This has been previously achieved by transferring the immobilized DNA templates from G1-phase to S-phase extracts (Heller et al., 2011). Since the pre-RC reconstitution reaction using purified proteins lack the inhibitors of origin activation that are otherwise present in the G1-phase extracts, we hypothesized that simple staging of the pre-RC assembly with purified proteins and origin activation with S-phase extract in a single reaction would bypass the need for template transfer. We assembled pre-RCs on bead bound DNA and added DDK directly to the pre-RC assembly reaction, followed by the addition of S-phase extract (Fig 2.2A). Pre-IC assembly in this reaction was monitored by western blot analysis of the DNA-bound fraction. Recruitment of pre-IC components Sld3, Cdc45, Sld2 and Dpb11 was dependent on reconstituted pre-RCs, but was unaffected in the presence of aphidicolin, a replicative DNA polymerase inhibitor (Fig 2.2A). Sld3 and Cdc45 were recruited to the pre-RC in DDK dependent fashion but were independent of CDK, consistent with reports that DDK promotes Sld3 and Cdc45 binding to early origins in G1 phase when CDK activity is low (Aparicio et al., 1997; Kamimura et al., 2001; Kanemaki and Labib, 2006; Tanaka et al., 2011). Recruitment of Sld2 and Dpb11, on the other hand, was dependent on both DDK and CDK (Fig 2.2A), in agreement with CDK promoting the formation of a ternary complex between Sld3, Sld2 and Dpb11 during initiation (Muramatsu et al., 2010; Tanaka et al., 2007; Zegerman and Diffley, 2007). These data

indicate that reconstituted pre-RCs support the ordered assembly of pre-ICs under the conditions used here. Mcm10 recruitment to the pre-RC was dependent on both DDK and CDK, but independent of DNA synthesis (Fig 2.2A), consistent with previous reports (Heller et al., 2011; Watase et al., 2012). Conversely, immunodepletion of Mcm10 from the S-phase extract (Fig 2.2B), while greatly reducing the DNA synthesis activity (Fig 2.7B), did not eliminate the recruitment of Cdc45, Sld3, or Dpb11 (Fig 2.2B), supporting previous observations that Mcm10 acts after pre-IC and CMG assembly (van Deursen et al., 2012; Watase et al., 2012). In *Xenopu*s egg extracts, aphidicolin induces the uncoupling of the CMG helicase from the replicative DNA polymerases leading to extensive DNA unwinding in the absence of DNA synthesis, which promotes the recruitment of RPA to the excess of single-stranded DNA (Byun et al., 2005; Pacek et al., 2006; Walter and Newport, 2000). Interestingly here we observed that yeast RPA recruitment was inhibited by aphidicolin (Fig 2.2A), suggesting that helicase uncoupling from the polymerase does not occur in the yeast system.

We tested the replication competence of complexes assembled using the modified approach in Fig 2.2A. As shown in Fig 2.2C, robust DNA synthesis dependent on reconstituted pre-RCs, DDK and CDK was observed, illustrating that our modified assay recapitulated regulated DNA replication.

Complete replication of plasmid DNA *in vitro*

As our modified approach obviates the need to transfer template DNA from G1- to S-phase extracts, we performed the reaction scheme of Fig 2.3A with pARS1 not coupled to the beads and monitored DNA replication over time. DNA replication products began to appear after a lag phase of 10-20

Figure 2.3 *In vitro* replication of free plasmid in solution

(A) Schematic of the replication reaction.

(B) Time course analysis of pARS1 replication. Replication products were analyzed by autoradiography after native agarose gel electrophoresis. Total ^{32}P-dCTP incorporation as determined by phosphorimaging is plotted over time on right. HMW: high molecular weight DNA.

(C) pARS1 replication products contain both covalently closed negatively supercoiled and nicked plasmid molecules. Replication products of pARS1 were analyzed by agarose gel-electrophoresis in the absence (left) or presence (right) of 1μg/ul of choloroquine and visualized by autoradiography.

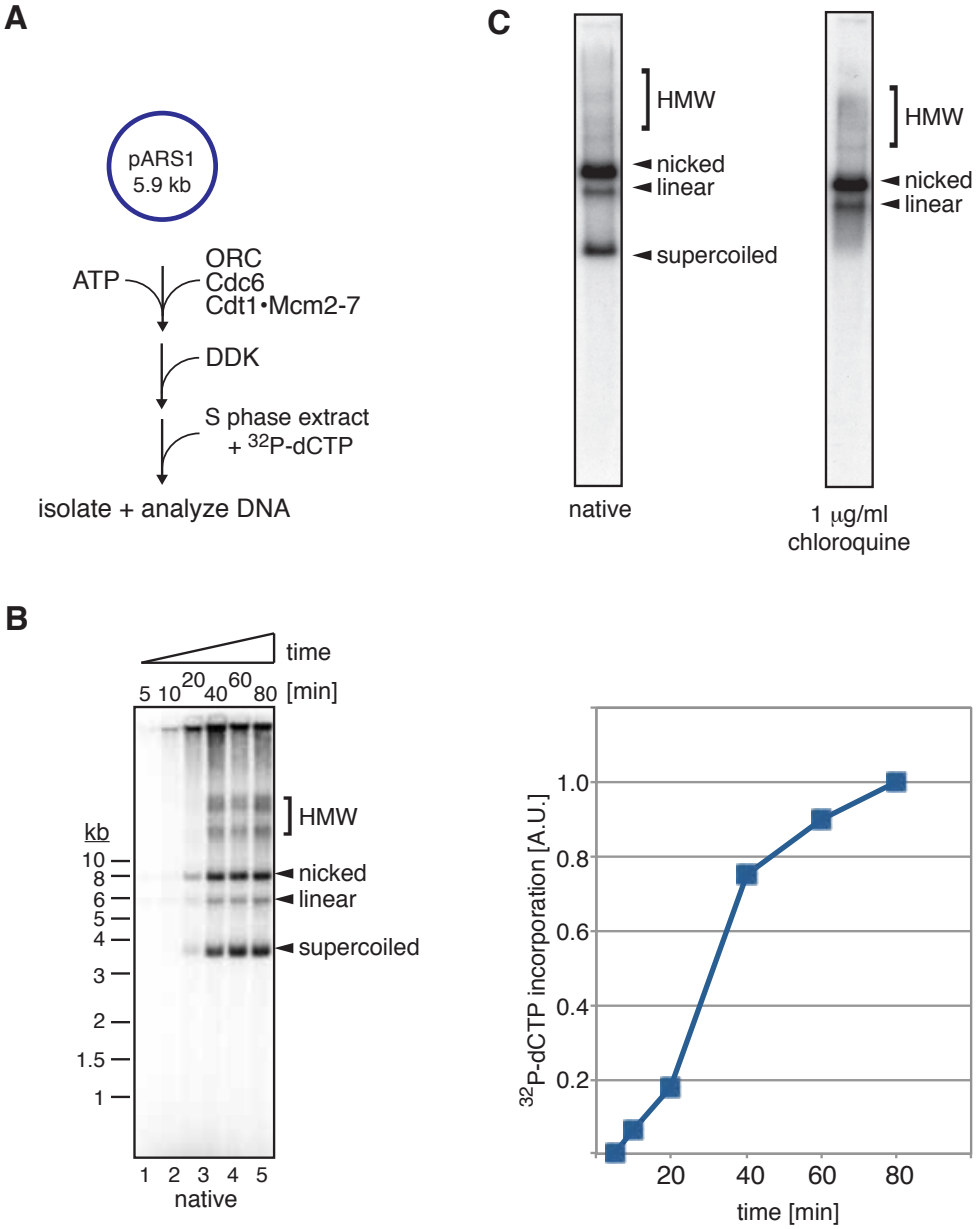
A
pARS1
5.9 kb
ATP
ORC
Cdc6
Cdt1•Mcm2-7
DDK
S phase extract
+ 32P-dCTP
isolate + analyze DNA
B
time
5 10 20 40 60 80 [min]
kb
10
8
6
5
4
3
2
1.5
1
HMW
nicked
linear
supercoiled
1 2 3 4 5
native
C
HMW
nicked
linear
supercoiled
native
HMW
nicked
linear
1 μg/ml
chloroquine
32P-dCTP incorporation [A.U.]
1.0
0.8
0.6
0.4
0.2
20
40
60
80
time [min]

min, accumulated over time and reached a plateau of DNA synthesis after 60 mins (Fig 3B). Native gel electrophoresis (Fig 2.3B, lanes 1-5) identified five main replication products: (i) negatively supercoiled plasmid, (ii) nicked plasmid, (iii) linear plasmid, (iv) a distribution of high-molecular weight (HMW) species, and (v) products that did not enter the gel. The identity of the negatively supercoiled and nicked DNA species was confirmed by agarose gel electrophoresis in the presence of chloroquine, a DNA intercalator that reduces the negative supercoiling. As, expected, the gel mobility of the nicked monomer was unchanged whereas the gel mobility of the negatively supercoiled monomer was reduced upon chloroquine intercalation (Fig 2.3C).

DNA supercoiling induced during DNA replication can be relaxed by both type I and type II topoisomerases, but only type II topoisomerases can decatenate daughter molecules (Wang, 2002). To test whether the generation of plasmid monomers in our system was dependent on Top2 present in the S-phase extract, we supplemented the extract with the Topo II inhibitor ICRF-193. While the total DNA synthesis was largely unaffected by ICRF-193, native gel electrophoresis of the replication products revealed a marked increase in HMW species and a concomitant loss of plasmid monomers (Fig 2.4A). Replication products obtained in the presence of ICRF-193 were predominantly close to full-length single-stranded nascent strands (ssl, Fig 2.4A, lane 4) whereas the generation of the faster migrating circular closed duplex DNA (ccc) was reduced as revealed by alkaline agarose gel electrophoresis. The identities of the slower and faster migrating bands were confirmed by the sensitivity of slower migrating band to Exonuclease III (Exo III) treatment (Fig 2.4B). Similar products were also observed previously during SV40 DNA replication *in vitro* (Ishimi et al., 1992). This data indicated

Figure 2.4 Characterization of the products from the replication reaction

(A) Replication in S-phase extract containing 1.25% DMSO (lanes 1,3) and 177uM ICRF-193 (lanes 2,4). Replication products were analyzed by autoradiography after native (lanes 1,2) or alkaline (lanes 3,4) agarose gel electrophoresis. Histogram on the left shows total ^{32}P-dCTP incorporation. ssl: single-stranded linear, ccc: covalently closed circular.

(B) Replication reaction were carried out as in Fig 3A, DNA isolated and either mock-treated (lane1) or treated with exonuclease III (Exo III, lane 2) prior to alkaline agarose gel electrophoresis.

(C) DNA isolated from replication of pARS1 in the presence of 177mM ICRF-193 was incubated with 4 units of human topoisomerase IIα (hTopoIIα) and analyzed by native gel electrophoresis

(D) DNA isolated from replication of pARS1 in the presence of 177mM ACRF-193 was incubated with Exonuclease III (Exo III) and analyzed by native gel electrophoresis.

(E) Native agarose gel electrophoresis of the sample as described in B.

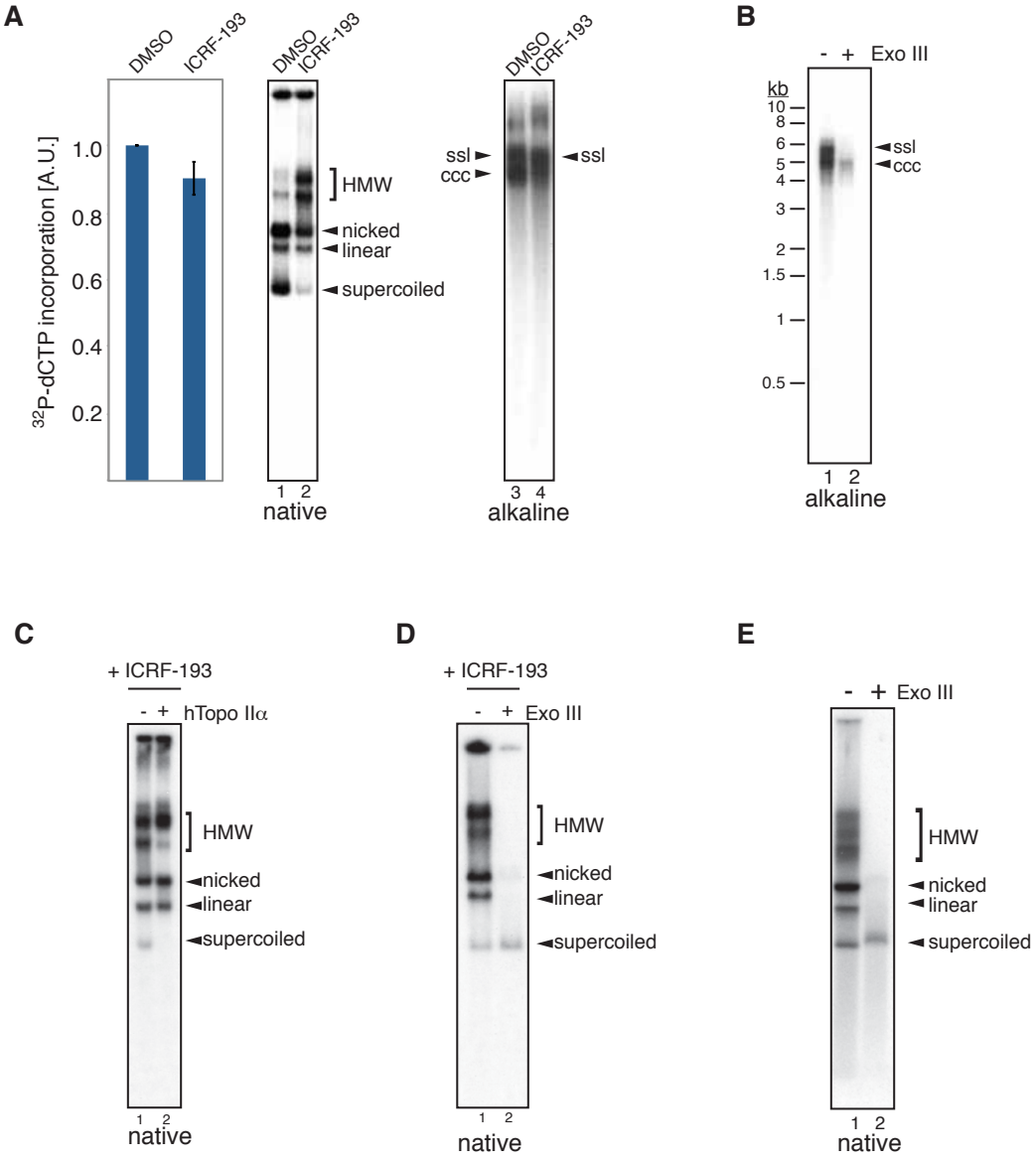
A
DMSO
ICRF-193
32P-dCTP incorporation [A.U.]
1.0
0.8
0.6
0.4
0.2
DMSO
ICRF-193
HMW
nicked
linear
supercoiled
1 2
native
DMSO
ICRF-193
ssl
ccc
ssl
3 4
alkaline
B
- + Exo III
kb
10
8
6
5
4
3
2
1.5
1
0.5
ssl
ccc
1 2
alkaline
C
+ ICRF-193
- + hTopo IIα
HMW
nicked
linear
supercoiled
1 2
native
D
+ ICRF-193
- + Exo III
HMW
nicked
linear
supercoiled
1 2
native
E
- + Exo III
HMW
nicked
linear
supercoiled
1 2
native

that Topo II inhibition by ICRF-193 blocks completion of DNA replication at a late step, as has also been seen in Xenopus extracts (Cuvier et al., 2008). A fraction of the HMW molecules was sensitive to treatment with purified human TopoIIα, implying that HMW species consist of catenated daughter molecules (Fig 2.4C). Most of the HMW molecules also appear to contain a free 3' end, as demonstrated by the sensitivity to Exo III (Fig 2.4D). This Exo III sensitivity of the high molecular weight products was independent of ICRF-193 treatment (Fig 2.4E). These data combined suggest that the HMW replication products contain a mixture of replication intermediates, such as precatenanes and partially nicked catenated dimers, and that decatenation of fully replicated plasmid daughters is catalyzed by Top2 in the extract. From this it follows that our system supports the initiation, elongation and termination stages of DNA replication.

Replication of plasmid DNA immobilized on beads yields predominantly shorter than full-length nascent strands (Fig 2.2C, lane 5). In striking contrast, the majority of the replication product obtained with free plasmid DNA template was full length to close to full length (Fig 2.4A, lane 1). To exclude the possibility that full-length ^{32}P-labeled DNA strands were the result of gap-filling synthesis, we probed the newly synthesized DNA with DpnI. This enzyme efficiently cleaves the DNA sequence GATC when fully methylated (GA^{m}TC), but shows reduced activity towards hemimethylated DNA, and does not cleave unmethylated DNA. Plasmid pARS1 consists of 23 copies of GATC recognition sequence. Sensitivity of the assay was increased by linearizing the DNA with EcoRI thus collapsing the distribution of topoisomers typically formed during the incubation with S-phase extract into a single band of linear DNA. Total DNA was detected by ethidium bromide staining whereas the

Figure 2.5 *In vitro* replication of free plasmid undergoes single round of replication

(A) DNA isolated from replication reaction was either mock-treated (lanes 1, 4) or treated with 0.4 units (lanes 2,5) or 2 units of DpnI after linearizing with EcoR1 to increase sensitivity, and analyzed by native agarose gel electrophoresis. An ethidum bromide stain of the gel is shown on the left (lanes 1-3), the corresponding autoradiograph is depicted on the right (lanes 4-6).

(B) DNA isolated from Replication products were linearized with restriction enzyme as indicated on top after linearization with NdeI to increase sensitivity and analyzed by native gel electrophoresis. . An ethidum bromide stain of the gel is shown on the left (lanes 1-3), the corresponding autoradiograph is depicted on the right (lanes 4-6).

(C) & (D) ^{32}P-dCTP is incorporated throughout the plasmid. (C) Map of pARS1; restriction sites used for analysis and sizes of resulting restriction fragments A-D are indicated. (D) Left: DNA isolated from a pARS1 replication reaction was isolated and analyzed by native agarose gel-electrophoresis and autoradiography before (lane1) and after (lane2) restriction digestion. Arrows indicate the positions of restriction fragment labeled A-D as in (C). Right: ^{32}P-dCTP incorporation into restriction fragments A-D was quantitated by phosphorimaging and plotted as % of total incorporation (blue bars); G/C content of each fragment was plotted as % of total G/C content of pARS1 (red bars).

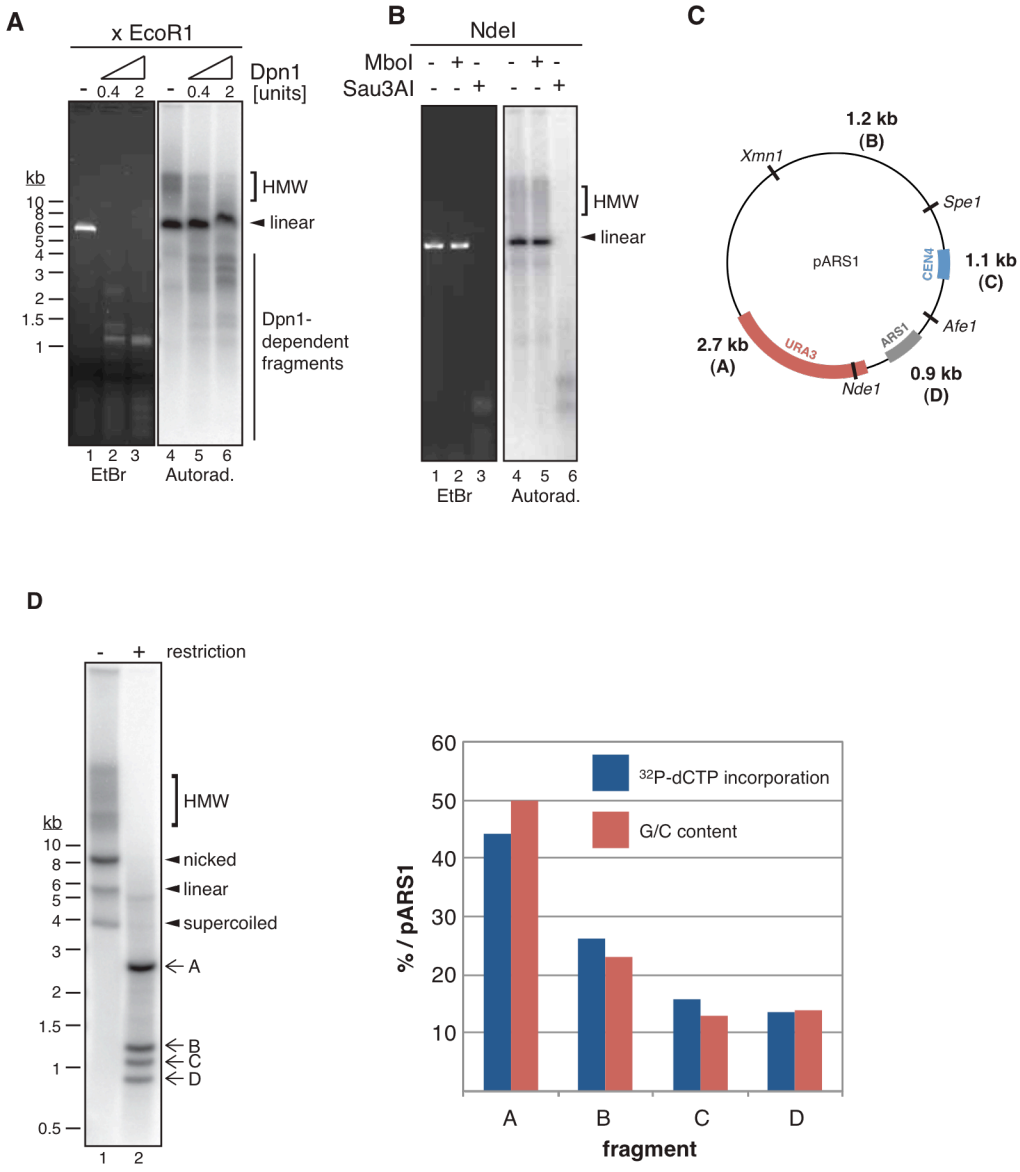
A
x EcoR1
Dpn1 [units]
- 0.4 2 - 0.4 2
kb
10
8
6
5
4
3
2
1.5
1
HMW
linear
Dpn1-dependent fragments
1 2 3 4 5 6
EtBr
Autorad.
B
NdeI
MboI - + - - + -
Sau3AI - - + - - +
HMW
linear
1 2 3 4 5 6
EtBr
Autorad.
C
1.2 kb (B)
Xmn1
Spe1
pARS1
CEN4
1.1 kb (C)
Afe1
ARS1
URA3
2.7 kb (A)
Nde1
0.9 kb (D)
D
- + restriction
kb
10
8
6
5
4
3
2
1.5
1
0.5
HMW
nicked
linear
supercoiled
A
B
C
D
1 2
60
50
40
30
20
10
% / pARS1
32P-dCTP incorporation
G/C content
A
B
C
D
fragment

replicated DNA molecule was detected by autoradiography. As can be seen in Fig 2.5A, the majority of fully methylated input linearized DNA (isolated from a *dam*$^{+}$ *E. coli* strain) was digested at the lowest concentration of DpnI (lanes1-3), whereas replicated plasmid DNA was resistant to cleavage under these conditions (lanes 4-6). Replicated DNA, is also resistant to cleavage by MboI (Fig 2.5B), recognizing the identical sequence as DpnI, but only when the DNA sequence is unmethylated on both strands. Product from the replication reaction, however, was sensitive to Sau3AI (Fig 2.5), which cleaves the same sequence as DpnI and MboI but is insensitive to DNA methylation state. Together, these data point that DNA molecules are replicated in a semi-conservative fashion in our system and that the plasmid DNA undergoes a single round of replication *in vitro.* Additionally, the products from replication reaction were digested with four unique restriction enzymes to generate four fragments of known length from the input plasmid (Fig 2.5C) and the proportion of [α-^{32}P]dCTP incorporated in each fragment was compared to the relative G/C content of the fragment. The continuous strand synthesis implied by the observation above is supported by the data that [α-^{32}P]dCTP is incorporated along the length of the plasmid DNA (Fig 2.5D).

Plasmid replication in solution exhibits hallmarks of cellular DNA replication initiation

The approach as described in Fig 2.3A, where pre-RC components are mixed with S-phase extracts raises the possibility that purified and endogenous pre-RC components interacted in the S-phase extract to form functional pre-RCs. In addition, we observed that closed circular plasmids underwent replication-independent nicking when incubated with S-phase

Figure 2.6 Protein requirements for plasmid replication *in vitro*

(A) Time-course analysis of pARS1 replication in the absence (lanes 1-4) or presence (lanes 5-8) of Cdc6 during the pre-RC assembly reaction were analyzed by native agarose gel electrophoresis; total [α-^{32}P]dCTP incorporation is plotted on the right.

(B) Replication reactions were carried out in the absence or presence of factors indicated on top of each panel. Replication products were analyzed by native (lanes 1-5) or alkaline (lanes 6-10) agarose gel electrophoresis and autoradiography; total [α-^{32}P]dCTP incorporation is plotted on the left.

(C) *In vitro* replication reaction with Cdt1•Mcm2-7 absent (lane 1) or present (lane 2) during pre-RC assembly were analyzed by native agarose gel electrophoresis and autoradiography; total [α-^{32}P]dCTP incorporation is plotted on the left.

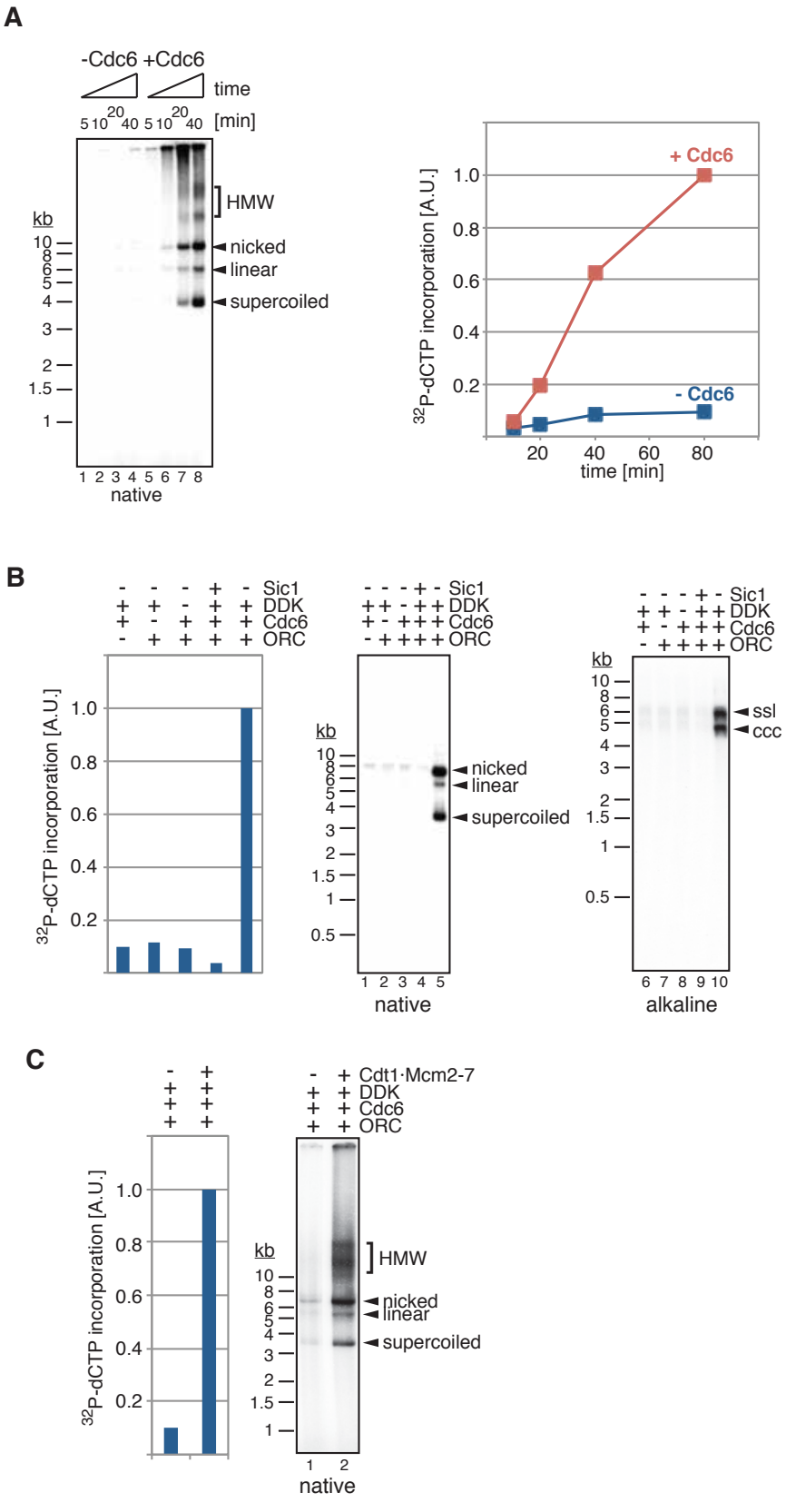
A
-Cdc6 +Cdc6
time
5 10 20 40 5 10 20 40 [min]
kb
10
8
6
5
4
3
2
1.5
1
HMW
nicked
linear
supercoiled
1 2 3 4 5 6 7 8
native
+ Cdc6
- Cdc6
32P-dCTP incorporation [A.U.]
1.0
0.8
0.6
0.4
0.2
20 40 60 80
time [min]
B
Sic1
DDK
Cdc6
ORC
32P-dCTP incorporation [A.U.]
1.0
0.8
0.6
0.4
0.2
kb
10
8
6
5
4
3
2
1.5
1
0.5
nicked
linear
supercoiled
1 2 3 4 5
native
ssI
ccc
6 7 8 9 10
alkaline
C
Cdt1·Mcm2-7
DDK
Cdc6
ORC
32P-dCTP incorporation [A.U.]
1.0
0.8
0.6
0.4
0.2
kb
10
8
6
5
4
3
2
1.5
1
HMW
nicked
linear
supercoiled
1 2
native

extract, which could theoretically provide and entry site for a DNA polymerase to perform strand displacement DNA synthesis. To exclude any potential origin independent mechanisms of DNA replication initiation in the S-phase extract, we re-evaluated the contribution of replication initiation factors towards DNA synthesis in our modified system. In the soluble system, DNA synthesis was dependent on purified Cdc6 (Fig 2.6A), ORC (Fig 2.6B, lanes 1, 6) and Cdt1•Mcm2-7 (Fig 2.6C), indicating that reconstituted pre-RCs are essential in this system and that purified pre- RC components do not form functional pre-RCs with endogenous pre-RC components that may be present in the S-phase extract. This may be expected given all budding yeast pre-RC components are subject to CDK dependent inhibition in S phase (Diffley, 2011). Moreover, DNA replication was dependent on DDK as well as CDK (Fig 2.6B). DNA synthesis in our system also required Mcm10 since the immunodepletion of Mcm10 from the S-phase extract significantly inhibited [α-^{32}P]dCTP (Fig 2.7B). This inhibition could be rescued by the re-addition of purified recombinant Mcm10 to the extract. Finally, DNA synthesis exhibited a pronounced sensitivity to aphidicolin (Fig 2.7A), confirming a role for replicative DNA polymerases during plasmid replication *in vitro*. Taken together, these data demonstrate that plasmid replication in solution described here exhibits hallmarks of cellular DNA replication initiation

In bacteria, negative supercoiling of the DNA template is essential for DNA duplex opening by the initiator, DnaA (Bramhill and Kornberg, 1988). We tested if the topology of the DNA template had any impact on DNA synthesis in our system. We found that negatively supercoiled, relaxed or linear plasmid forms were replicated with comparable efficiencies, indicating that negative supercoiling is not essential for functional pre-RC formation and replication

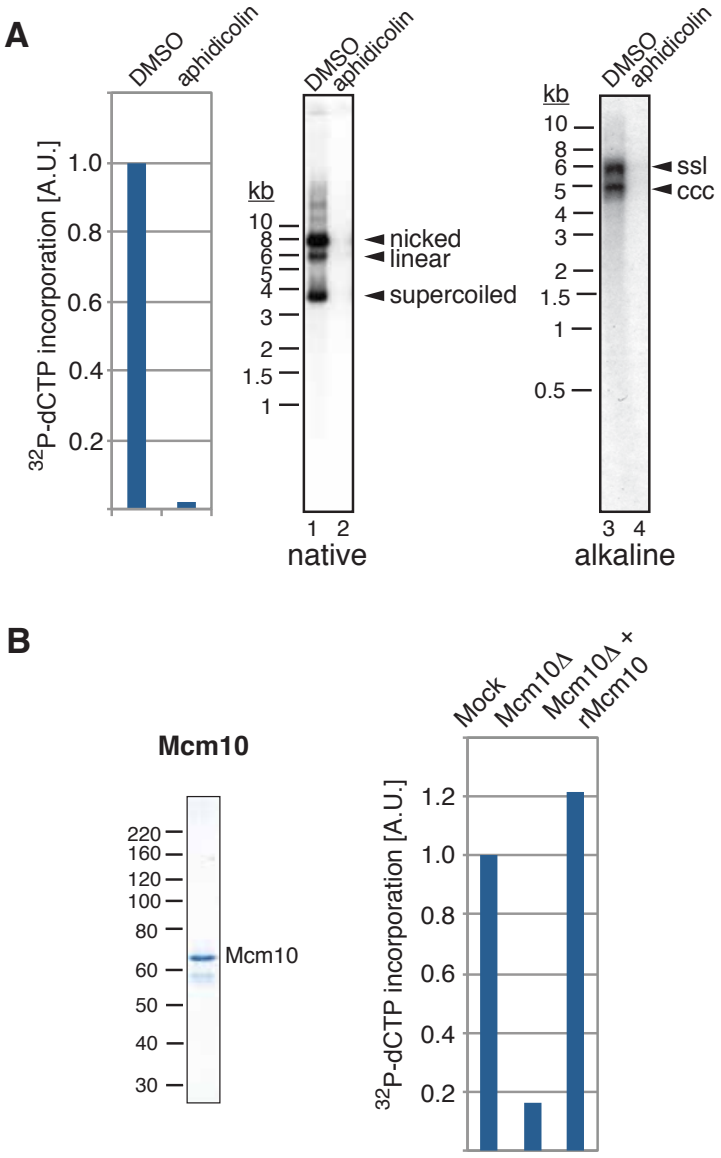

Figure 2.7 DNA replication *in vitro* is dependent on replicative DNA polymerases and Mcm10

(A) *In vitro* replication was performed in the presence of 1.25% DMSO (lanes 1, 3) or 37 μM aphidicolin (lanes 2, 4). Products were analyzed by native (lanes 1-2) or alkaline (lanes 3-4) gel electrophoresis and autoradiography. Total ^{32}P-dCTP incorporation is plotted on the left.

(B) Left: Purified Mcm10 protein was separated by SDS-PAGE and stained with Coomassie. Size markers (kDa) is on left of the gel. Right: ^{32}P-dCTP incorporation was monitored in mock-depleted, Mcm10-myc-depleted, or Mcm10-myc-depleted extract supplemented with purified recombinant Mcm10.

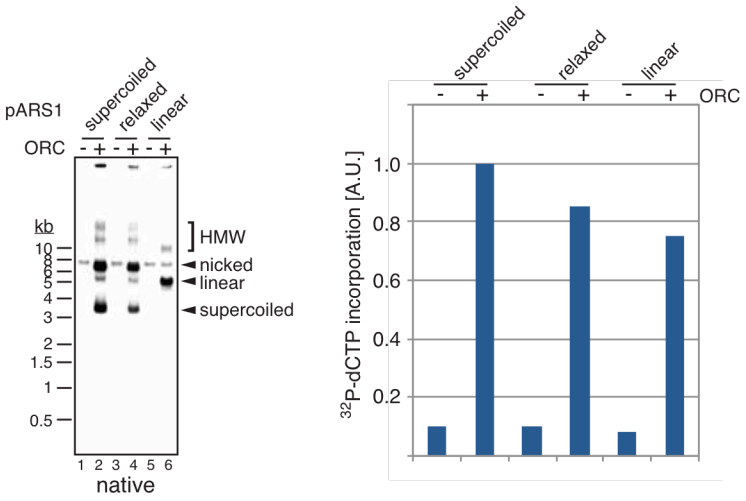

Figure 2.8 Negative supercoiling is not essential for replication initiation *in vitro* pARS1 template that was negatively supercoiled (lanes 1,2), relaxed with vaccinia topoisomerase (lanes 3.4), or linearized with SmaI (lanes 5.6) was subjected to *in vitro* replication in the absence or presence of purified ORC as indicated; replication products were analyzed by native agarose gel electrophoresis and autoradiography (left panel). hHstogram of total 32-P dCTP incorporation was determined by phosphorimager analysis. (Right panel).

initiation *in vitro,* (Fig 2.8) as has been seen in the extract based system previously (Heller et al., 2011).

Discussion

We have demonstrated that pre-RCs reconstituted with purified budding yeast proteins support cell-free DNA replication. Replication of plasmid DNA in our system results in the generation of covalently closed circular daughter molecules, indicating that the system recapitulates all stages of DNA replication, including initiation, elongation, and termination. However, only a

small fraction of input DNA molecules seem to be replicated in this system since majority of DNA, post replication reaction seem to be sensitive to Dpn1, an enzymes that cleaves fully methylated input plasmid. Since elongation seems to be efficient once initiation has occurred, as replicated DNA molecules are mostly full-length, we presume that a step preceding elongation is limiting overall levels of replication. This notion is also supported by the observation that replication products began to appear only after a lag phase of 10-20 min.

DNA replication in this system requires the preassembly of the pre-RCs and exhibits the hallmark of cellular DNA replication initiation upon S-phase extract addition. Mcm2-7 double hexamers loaded around double-stranded DNA are, therefore, true intermediates of the eukaryotic DNA replication initiation reaction. Thus, activation of the Mcm2-7 helicase is predicted to require the transient opening of the topologically closed Mcm2-7 rings present in the double hexamer and specific extrusion of the lagging strand template in order to form active CMG helicase complexes bound around the leading-strand template (Fu et al., 2011; Moyer et al., 2006). This raises a very interesting question about how the DNA duplex might be opened at eukaryotic origins. In *E. coli*, negative supercoiling of the DNA template is essential for origin unwinding by the initiator, DnaA. In contrast, as demonstrated here and by others previously (Heller et al., 2011), negative supercoiling of the template DNA is not required for replication initiation in budding yeast. DNA supercoiling also seems to be dispensable for DNA replication in *Xenopus* extracts (Yardimci et al., 2010). Additionally, despite the structural homology of AAA+ subunits of ORC to DnaA (Clarey et al., 2006; Erzberger and Berger, 2006; Speck et al., 2005), ORC does not exhibit DNA melting activity, which agrees

with Mcm2-7 being loaded around double stranded DNA. Our finding that ORC can be eluted from the DNA after Mcm2-7 loading without disrupting the replication competence of the loaded Mcm2-7 double hexamers suggests that ORC is also expendable for duplex opening at a step after the loading of Mcm2-7 double hexamer. Therefore, initial origin unwinding in eukaryotes is most likely mediated in a Mcm2-7 dependent mechanism.

The intricacy of the Mcm2-7 remodeling reaction during the origin activation needs to be coordinated with the progression of S-phase to prevent the generation of vulnerable single-stranded DNA in the absence DNA synthesis. This may explain the involvement of numerous initiation factors for Mcm2-7 activation. We demonstrate that DDK can be washed away after phosphorylation of purified Mcm2-7 complexes supporting the notion that Mcm2-7 are the only essential targets for DDK during origin activation. We find that DDK and CDK promote the ordered recruitment of the pre-IC components Sld3, Cdc45, Dpb11 and Sld2 to reconstituted pre-RCs in a pattern that mimics pre-IC assembly *in vivo*, suggesting that reconstituted pre-RCs initiate the DNA replication *in vitro* by a physiological mechanism.

Budding yeast Mcm10 appears to play a late role in Mcm2-7 helicase activation after pre-IC formation and CMG assembly (Ricke and Bielinsky, 2004; van Deursen et al., 2012; Watase et al., 2012). In support of this notion, we find that pre-IC assembly *in vitro* occurs in the absence of Mcm10. There is some controversy regarding the timing of budding yeast Mcm10 association with the pre-RC, with some reports suggesting an association of Mcm10 with pre-RCs as early as G1-phase (Ricke and Bielinsky, 2004; van Deursen et al., 2012), and others suggesting a pre-IC-dependent recruitment of Mcm10 to origins (Heller et al., 2011; Watase et al., 2012). Our observation that stable

Mcm10 association with reconstituted pre-RC in S-phase extract is dependent on both DDK and CDK is consistent with the latter studies. The discrepancies in the observed Mcm10 association timing between multiple reports may reflect that recruitment of Mcm10 to the origin is influenced by the experimental conditions, or that the stability of Mcm10 binding to Mcm2-7 increases upon pre-IC formation.

An analogous cell-free replication system for budding yeast has also been reported (On et al., 2014) where mass spectrometry based proteomics approach was used to screen for proteins that bound to pre-RCs in a DDK dependent fashion. This approach led the authors to conclude that most or all of the core proteins involved in DNA replication initiation and elongation have been previously reported. This information, combined with our data that pre-RCs reconstituted with purified proteins can support regulated DNA replication sets up a stage to potentially reconstitute complete DNA replication with a set of purified proteins

Materials and methods

Proteins

Unless stated otherwise, all the proteins purified from budding yeast used the overexpression strain. To obtain an overexpression strain, the protein of interest was cloned into a vector consisting of bidirectional inducible Gal1-10 promoter into W303a (see the table below). Gal4 is a positive regulator of GAL genes in response to galactose and therefore overexpressed as well. ORC and Cdt1•Mcm2-7 were purified as previously described (Frigola et al., 2013).

Purification of Cdc6 from bacteria

pET15b/His-Cdc6 was transformed into BL21 DE3 Codon+ RIL cells. 3 L of cells were grown at 37 °C to a density of OD_{600} = 0.5-0.8. Cells were chilled on ice, supplemented with 2 % ethanol, and induced with 1mM IPTG overnight at 17 °C. Cells were harvested at 5000 rpm in a SLA-3000 rotor (Sorvall) for 10 minutes, washed once in PBS 1X and stored at −80°C. Cells were resuspended in buffer C1 (25 mM Hepes-KOH pH7.6 / 0.4 M KCl / 0.05% NP-40 / 5 mM $Mg(OAc)_2$ / 1 mM ATP / 10 % glycerol) / 10 mM imidazole / 2 mM β-mercaptoethanol (βMe) / protease inhibitors (Roche, complete protease inhibitor coktail), supplemented with 1mg/mL of lysozyme and incubated for 30 minutes at 4°C with agitation. The lysate was sonicated on ice and centrifuged for 45 minutes at 18,000 rpm using an SS-34 rotor (Sorvall). The soluble phase was subjected to Ni-chelate chromatography in buffer C1 and bound protein eluted from the resin using a gradient of 0.025 – 1M imidazole. His-Cdc6-containing fractions were pooled, concentrated using Microcon Ultracel 10,000 MWCO (Millipore), and fractionated by gel- filtration over a 120mL Superdex 200 HiLoad 16/60 (GE Healthcare) column equilibrated in buffer C1 / 2mM βMe. Peak fractions were pooled, dialyzed against buffer C2 (25 mM Hepes-KOH pH7.6 / 0.05 % NP-40/5 mM $Mg(OAc)_2$ /1mMATP/10%glycerol)/0.15MKCl/2mMβMe, and subjected to fractionation over a 1 mL MonoQ 5/50 GL column (GE Healthcare) column equilibrated in buffer C2 / 0.15 M KCl. His-Cdc6 was recovered in the flow-through and subjected to fractionation over a 1 mL MonoS 5/50 GL column (GE Healthcare) using an elution gradient of 0.15 – 0.5 M KCl over 20 column

volumes. Peak fractions containing His-Cdc6 were pooled, dialyzed against buffer C2 / 0.3 M K-glutamate and stored in aliquots. 3 to 6 mg of purified His-Cdc6 was obtained from a 3L culture.

Purification of DDK from yeast

50 L of cells (strain YMC5) were grown in YP-raffinose (2 %) at 30 °C to a cell density of $2x10^7$ cells/mL. Protein expression was then induced by adding galactose (2 %) for 3 to 4 hours at 30°C. Cells were harvested, washed twice with ice-cold 25 mM Hepes-KOH pH 7.6 / 1 M sorbitol, then washed once with buffer D (45 mM Hepes-KOH pH 7.6 / 0.05 % NP-40 / 10 % glycerol) / 0.1 M NaCl. The pellet was resuspended in 0.5 volumes of buffer D / 0.1 M NaCl / 2 mM βMe / protease inhibitors, and frozen dropwise in liquid nitrogen. Frozen drops of cells were crushed using a freezer mill (SPEX CertiPrep 6850 Freezer/Mill) with 6 cycles of 2 minutes crushing at a rate of 15 impacts per second. Frozen cell powder was thawed at room temperature, resuspended with 1 volume of buffer D / 0.1 M NaCl / 2 mM βMe / protease inhibitors, the concentration of NaCl was adjusted to 0.3 M, and the suspension was centrifuged for one hour at 47,500 rpm using a T-865 rotor (Thermo Scientific). The clear soluble phase was recovered and subjected to IgG immunoprecipitation by adding 0.5mL of packed IgG Sepharose 6 Fast Flow (GE Healthcare) per 50 mL of extract. After 4 hours at 4°C the beads were collected and washed with 10 bed volumes of buffer D / 0.3 M NaCl / 2 mM βMe. Elution of the captured material was carried out overnight at 4°C by resuspending the beads in 1 bed volume of buffer D / 0.3 M NaCl / 2 mM βMe and adding an equal amount of TEV protease. On the next day, the flow-through was recovered and concentrated using a Microcon Ultracel 10,000

MWCO, and treated with Lambda Protein Phosphatase (NEB) by bringing the $MnCl_2$ concentration to 1mM final and adding 10U of λPPase per 20μL of sample and incubating the reaction for 1h at 30°C. Fractionation by gel filtration was then performed over a 120 mL Superdex 200 HiLoad 16/60 equilibrated in buffer D / 0.3 M NaCl / 2 mM βMe. Peak fractions were pooled, dialyzed against buffer D / 0.15 M NaCl / 2 mM βMe and subjected to fractionation over a 1 mL MonoQ 5/50 GL column using an elution gradient of 0.15 – 0.5 M NaCl over 20 column volumes. Peak fractions were pooled and stored in aliquots. 0.5 to 1 mg of purified Cdc7•Dbf4 complex was recovered from a 50L culture.

Purification of Mcm10 from bacteria

The MCM10 open reading frame was cloned into pET15b to yield pET15b/Mcm10. pET15b/Mcm10 was transformed into BL21 DE3 Codon+ RIL cells. 1 L of cells was grown at 37°C to a density of OD_{600}= 0.6. Cells were chilled on ice and induced with 1 mM IPTG for 3 hr at 30°C. Cells were harvested at 5000 rpm in a SLA-3000 rotor (Sorvall) for 10 minutes, washed once in PBS and stored at −80°C. Cells were resuspended in buffer C (50 mM Tris pH7.5 / 1 mM EDTA / 0.05 % NP-40 / 10% glycerol) / 300 mM NaCl / 2 mM β-mercaptoethanol / protease inhibitors (Roche, complete protease inhibitor coktail), supplemented with 1 mg/mL of lysozyme and incubated for 30 minutes at 4°C with agitation. The lysate was sonicated on ice and centrifuged for 20 minutes at 18,000rpm using an SS- 34 rotor (Sorvall). Ammonium sulfate was added to 30% saturation to the soluble phase and the precipitate was resuspended in buffer C / 300 mM NaCl / 10 mM imidazole / 2 mM β-mercaptoethanol. The extract was incubated with Ni-NTA agarose

beads for 2 hr at 4°C and the bound proteins were eluted with 10 column volumes of buffer C / 200 mM imidazole. His-Mcm10 containing fractions were pooled and dialyzed against buffer D (25 mM Hepes-KOH pH7.6 / 0.02 % NP40 / 10 % glycerol) / 100 mM NaCl and subjected to fractionation over a 1 mL MonoS 5/50 GL column (GE Healthcare) using an elution gradient of 0.1-1 M NaCl. Peak fractions were pooled and the His-tag was cleaved off using thrombin at the concentration of 0.1U/ug of Mcm10. The product from the cleavage reaction was fractionated by gel- filtration over a 120 mL Superdex 200 HiLoad 16/60 (GE Healthcare) column equilibrated in buffer D / 300mM NaCl / 2mM β-mercaptoethanol. Peak fractions were pooled, and the salt concentration was reduced by dialysis against buffer D / 150 mM NaCl. Finally, the sample was subjected to fractionation over a 1 mL MonoS 5/50 GL column (GE Healthcare) using an elution gradient of 0.15-1 M NaCl in buffer D. Peak fractions containing Mcm10 were mixed and dialyzed against buffer D / 300 mM K-glutamate, and aliquots snap-frozen in liquid nitrogen and stored at −80°C.

Purification of Sic1 from bacteria

Sic1 was expressed as a 6x His-tag fusion protein in BL21 DE3 Codon+ RIL cells. Cells were grown to an OD_{600}= 0.6 and induced with 0.1 mM IPTG at 37°C for 3 hours. Cells were harvested by centrifugation, washed once with PBS, and lysed by sonication in 50 mM Tris-HCl pH 8.0 / 300 mM NaCl / 20 mM imidazole / 1% NP-40 / 1 mM PMSF. Extract was clarified by centrifugation and rotated with Ni- NTA agarose for 2 hours at 4°C. Ni-NTA resin was recovered by gentle centrifugation, washed with 50 mM Tris-HCl / 300 mM NaCl / 20 mM imidazole, and bound proteins were eluted with 50 mM

Tris-HCl/ 300 mM NaCl / 400 mM imidazole. Peak fractions were pooled and fractionated by gel-filtration on a Superdex 200 HR 10/30 in 45 mM Hepes-KOH pH 7.6 / 300 mM KCl / 1 mM EDTA / 1 mM EGTA / 10% glycerol / 1 mM DTT. Peak fractions off the gel-filtration were pooled, dialyzed against 45 mM Hepes- KOH pH 7.6/ 100 mM KCl / 1 mM EDTA / 1 mM EGTA / 10% glycerol / 1 mM DTT, and fractionated on MonoQ ion-exchange resin using an salt gradient elution from 0.1 M to 1 M KCl over 20 column volumes.

Topoisomerases

Vaccinia topoisomerase was a kind gift of Dr. Stewart Shuman (MSKCC). Human Topoisomerase II α was purchased from Sigma-Aldrich.

DNA templates

pARS1 used in this chapter of the thesis is pARS/WTA (Marahrens & Stillman, 1992). Plasmids used in the soluble reaction were purified from *E. coli* using Plasmid Maxipre Kit (QIAGEN) in accordance with manufacturer's instructions. For the reactions using pARS1 coupled to magnetic beads, pARS1 was randomly biotinylated using the PHOTOPROBE (Long Arm) Biotin Kit (Vector Laboratories) according to manufacturer's guide. Following biotinylation, DNA was incubated with streptavidin-dynabeads() overnight and unbound DNA was washed away.

S-phase extract

S-phase extract used in this chapter of the thesis was prepared as described previously (Heller et al., 2011).

Replication assay

The incubation steps during the replication reaction were performed with agitation in case of immobilized template and without agitation when template used was free in solution. Pre-RCs were reconstituted with 50 nM ORC, 50 nM Cdc6, and 250 nM Cdt1·Mcm2-7, for 30 min at 30°C on 5 nM plasmid DNA (either coupled to beads or free) in 40 µl of 25 mM Hepes-KOH pH 7.6, 0.12 M KOAc, 10 mM $Mg(OAc)_2$, 0.02% NP-40, 5% glycerol, 1 mM DTT, and 5 mM ATP. Purified DDK was then added into the pre-RC assembly reaction to the final concentration of 50 nM. Incubation was continued for 20 min, before adding 40 µl of S-phase extract supplemented with 5 mM ATP, 0.1 mM dNTPs (dATP/dTTP/dGTP) each, 0.2 mM NTPs (UTP/GTP/CTP) each, 10 µCi of [α-^{32}P]dCTP (3,000 Ci/mmol, Perkin Elmer), 40 mM creatine phosphate (Roche), 0.01 mg/ml creatine kinase (Roche), for 45 min at 30°C. Reactions were stopped by adding 15 mM EDTA, 0.2% SDS, and 20 µg of proteinase K, and incubation for 30 min at 37°C. DNA was isolated by phenol/chloroform extraction and ethanol precipitation, and fractionated on native (1 × TAE) or alkaline (30 mM NaOH, 2 mM EDTA) 0.8% agarose gels. Gels were dried onto Whatman paper and analyzed by phosphorimaging.

Pre-IC assembly

To monitor pre-IC assembly, replication reactions were carried out on plasmid DNA immobilized on paramagnetic beads as described in Materials and Methods, including 0.1 mM dCTP instead of [α-^{32}P]dCTP. After 40 min incubation in the S phase extract, beads were recovered using a magnetic rack, washed twice with 0.4 ml of 25 mM Hepes-KOH pH 7.6 / 0.3 M K-glutamate / 5 mM $Mg(OAc)_2$ / 0.02 % NP-40 / 10 % glycerol / 1 mM EDTA / 1

mM EGTA / 1 mM DTT, boiled in SDS sample buffer, and analyzed by SDS-PAGE and Western blotting.

Mcm10 depletion and add-back

7.5µg monoclonal myc-antibody was bound to Dynabead protein G (10 µl) for 1 hr @30°C. Beads thus coupled to myc-antibody or uncoupled beads (mock) were rotated for depletion with 100µl S-phase extract prepared from YSD8 for 1hr @4°C immediately before usage of the extract in the *in vitro* replication assay. To rescue Mcm10 depletion, Mcm10-depleted extract was supplemented with 100 fmol of purified recombinant Mcm10.

Antibodies

Monoclonal antibodies SB49 (Orc6) and 9H8/5 (Cdc6), and polyclonal antibodies against Dpb11, Sld2, and Sld3 were a gift from John Diffley (CRUK). Polyclonal Cdc45 antibody was a gift from Bruce Stillman (CSHL). Polyclonal RPA antibody was purchased from Agrisera (AS07 214). Goat polyclonal antibodies against Mcm2 (sc-6680), Mcm7 (sc-6688), and Mcm5 (sc-6687) were purchased from Santa Cruz Biotechnology. Monoclonal antibody 9E10 (c-myc) was purchased from Clontech (631206).

Table 2.1. List of yeast strains used in chapter two

Name	Genotype
W303-1a	*MATa ade2-1 ura3-1 his3-11,15 trp1-1 leu2-3,112 can1-100*
YDR89	*W303-1a cdc7-4 **Δ**pep4::kanMX **Δ**bar1::hphNT1 ura3-1::GALp-SLD3(URA3) trp1-1::GALp-CDC45(TRP1) leu2-3,112::GALp-SLD2/DPB11(LEU2)*
YSD8	*YDR89 MCM10::MCM10-9myc(natNT2)*
YMC5	*W303-1a **Δ**pep4::hphNT1 his3-11,15::GALp-GAL4(HIS3) leu-3::GALp-DBF4-TAPtcp/CDC7-myc(LEU2/TRP1)*

CHAPTER THREE

CHROMATIN CONSTRAINS THE INITIATION AND ELONGATION OF DNA REPLICATION*

Introduction

Biochemical reconstitution approaches in bacterial and viral systems have been essential for elucidating mechanistic principles of DNA replication. In contrast, a reconstituted system to study eukaryotic chromosomal DNA replication, which exhibits additional levels of complexity that derive from the constraints of the cell cycle and the packaging of chromosomal DNA into chromatin, has not yet been available.

A multi-step mechanism ensures that the activity of the numerous replication origins distributed along the length of each chromosome is coordinated with the cell cycle (Bell and Labib, 2016). In the first step, which can only occur at the end of mitosis and during G1 phase, (i.e. when cyclin-dependent kinase (CDK) activity is low, the origin recognition complex (ORC)), Cdc6, and Cdt1 load the replicative DNA helicase, Mcm2-7, in inactive double-hexameric form around DNA at the origin. Origin activation in the subsequent S phase entails the activation of the Mcm2-7 helicase and concurrent assembly of two oppositely oriented replisomes around the forks flanking the replication bubble. In a process that involves the initiation factors Sld3·Sld7, Dpb11, Sld2, and DNA polymerase ε (Pol ε), two cell cycle-regulated protein kinases, Cdc7·Dbf4 (DDK) and CDK, control the activation of the Mcm2-7

** Devbhandari, S., Jiang, J. Kumar, C., Whitehouse I., and Remus D. (2017). Chromatin Constrains the Initiation and Elongation of DNA Replication. Molecular cell 65, 131-141.*

DNA helicase during origin firing by promoting the assembly of the essential helicase subunits Cdc45 and GINS into the CMG (Cdc45-MCM-GINS) DNA helicase complex. Activation of the CMG depends on Mcm10, and is thought to induce origin unwinding, which promotes subsequent recruitment of the single-stranded DNA binding protein, RPA, and DNA polymerase α-primase (Pol α). Pol α primes DNA synthesis by the replicative DNA polymerases, Pol δ and Pol ε (Kunkel and Burgers, 2008). Although it is generally assumed that Pol ε synthesizes the leading strand, and Pol δ the lagging strand, this strict strand assignment is still a matter of debate (Stillman, 2015), and the ability of cells to complete DNA replication in the absence of DNA synthesis by Pol ε likely indicates that the strand specificity of DNA polymerases is to some degree flexible (Dua et al., 1999; Kesti et al., 1999). DNA replication terminates when two opposing forks emanating from adjacent origins meet, which leads to the ubiquitin-dependent removal of the CMG from chromatin (Bell and Labib, 2016).

The antiparallel configuration of the parental DNA duplex strands dictates that one daughter strand, the lagging strand, be replicated discontinuously in the form of short Okazaki fragments, while the other strand, the leading strand, can be synthesized continuously. Pol α primes DNA synthesis by synthesizing RNA/DNA hybrid primers of approximately 30 nt length on the template strands, necessitating the removal of the RNA from the 5' ends of Okazaki fragments prior to ligation by DNA ligase. Okazaki fragment processing occurs via concerted strand displacement by Pol δ and nucleolytic resection of the resulting 5' flap by the structure-specific endonuclease Fen1 (Balakrishnan and Bambara, 2013). How Okazaki fragment synthesis is regulated is not clear, but the nucleosomal repeat of nascent chromatin behind

the replication fork has been implicated in determining Okazaki fragment length *in vivo*, indicating that lagging strand synthesis and chromatin assembly are functionally linked (Smith and Whitehouse, 2012).

Results

Regulated origin activation on plasmids free in solution

To reconstitute budding yeast DNA replication with purified proteins we first assembled the minimal components required for regulated origin activation (Yeeles et al., 2015). To this end we purified the factors required for Mcm2-7 loading (ORC, Cdc6, Cdt1·Mcm2-7), CMG formation (DDK, Cdc45, Sld3·Sld7, Clb5·Cdk1, Sld2, Dpb11, GINS, Pol ε), CMG activation (Mcm10), and for initiating DNA synthesis (Pol α, RPA) (Fig 3.1A). In addition, we purified Ctf4, which has been implicated in tethering Pol α to the replisome (Bell and Labib, 2016), and topoisomerases I (Top1) and II (Top2), which are implicated in relieving topological stress during replication fork progression. To test the ability of this set of factors to initiate of DNA replication we followed the reaction scheme outlined in Fig 3.1B. A similar approach was reported recently (Yeeles et al., 2015), in which the individual steps were carried out with intervening washes on plasmid DNA immobilized on paramagnetic beads. However, we sought to perform the reaction on plasmid DNA free in solution to permit the observation of plasmid replication intermediates and to avoid replication termination defects inherent to the coupling of DNA to beads. First, Mcm2-7 loading was performed with ORC, Cdc6, and Cdt1·Mcm2-7 in the presence of ATP on the origin-containing plasmid pARS1 (4.8 kb). Then,

Figure 3.1 Reconstitution of origin activation on plasmid DNA free in solution

(A) Purified budding yeast replication initiation proteins analyzed by SDS-PAGE and Coomassie stain.

(B) Reaction scheme. pARS: ARS-containing plasmid.

(C) Nascent DNA products obtained with pARS1 (4.8 kb) as described in (B) were analyzed by alkaline agarose gel-electrophoresis and autoradiography. Initiation factors were individually omitted from the reaction as indicated. RC: Rolling circle; ssL: single-stranded full-length linear.

(D) Analysis of DNA products obtained with pARS305 (9.8 kb) as in (C). RC: Rolling circle; ssL: single-stranded full-length linear.

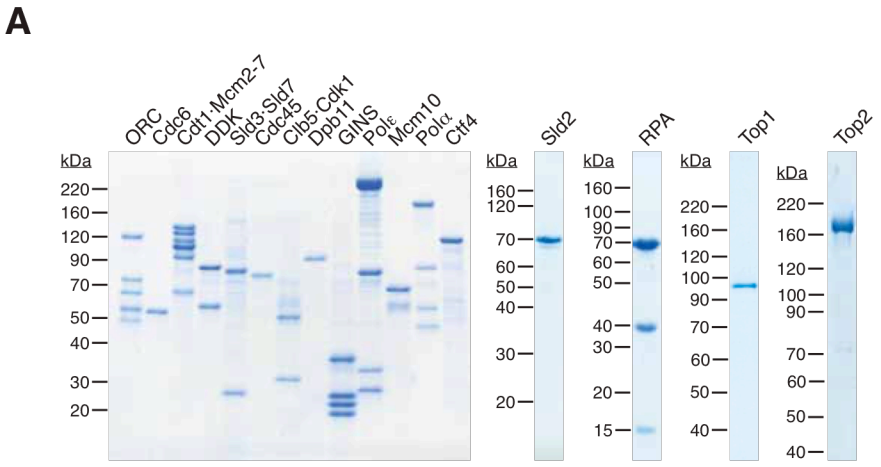
A
ORC
Cdc6
Cdt1·Mcm2-7
DDK
Sld3·Sld7
Cdc45
Clb5·Cdk1
Dpb11
GINS
Polε
Mcm10
Polα
Ctf4
Sld2
RPA
Top1
Top2
kDa

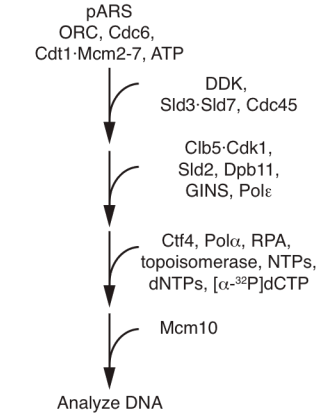
B
pARS
ORC, Cdc6,
Cdt1·Mcm2-7, ATP
DDK,
Sld3·Sld7, Cdc45
Clb5·Cdk1,
Sld2, Dpb11,
GINS, Polε
Ctf4, Polα, RPA,
topoisomerase, NTPs,
dNTPs, [α-32P]dCTP
Mcm10
Analyze DNA

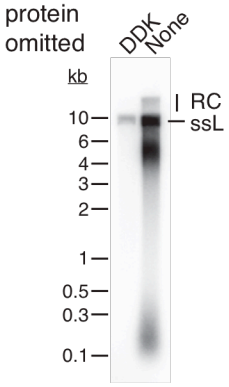
D
protein
omitted
DDK
None
kb
RC
ssL

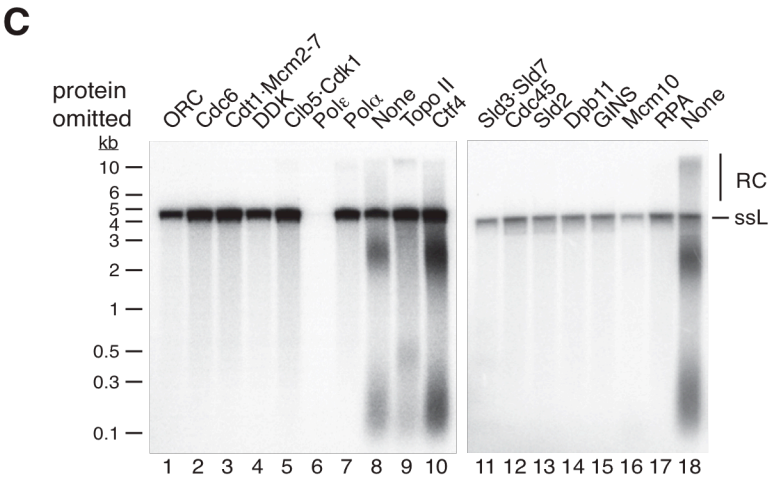
C
protein
omitted
ORC
Cdc6
Cdt1·Mcm2-7
DDK
Clb5·Cdk1
Polε
Polα
None
Topo II
Ctf4
Sld3·Sld7
Cdc45
Sld2
Dpb11
GINS
Mcm10
RPA
None
kb
RC
ssL
1 2 3 4 5 6 7 8 9 10 11 12 13 14 15 16 17 18

purified DDK was added to phosphorylate Mcm2-7 double hexamers (DHs) formed in this reaction (Gros et al., 2014), followed by the addition of Cdc45 and Sld3·Sld7, which form a complex with Mcm2-7 after DDK phosphorylation (Gros et al., 2014; Heller et al., 2011; Tanaka et al., 2011; Yeeles et al., 2015). We then performed the CDK-dependent step of the CMG assembly reaction by adding Clb5·Cdk1, Sld2, Dpb11, GINS, and Pol ε to the reaction mix. Subsequently, we added Ctf4, Pol α, RPA, and topoisomerase II to the reaction, and supplemented with NTPs and dNTPs to support the formation of RNA/DNA primers by Pol α and DNA synthesis; [α-^{32}P]dCTP was included to monitor DNA synthesis. Finally, to initiate origin activation, we added Mcm10 into the reaction mix.

Analysis of the DNA products by alkaline agarose gel-electrophoresis revealed the generation of four distinct labeled DNA products (Fig 3.1C, lanes 8 and 18): Full-length single-stranded DNA (ssL); longer than unit-length (> 4.8 kb) nascent strands; long nascent strands of approximately half unit length (2-3 kb); and short nascent strands of approximately 100-300 bases. Formation of the labeled full-length single-stranded DNA (ssL) is dependent on Pol ε (Fig 3.1C lane 6), but not on other components of the reaction, indicating that this product results from replication-independent labeling of nicks present in the template by Pol ε, Generation of longer than unit-length nascent strands depends on most initiation factors, but not on topoisomerase or Ctf4, nor priming by Pol α (Fig 3.1, lane 7), indicating that these nascent strands are the product of rolling-circle (RC) replication carried out by Pol ε in conjunction with the CMG, primed by a nick in the template. The generation of the half unit-length and short nascent strands is strictly dependent on 15 of the 16 proteins added into the reaction, the exception being Ctf4 (lane 10), indicating that

these products are the result of canonical origin activation and Pol α-primed DNA synthesis.

The discrete size distribution of the half unit-length nascent strands is consistent with these products resulting from leading strand synthesis by two opposing forks emanating from a common origin and terminating at the opposite pole of the plasmid circle. Supported by results presented below, the short, 100-300 nt, nascent strands are likely to be nascent lagging strand products. In agreement with these interpretations, we found that the length of the short nascent strands is independent of the length of the template, whereas the average length of the long nascent strands correlates with template size. Thus long nascent strands reach a length of 4-6 kb, i.e. approximately half unit-length, on a 10 kb plasmid template, while the short nascent strands remain unchanged in length at 100-300 bases (Fig 3.1D). Moreover, quantitation of the relative amounts of the half unit-length and short nascent strands synthesized in lanes 8, 10, and 18 of (Fig 3.1C) reveals that these products are generated at similar levels, which is consistent with the notion that these nascent strands derive from coordinated leading and lagging strand synthesis at the fork. From these observations we conclude that the purified proteins described above support regulated bidirectional origin activation *in vitro*.

Both Topo I and Topo II support fork progression, but only Topo II supports decatenation of plasmid daughters

Nascent strands obtained in the absence of topoisomerase, except for those derived from rolling circle replication, were significantly shorter than half unit-length (Fig 3.1C, lane 9), probably because replication fork progression in

topologically closed template DNA is inhibited in the absence of topoisomerase by the accumulation of positive supercoils ahead of the forks (Wang, 2002). Consistent with this notion, we found that both Topo I and Topo II could support replication fork progression. Both budding yeast Top2 and human Topo II (hTopo II) could be used interchangeably in our experiments without qualitative differences in the resulting replication products, indicating that species-specific interactions are not required for Topo II function during budding yeast DNA replication *in vitro*; hTopo II was more active in these assays, possibly due to its greater specific activity.

A time course of DNA synthesis in the presence of either Top1 or hTopo II revealed a lag time of 1-2 minutes upon addition of Mcm10, after which Top1 and hTopo II supported DNA synthesis at similar rates, reaching a plateau after around 45 minutes (Fig 3.2B). We find that approximately 10-15 fmol of plasmid DNA molecules, or 10 % of the input, are ultimately synthesized per reaction under our standard conditions. Analysis of the DNA products obtained in both time course experiments by alkaline agarose gel-electrophoresis revealed that the long nascent strands reached half unit length (2-3 kb) after approximately 6-8 minutes, while maximal extension of the rolling circle replication products was observed after 30-45 minutes (Fig 3.2A), demonstrating that both Topo I and Topo II support replication fork progression. However, analysis of the replication products by native agarose gel-electrophoresis revealed that DNA replication in the presence of Top1 results in the accumulation of slow migrating replication intermediates, while DNA replication in the presence of Topo II culminated in the formation of nicked plasmid monomers (Fig 3.2B), consistent with the well-documented ability of Topo II, but not Topo I, to support decatenation of double-stranded

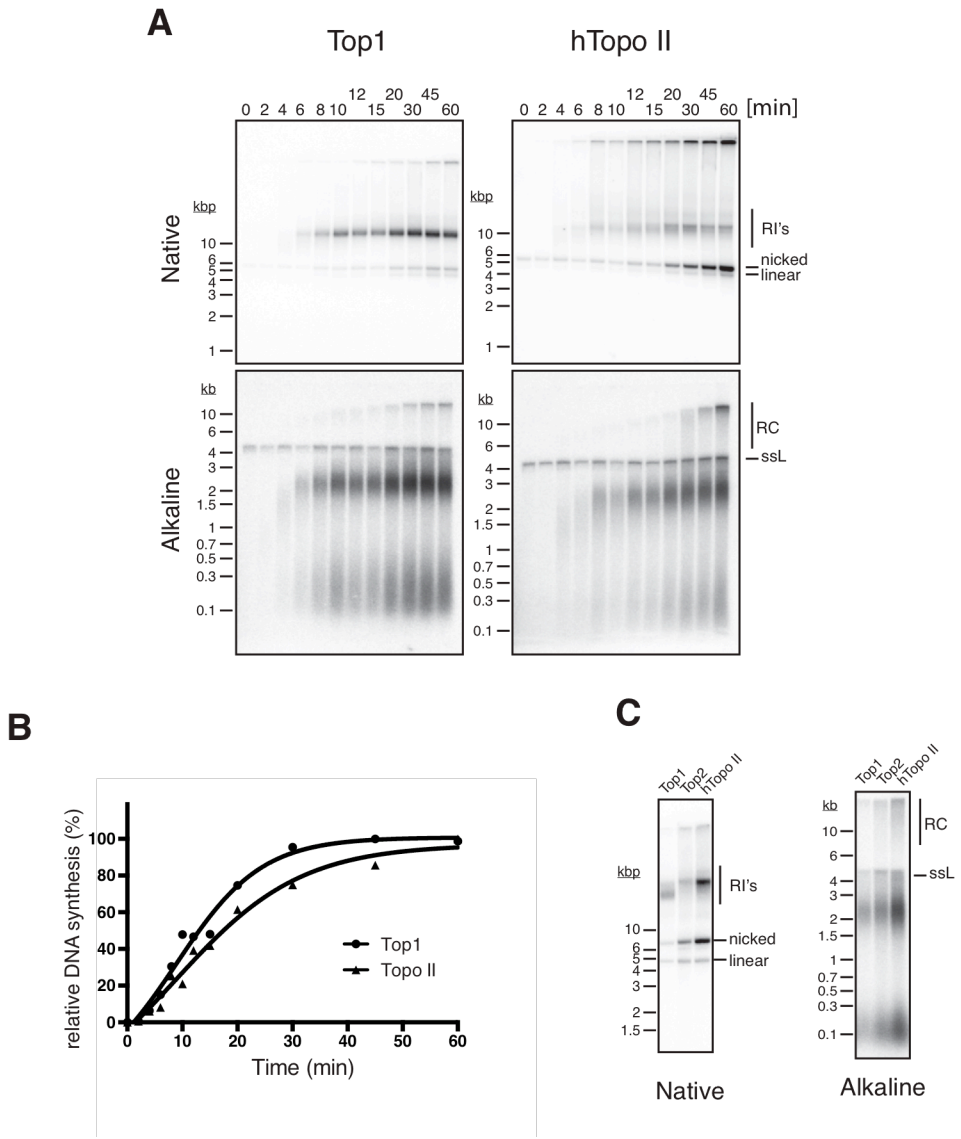

Figure 3.2 Both Topo I and Topo II support replication elongation, but only Topo II supports decatenation of plasmid daughter molecules

(A) Reactions were performed with pARS1 (4.8 kb) according to the scheme of Fig. 3.1B. At indicated times after addition of Mcm10 aliquots were withdrawn from each reaction and processed for analysis by native (top) or alkaline (bottom) agarose gel-electrophoresis and autoradiography. RI's: replication intermediates.

(B) Quantification of native gels from (A).

(C) Reactions were performed with pARS1 (4.8 kb) according to the scheme of Fig. 3.1B using either Top1, Top2, or human Topo II (hTopo II) as indicated. DNA products were analyzed by native (top) or alkaline (bottom) agarose gel-electrophoresis and autoradiography.

DNA (Corbett and Berger, 2004). Side-by-side analysis of replication products obtained in the presence of Top1, Top2, or hTopo II by alkaline agarose gel-electrophoresis demonstrated that all three topoisomerases support the synthesis of half unit-length and short nascent strands, but that replication intermediates obtained with Top1 migrated slightly faster in a native agarose gel than those obtained with the type II enzymes, which may suggest that the slower migrating replication intermediates obtained with Top1 or Top2 differ in their molecular structure (Fig 3.2C). These results raise the question whether the inability of Top1 to resolve replicated daughter molecules is because of either a termination defect or its inability to decatenate nicked daughter molecules.

PCNA clamp loading inhibits primer extension by Pol α

To dissect the relative contributions of Pol ε and Pol α to DNA synthesis in the minimal system described above we took two approaches: The role of Pol ε was assessed by substituting wildtype Pol ε with a catalytically inactive variant that harbors a mutation in the DNA polymerase active site, while the role of Pol α was assessed by supplementing the system with the components necessary for RFC-catalyzed PCNA clamp-loading, a reaction that was previously shown to inhibit primer extension by human Pol α (Mossi et al., 2000; Tsurimoto et al., 1990; Tsurimoto and Stillman, 1991; Yuzhakov et al., 1999).

Although the POL2 gene is essential *in vivo*, the catalytic activity of Pol2 is dispensable for viability (Dua et al., 1999; Kesti et al., 1999). To eliminate Pol ε DNA polymerase activity, we substituted the metal-coordinating aspartate 640 of the N-terminal Pol2 DNA polymerase active site

Figure 3.3 PCNA clamp loading inhibits primer elongation by Polα

(A) Purified budding yeast factors.

(B) Reactions were carried out with pARS1 (4.8 kb) according to the scheme in Fig. 3.1B, using either wildtype Pol ε (lanes 1 and 2) or Pol ε^{pol-} (lanes 3 and 4) either in the absence or presence of Pol α as indicated. DNA products were analyzed by alkaline agarose gel-electrophoresis and autoradiography.

(C) Reactions were carried out with pARS1 (4.8 kb) according to the scheme in Fig. 3.1B, using either Pol ε^{pol-} (lanes 1-3) or wildtype Pol ε (lanes 4-9), and with increasing concentrations of either RPA (Lanes 1-6) or *E. coli* SSB (lanes 7-9). Reaction products were analyzed by alkaline agarose gel-electrophoresis and autoradiography. The concentrations indicated for SSB refer to SSB tetramer.

(D) Reaction scheme.

(E) Reactions were carried out with pARS1 (4.8 kb) according to the scheme in (D) using either Pol ε^{pol-} (lanes 1-4) or wildtype Pol ε (lanes 5-8) either in the absence or presence of RFC and PCNA as indicated.

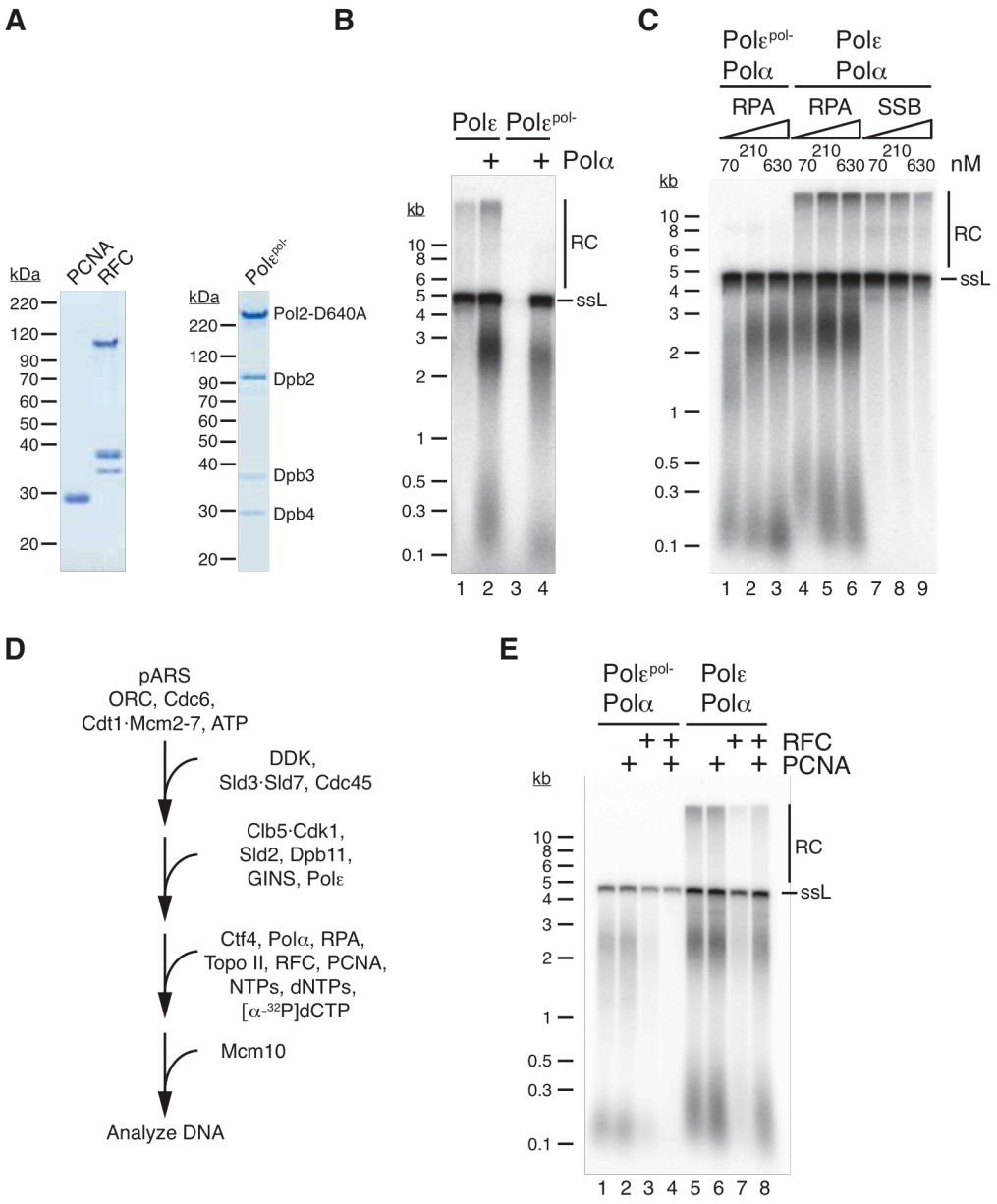
A
kDa
PCNA
RFC
220
120
90
70
60
50
40
30
20
kDa
Pol2-D640A
Dpb2
Dpb3
Dpb4
B
Polε
Polε^pol-
+
+
Polα
kb
RC
ssL
C
Polε^pol-
Polα
Polε
Polα
RPA
RPA
SSB
70
210
630
nM
kb
RC
ssL
D
pARS
ORC, Cdc6,
Cdt1·Mcm2-7, ATP
DDK,
Sld3·Sld7, Cdc45
Clb5·Cdk1,
Sld2, Dpb11,
GINS, Polε
Ctf4, Polα, RPA,
Topo II, RFC, PCNA,
NTPs, dNTPs,
[α-32P]dCTP
Mcm10
Analyze DNA
E
Polε^pol-
Polα
Polε
Polα
RFC
PCNA
kb
RC
ssL

(Hogg et al., 2014) with alanine (Pol2-D640A) to yield Pol ε^{pol-} (Fig 3.3A). Inactivation of the Pol ε DNA polymerase activity eliminated the rolling circle replication products, but permitted reduced synthesis of half-unit-length and short nascent strands, indicating that Pol α does not support rolling circle replication with the CMG, but does support the synthesis of nascent strands resulting from origin activation (Fig 3.3B). However, the average length of nascent strands synthesized by Pol α in the presence of Pol ε^{pol-} was markedly reduced relative to those synthesized in the presence of Pol ε, and we subsequently found that nascent strand synthesis by Pol α was significantly stimulated by RPA (Fig 3.3C, lanes 1-3). These data indicate that both Pol ε and Pol α can account for the synthesis of short and long nascent strands. *E. coli* SSB could not substitute for RPA in the generation of the long and short nascent strands, despite being able to support rolling circle replication by Pol ε/CMG, indicating that specific interactions are important for RPA function during DNA replication (Fig 3.3C, lanes 4-9).

To investigate if clamp loading restricts primer extension by Pol α after budding yeast origin activation *in vitro*, we purified the budding yeast RFC clamp loader and PCNA clamp (Fig 3.3A) and supplemented the origin activation reaction with these proteins as outlined in the reaction scheme of Fig 3.3D. While the synthesis of short and long nascent strands by Pol α in the presence of Pol ε^{pol-} was unaffected by PCNA alone, RFC alone strongly reduced the synthesis of nascent strands by Pol α, and addition of both PCNA and RFC essentially abolished the synthesis of nascent strands by Pol α (Fig 3.3E, lanes 1-4) indicating that RFC can displace Pol α from the 3' primer terminus during PCNA loading and thereby restrict primer extension by Pol α. RFC alone, but not PCNA alone, also inhibited nascent strand synthesis in the

presence of wild-type Pol ε, α (Fig 3.3E lanes 5-7). Importantly, however, both short and long nascent strands were synthesized by Pol ε if PCNA loading by RFC had occurred prior to DNA synthesis (Fig 3.3E lane 8), suggesting that Pol ε can displace RFC from 3' primer ends after PCNA loading. Together these observations suggest that budding yeast Pol α and Pol ε can engage in an RFC/PCNA-mediated polymerase switch mechanism analogous to that reported for Pol α and Pol δ during SV40 replication (Tsurimoto et al., 1990; Tsurimoto and Stillman, 1991). Thus, although Pol α can contribute to the synthesis of nascent strands after budding yeast origin activation *in vitro* (Fig 3.3B and 3.3C), PCNA loading by RFC will normally restrict Pol α activity to the synthesis of short primers only.

DNA synthesis by Pol δ is unrestricted on naked DNA

The bimodal distribution of nascent strands observed in the experiments above is a consequence of the omission of factors required for nascent strand ligation. Daughter strand ligation should require the removal of the RNA primer from the 5' end of nascent fragments to generate DNA nicks that can be ligated by DNA ligase I. Consistent with this notion, addition of purified budding yeast Cdc9 (DNA ligase I; Fig 3.5A) alone to the reaction outlined in Fig 3.3B was not sufficient to support ligation of nascent strands (Fig 3.4). Therefore, to complement the origin activation system with the canonical lagging strand machinery we purified budding yeast Pol δ and Fen1 in addition to Cdc9 (Fig 3.5A), and supplemented the reaction outlined in Fig 3.3D with these three components prior to addition of Mcm10. Because of the presence of RFC and PCNA, which suppress primer extension by Pol α (Fig3.3E), nascent strands formed under these conditions are synthesized

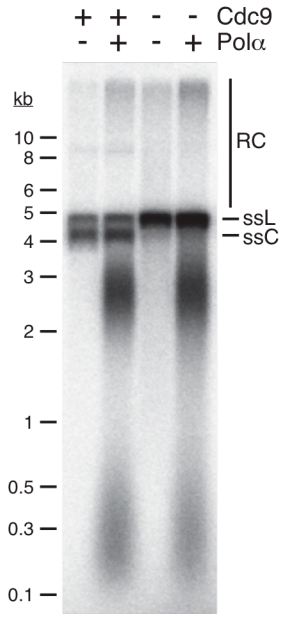

Figure 3.4 Cdc9 cannot ligate nascent strands synthesized by Pol α and Pol ε Reactions were performed as schematized in Fig 3.3D in absence or presence of purified Cdc9 and Pol α as indicated. DNA was analyzed by alkaline agarose gel-electrophoresis and autoradiography.

either by Pol ε or Pol δ. Addition of Pol δ increased the total amount of DNA synthesis approximately four-fold. Unexpectedly, however, nascent strands synthesized in the presence of Pol δ and Pol ε formed long heterogenous smears, contrary to the discrete bimodal length distribution of nascent strands synthesized by Pol ε in the absence of Pol δ (Fig 3.5C). Rolling circle replication was also markedly increased in the presence of Pol δ. The majority of the heterogenous nascent strands are synthesized in an origin activation-dependent manner, while a small fraction of rolling circle products was also generated in the absence of regulated origin activation, probably via strand displacement synthesis by PCNA-Pol δ primed at nicks in the DNA template

Figure 3.5 Nucleosome assembly limits Okazaki fragment length

(A) Purified budding yeast factors.

(B) Reaction scheme.

(C) Reactions were carried out with pARS1 (4.8 kb) according to the scheme in (B) but without nucleosome assembly in the first step, either in the absence (lanes 1 and 2) or presence (lanes 3 and 4) of Pol δ, and either in the absence (lanes 1 and 3) or presence (lanes 2 and 4) of Cdc9. Reaction products were analyzed by alkaline agarose gel-electrophoresis and autoradiography.

(D) Reactions were carried out with pARS1 (4.8 kb) according to the scheme in (B) either in the absence (lanes 1 and 2) or presence (lanes 3 and 4) of Pol δ, and either in the absence (lanes 1 and 3) or presence (lanes 2 and 4) of Cdc9. Reaction products were analyzed by alkaline agarose gel-electrophoresis and autoradiography.

(E) Reactions were carried out with pARS1 (4.8 kb) according to the scheme in Fig 3.5B, excluding Cdc9, and with either Pol ε^{pol-} (lane 1) or wildtype Pol ε (lane 2). DNA products were analyzed by alkaline agarose gel-electrophoresis and autoradiography.

(F) Reactions were carried out with pARS1 (4.8 kb) according to the scheme in (B) either in the absence or presence of Cdc9, *S. cerevisiae* Fen1 (yFen1), or with human Fen1 (hFen1), as indicated. Reaction products were analyzed by alkaline agarose gel-electrophoresis and autoradiography.

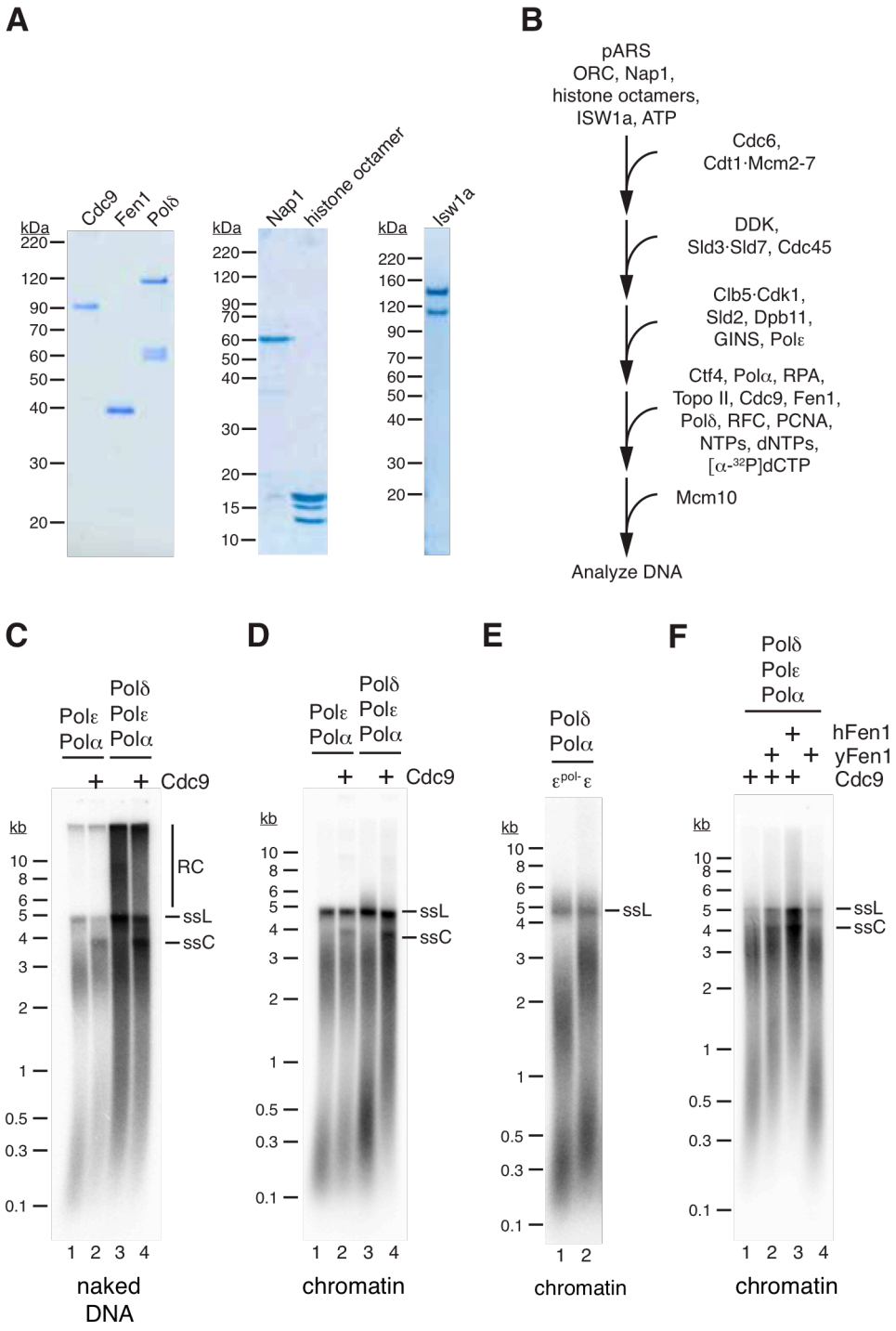
A
kDa
Cdc9
Fen1
Polδ
220
120
90
70
60
50
40
30
20
kDa
Nap1
histone octamer
220
120
90
70
60
50
40
30
20
15
10
kDa
Isw1a
220
160
120
90
70
60
50
40
30
20
B
pARS
ORC, Nap1,
histone octamers,
ISW1a, ATP
Cdc6,
Cdt1·Mcm2-7
DDK,
Sld3·Sld7, Cdc45
Clb5·Cdk1,
Sld2, Dpb11,
GINS, Polε
Ctf4, Polα, RPA,
Topo II, Cdc9, Fen1,
Polδ, RFC, PCNA,
NTPs, dNTPs,
[α-32P]dCTP
Mcm10
Analyze DNA
C
Polε
Polα
Polδ
Polε
Polα
+ + Cdc9
kb
10
8
6
5
4
3
2
1
0.5
0.3
0.1
RC
ssL
ssC
1 2 3 4
naked
DNA
D
Polε
Polα
Polδ
Polε
Polα
+ + Cdc9
kb
10
8
6
5
4
3
2
1
0.5
0.3
0.1
ssL
ssC
1 2 3 4
chromatin
E
Polδ
Polα
εpol-ε
kb
10
8
6
5
4
3
2
1
0.5
0.3
0.1
ssL
1 2
chromatin
F
Polδ
Polε
Polα
+ hFen1
+ + yFen1
+ + + Cdc9
kb
10
8
6
5
4
3
2
1
0.5
0.3
0.1
ssL
ssC
1 2 3 4
chromatin

(Fig 3.6A) (Ayyagari et al., 2003). DNA synthesis by Pol δ was assessed in the presence of Pol ε^{pol-}, which revealed that synthesis of long nascent strands by Pol δ was strictly dependent on RFC/PCNA, whereas nascent strands obtained in the absence of RFC/PCNA corresponded to Pol α products only

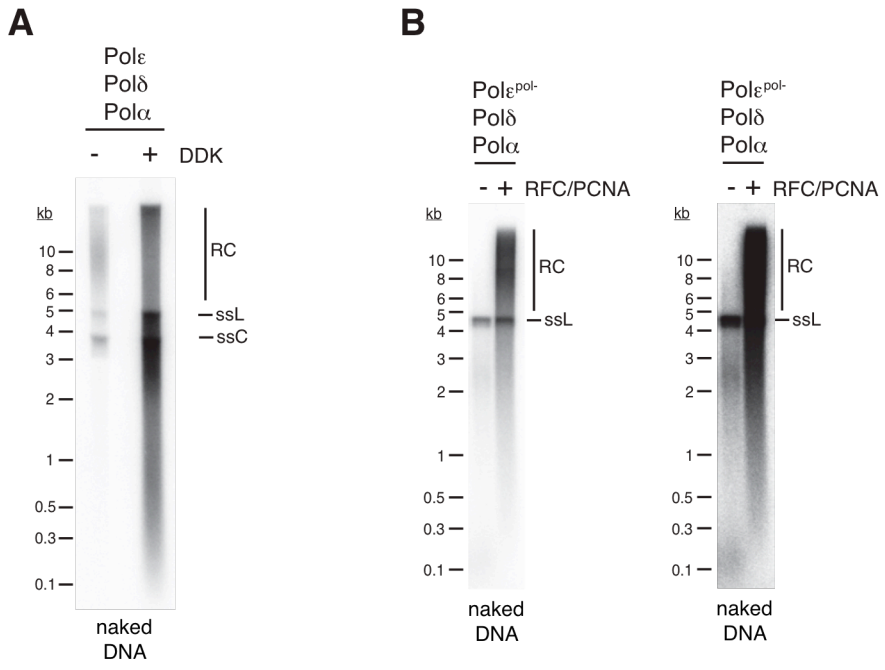

Figure 3.6 Heterogenous DNA synthesis by Pol δ on naked DNA is dependent on origin activation and clamp loading

(A) Reactions were carried out in presence of Cdc9 as in Fig 3.5C, either in absence or presence of DDK as labeled.

(B) Left; Reactions were carried out on pARS1 (4.8kb) as schematized in Fig 3.1B with Pol ε^{pol-} replacing wildtype Pol ε, and including Pol δ. RFC and PCNA were either absent or present as indicated. DNA products were analyzed by alkaline agarose gel-electrophoresis and autoradiography. Right; Same gel as in left with different contrast level to visualized products synthesized by Pol α in the absence of RFC/PCNA.

(Fig 3.6B), consistent with Pol δ being dependent on PCNA for processive DNA synthesis (Prelich et al., 1987). Although the ability of Cdc9 to ligate nicked plasmid circles was apparent from the conversion of full-length single-stranded linear DNA (ssL) to single-stranded circular closed DNA (ssC) in the gel analysis of Fig 3.5C, the heterogeneity of the nascent strands obtained in the presence of Pol δ under these conditions compromised our ability to clearly assess the ligation of nascent strands by Cdc9. We conclude that PCNA-Pol δ synthesizes heterogeneously long nascent strands after origin activation on naked plasmid DNA.

Nucleosome assembly limits Okazaki fragment length

Motivated by the observation that Okazaki fragment length *in vivo* appears to be determined by the nucleosomal repeat of nascent chromatin (Smith and Whitehouse, 2012), we directly tested the influence of chromatin on nascent strand synthesis in our system. To this end we assembled plasmid DNA into nucleosome arrays using purified Nap1, yeast histone octamers, and Isw1a (Fig 3.5A) (Vary et al., 2004). We assembled nucleosomes on plasmid DNA in the presence of ORC prior to Mcm2-7 loading and performed the DNA replication reaction as indicated in Fig 3.5 B. In the absence of Pol δ, Pol ε synthesized long and short nascent strands on chromatin that exhibited a size distribution similar to those obtained on naked DNA (compare Fig 3.5 D, lanes 1 and 2, to Fig 3.5C, lanes 1 and 2). Strikingly though, on the chromatin template we were able to observe a canonical bimodal distribution of nascent strands characteristic for leading and lagging strand products even in the presence of Pol δ (compare Fig 3.5D, lanes 3 and 4, to Fig 3.5C, lanes 3 and 4).

While the length distribution of the longer nascent strands obtained with Pol ε and Pol δ was very similar to that of strands synthesized by Pol ε in the absence of Pol δ, the shorter nascent strands, which we show below are lagging strand products, were on average almost twice as long in the presence of Pol δ compared to those obtained with Pol ε alone, similar to the average Okazaki fragment length observed *in vivo* (Smith and Whitehouse, 2012), suggesting that Pol δ contributes primarily to the synthesis of the lagging strand in the presence of Pol ε. In the absence of DNA synthesis by Pol ε, however, we found that Pol δ was also capable of synthesizing both short and long nascent strands, although both species were shorter than when synthesized by Pol δ alone (Fig 3.5E). Thus, both Pol ε and Pol δ may contribute to the synthesis of nascent lagging strands, whereas Pol ε alone can synthesize fully extended longer nascent strands. Importantly, however, nascent lagging strands obtained in the presence of both Pol δ and Pol ε, but not those synthesized by Pol ε alone, could be ligated by Cdc9 (Fig 3.5D) and this ligation was dependent on Fen1 (Fig 3.5F**)** indicating that the reaction recapitulates canonical nascent strand maturation. As both human and budding yeast Fen1 supported ligation (Fig 3.5F), species-specific interactions are not required for the nucleolytic processing of Okazaki fragments.

In conclusion, these data demonstrate that chromatin restricts excessive strand displacement or nick translation synthesis by Pol δ to yield canonical nascent leading and lagging strands. While both Pol δ and Pol ε can principally contribute to the synthesis of nascent leading and lagging strands, only nascent lagging strands synthesized by Pol δ can be functionally matured into a continuous daughter strand by Fen1 and Cdc9.

Nucleosomes inhibit progression of Pol δ

Intriguingly, the above results demonstrated that nascent strand synthesis by Pol ε was unaffected by the chromatinization of the template (compare Fig 3.5C, lane 1, to Fig 3.5D, lane 1), whereas the length of nascent strands synthesized specifically by Pol δ was significantly reduced on chromatin (compare Fig 3.5E, lane 1, to Fig 3.6B, lane 2). Thus the shortening of the nascent lagging strands synthesized by Pol δ is not due to differences in the rate of primer synthesis by Pol α on naked DNA and chromatin under these conditions. Instead, these observations indicate that restriction of Pol δ progression during lagging strand synthesis by nucleosomes is the primary reason for the generation of discrete nascent strands in the complete reaction on chromatin. Such a mechanism implies that nucleosomes are formed on the plasmid daughters. Indeed our replication reaction is performed in the presence of the chromatin assembly system, and we found that MNase digestion of daughter strands yields nucleosomal fragment sizes, consistent with nucleosomal packaging of the replicated DNA (Fig 3.7). To directly test the effect of nucleosomes on the DNA polymerase activity of Pol δ and Pol ε in greater detail we employed a linear oligonucleotide-based template composed of a 256 nt template encompassing the 601 nucleosome positioning sequence (Lowary and Widom, 1998), with a 29 nt single-stranded gap between the radiolabeled primer and the 601-containing duplex (Fig 3.8). In this system Pol δ efficiently extends the radiolabeled primer to fill the gap in an RFC/PCNA-dependent manner (Fig 3.8B). Pol ε is similarly proficient in gap-filling, but does not require association with PCNA under these conditions (Fig 3.8C). In the presence of Fen1, Pol δ catalyzed nick-translation synthesis through the

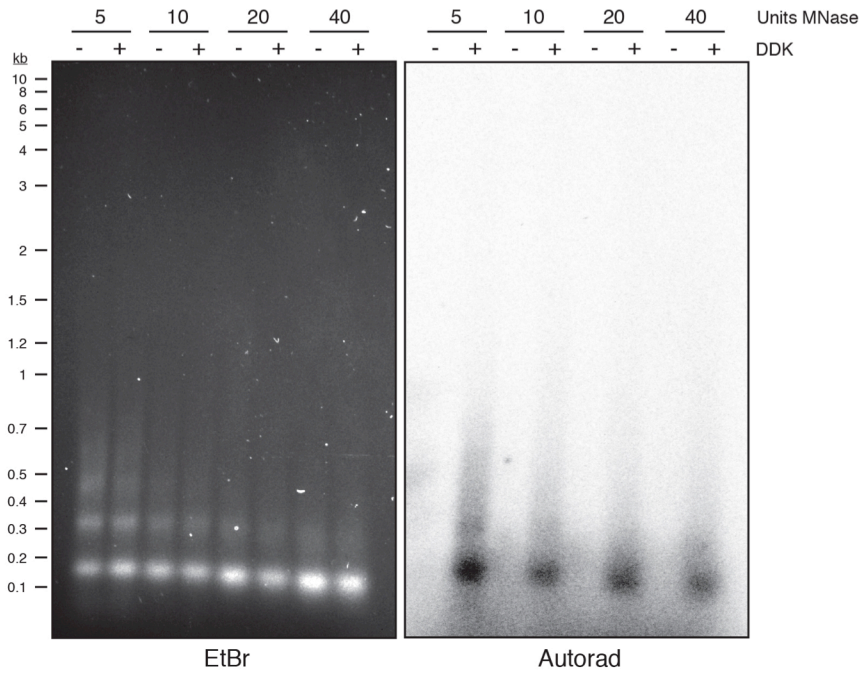

Figure 3.7 Daughter strands are assembled into nucleosomes
Reactions were carried out as outlined in figure 3.5B either in the absence or presence of DDK, as indicated. One hour after the addition of Mcm10 , micrococcal nuclease (MNase) was added to the reaction, and incubation was continued for an additional 15 minutes. DNA was isolated from the reactions and fractionated by native agarose gel-electrophoresis. Total DNA was analyzed by staining the gel with ethidium-bromide (EtBr, left), replication products in the gel were analyzed by autoradiography.

downstream duplex to generate up to full-length, 256 nt, daughter strands(Fig 3.8D, lanes 1-3). Pol ε, on the contrary, was unable to perform nick-translation in the presence of Fen1 (Fig 3.8D, lanes 4 and 5). Importantly, in the presence of a nucleosome at the 601 sequence, nick-translation by Pol δ/Fen1 did not progress beyond the midpoint of the nucleosome (Fig 3.8D, lane 8), demonstrating that nucleosomes pose a significant barrier to Pol δ progression.

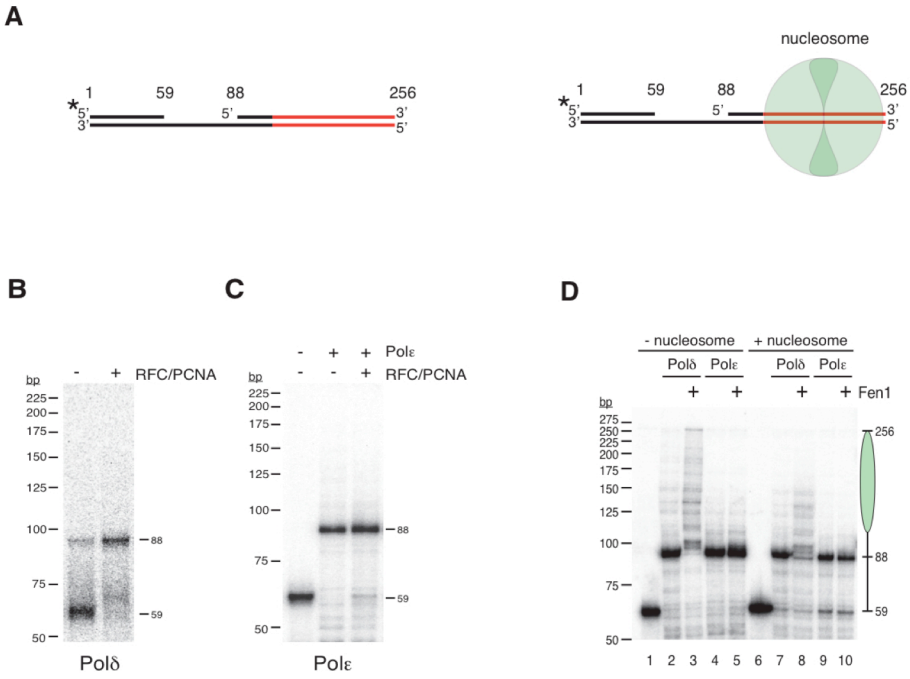

Figure 3.8 Nucleosomes limit strand displacement by Pol δ

(A) Primer-template schematic. Red, 601 nucleosome positioning sequence; base pair positions are indicated above the substrate DNA; * indicates ^{32}P label position on the 5' end. Left; substrate without nucleosome (used in (B) and (C) as follows). Right; nucleosome is in green (used in (D))

(B) Primer-template extension assay: The primer-template was incubated with Pol δ, ATP, dNTP mix, and RFC/PCNA as indicated. Reaction products were analyzed by denaturing polyacrylamide gel-electrophoresis and autoradiography. Positions of the primer (59 bp), gap-filling product (88 bp), and full-length product (259 bp) are indicated on the right

(C) As in (B) but Pol ε was used instead of Pol δ.

(D) As in (B) with following modifications. Primer-template either without (lanes 1-5) or with (lanes 6-10) a nucleosome assembled at the 601 sequence was used. hFen1 and either Pol d or Pol e, as indicated were used as indicated. Reaction products were analyzed by denaturing polyacrylamide gel-electrophoresis and autoradiography. The nucleosome position is indicated by the green oval.

Note: This figure was contributed by Jieqing Jiang.

The ability of Pol δ, but not Pol ε, to perform nick-translation synthesis together with Fen1 provides a mechanistic basis for the observation that lagging strand maturation can only occur if Okazaki fragments are synthesized by Pol δ (Fig 3.5D). Moreover, the above results suggest that the length of nascent strands synthesized by Pol ε is limited by the inability of Pol ε to synthesize DNA through a downstream 5' end, whereas the generation of discretely sized nascent strands by Pol δ requires the inhibition of Pol δ-catalyzed strand displacement activity by nucleosomes in the template.

Completion of plasmid replication

We have demonstrated above that nascent strands synthesized by Pol α and Pol ε in the absence of Pol δ cannot be processed into mature daughter strands (Fig 3.5 D), which is consistent with Pol δ being essential for DNA replication *in vivo*. To test if the generation of fully replicated, covalently-closed plasmid daughter molecules was supported in reactions employing all three replicative DNA polymerases, we followed the scheme of Fig 3.5B, using either naked DNA or chromatin as a template. To separate covalently closed from nicked plasmid daughter molecules, we analyzed the DNA products by agarose gel electrophoresis in the presence of a high concentration of ethidium bromide, which induces positive supercoiling of topologically closed DNA molecules.

In the replication control on naked DNA (Fig 3.9, lane 1) we observed low levels of origin activation-independent strand-displacement synthesis as before (Fig 3.6A), as well as background levels of end-labeled linear molecules and covalently closed plasmid monomers that derive from the labeling of nicks in the plasmid template. Regulated initiation of DNA

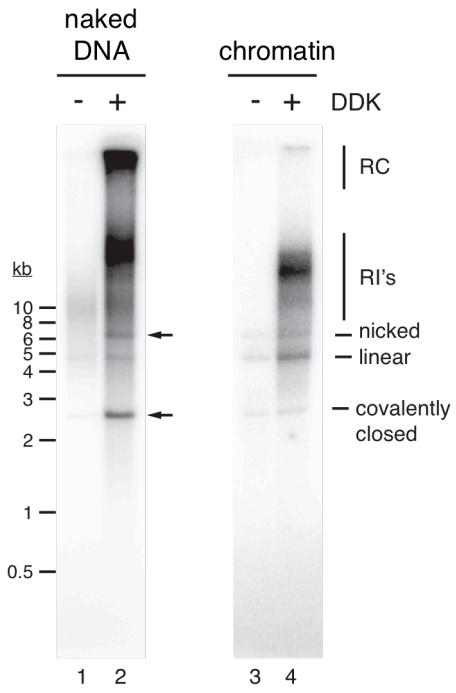

Figure 3.9 Generation of fully replicated plasmid daughter molecules Reactions were performed with pARS1 (4.8 kb) according to the scheme of Fig. 4B, using either naked DNA (lanes 1 and 2) or chromatin (lanes 3 and 4) as a template. DNA products were analyzed by native agarose gel-electrophoresis in the presence of 0.5 mg/ml ethidium bromide and autoradiography. Arrows indicate the positions of nicked and covalently closed plasmid daughter molecules

replication under these conditions resulted in significant increases in the levels of DNA products migrating at the position of rolling circles replication products near the well, replication intermediates, nicked monomers, and covalently-closed monomers (Fig 3.9, lane 2). The large fraction of replication intermediates indicates that most daughter molecules resulting from regulated origin activation were either incompletely replicated or had failed to be decatenated, which contrasts with the efficient generation of fully replicated, but nicked, plasmid daughter monomers observed in the two-polymerase

system earlier (Fig 3.2A). Nonetheless, the generation even of low levels of nicked and covalently closed plasmid daughter monomers (arrows in Fig 3.9) indicates that completion of DNA replication and subsequent decatenation by Topo II had occurred at least in a fraction of the plasmid molecules. These data indicate that even though Okazaki fragment maturation is more readily detectable when Okazaki fragments generated on chromatin template exhibit a short discrete size distribution (Fig 3.5D), heterogenously long Okazaki fragments generated on naked DNA (Fig 3.5C) can also be matured into a complete daughter strand. As before (Fig 3.5D), rolling circle replication was almost completely suppressed on chromatin. Strikingly, however, essentially all plasmid daughters generated from the chromatin template were incompletely replicated, migrating at the position of replication intermediates (Fig 3.9, lanes 3 and 4). Since nascent leading strands reached half unit length also on chromatin (Fig 3.5D), fork progression is not grossly defective under these conditions. Instead, nucleosomal packaging appears to inhibit replication termination. It will be of interest in the future to determine what limits the completion of DNA replication both on naked DNA and on chromatin.

Chromatin promotes origin specificity during DNA replication *in vitro*

A hallmark of plasmid replication in budding yeast cells is the dependency on specific origin sequences (Marahrens and Stillman, 1992). Contrary to the situation *in vivo*, we and others have previously found that plasmid DNA molecules can be replicated in a regulated manner even in the absence of specific origin DNA sequences in yeast cell extracts (Gros et al., 2014; On et al., 2014). Because those previous studies employed naked plasmid DNA as a template, we decided to determine the site of replication

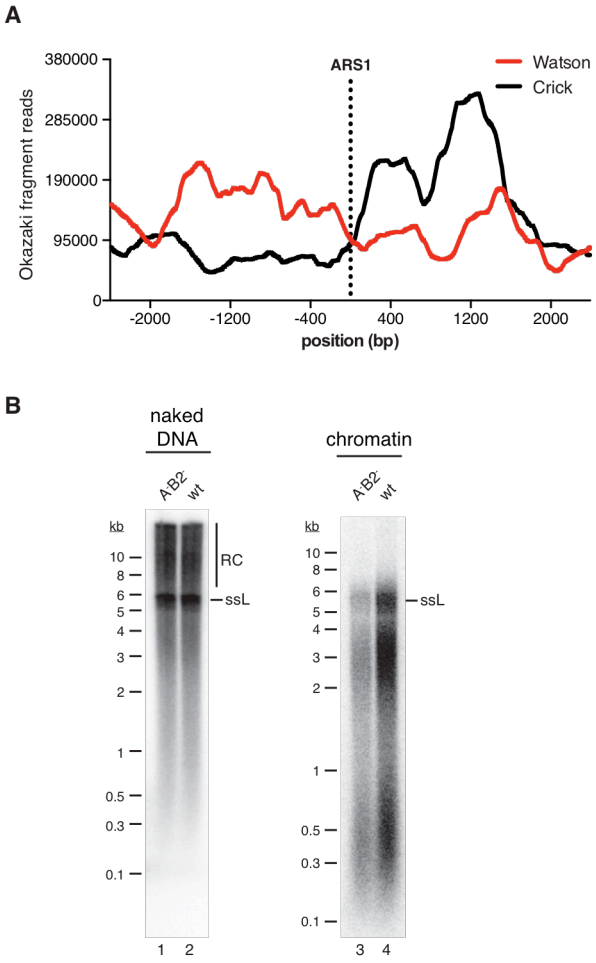

Figure 3.10 DNA replication initiates at origins in chromatin templates

(A) Okazaki fragment distribution on the Watson (red) and Crick (black) strands of pARS1 (4.8 kb). Sequence reads at every base pair were plotted over the linear coordinates of the plasmid sequence on the X-axis, with the position of ARS1 at 0 indicated by the vertical dotted line.

(B) Reactions were performed with pARS1-wt or pARS1-A$^-$B2$^-$ (5.9 kb) according to the scheme of Fig. 3.5B, excluding Cdc9, using either naked DNA (lanes 1 and 2) or chromatin (lanes 3 and 4) as a template. DNA products were analyzed by alkaline agarose gel-electrophoresis and autoradiography.

Note: Fig 3.10 A was contributed by Charanya Kumar

initiation on our chromatinized template by isolating and sequencing Okazaki fragments generated in the complete system on chromatinized pARS1 (4.8 kb) (Smith and Whitehouse, 2012). Intriguingly, we observed a pronounced transition in Okazaki fragments mapping to the Watson or Crick strand at the position of ARS1, demonstrating that DNA replication initiates preferentially at ARS1 under these conditions (Fig 3.10 A). Moreover, due to the distinct strand bias this data demonstrates that the short nascent fragments detected in our assay are indeed Okazaki fragments. To test the dependency on origin sequences, we compared the replication efficiency of plasmids harboring wildtype ARS1 to a variant carrying inactivating mutations in the A and B2 elements. Naked plasmid DNA molecules supported DNA replication at essentially identical levels irrespective of the presence of a functional ARS1 sequence (Fig 3.10B), as observed previously in extracts (Gros et al., 2014). In contrast, plasmids harboring wildtype ARS1 replicated on average three-fold more efficiently after assembly into chromatin than plasmids harboring a mutant origin (Fig 3.10B). Thus, chromatin promotes origin specificity during DNA replication *in vitro*.

Discussion

We have shown that origin-containing plasmids can be replicated free in solution by the stepwise addition of 24 purified budding yeast proteins. The system exhibits essential hallmarks of cellular eukaryotic DNA replication, including regulated, bidirectional origin activation, coordinated leading and lagging strand synthesis by the three eukaryotic replicative DNA polymerases, and canonical Okazaki fragment processing. Using this system we identify a

dual regulatory role for chromatin during DNA replication: Imposing replication origin specificity, and determining canonical Okazaki fragment length.

On naked DNA we find that Pol δ and Fen1 support excessive strand displacement/nick-translation synthesis, leading to the synthesis of Okazaki fragments that are abnormally long and heterogenous. In contrast, nucleosome assembly during the DNA replication reaction delimits the average length of Okazaki fragments *in vitro*, yielding Okazaki fragments that exhibit a length similar to that observed *in vivo* (Smith and Whitehouse, 2012). Consistent with these findings, Okazaki fragment length is significantly increased in budding yeast cells compromised for replication-coupled chromatin assembly upon deletion of Rtt106 or subunits of the CAF-1 complex (Smith and Whitehouse, 2012; Yadav and Whitehouse, 2016). We demonstrate that nucleosomes in the template specifically affect lagging strand synthesis by Pol δ after origin activation, whereas nascent strands synthesized by Pol ε were indistinguishable either in the absence or presence of nucleosome assembly. Moreover, we find that Pol δ can extend a primer by nick-translation with Fen1 only up to the midpoint of a downstream nucleosome, which is consistent with the observation that Okazaki fragment ligation junctions accumulate genome wide around nucleosome dyads *in vivo* (Smith and Whitehouse, 2012). Together these observations establish that inhibition of Pol δ progression through nucleosomal DNA is a key determinant of Okazaki fragment length in eukaryotes.

At first sight this notion seems contradictory to our finding that Pol α and/or Pol ε in the absence of Pol δ can synthesize short nascent lagging strands with a length distribution similar to canonical Okazaki fragments even on naked DNA. Importantly, however, we find that these nascent strands are

not ligatable and thus are not functional Okazaki fragments. This can be explained by our observation that Pol ε, unlike Pol δ, does not exhibit strand displacement or nick-translation activity with Fen1, as has also been observed previously (Garg et al., 2004), which is prerequisite for primer removal by Fen1. We speculate that the similar length distribution of canonical Okazaki fragments and nascent lagging strands synthesized by Pol α/Pol ε is coincidental and that nascent lagging strand lengths in the latter case are determined by the rate of primer synthesis by Pol α and subsequent gap-filling synthesis by Pol ε (or Pol α in the absence of RFC/PCNA).

A mechanism whereby nucleosomes inhibit progression of Pol δ requires chromatin to be rapidly assembled on the daughter strands behind the fork. In addition, nucleosomes need to be disassembled ahead of the fork to allow fork progression and recycling of the parental histones onto the replicated daughter strands. Numerous factors have been implicated in mediating replication-coupled chromatin assembly and disassembly (Alabert and Groth, 2012). Our findings suggest that Nap1 and Isw1a can promote both replication fork progression through nucleosomal DNA and assembly of nucleosomes on daughter strands *in vitro*; the intrinsic H3/H4 chaperone activity of the Mcm2 N-terminal tail may also contribute to these events (Clement and Almouzni, 2015). However, we note that the level of DNA synthesis is 5- to 6-fold reduced on chromatin relative to naked DNA, and the assembly of extended nucleosomal arrays on the daughter strands is inefficient, indicating that additional histone chaperones and chromatin remodeling factors may facilitate efficient chromatin replication *in vitro*. It will be interesting to exploit the system described here to analyze how known

replication-coupled chromatin assembly factors, such as CAF-1, Rtt106, FACT, and Asf1, coordinate their activities at the replication fork.

The rolling circle replication observed in the system described here, dependent on formation of CMG helicase as well as the polymerase activity of Pol ε, was enhanced by the presence of Pol δ. On the other hand, chromatinization of the template completely suppressed this replication. This raises an intriguing question regarding the potential mechanism by which chromatin inhibits rolling circle replication. One possibility is that chromatinization of the DNA significantly reduces the nicking of the template during the reaction resulting in reduced availability of nicks for priming the rolling circle replication. Alternatively, as rolling circle replication requires the recognition of the nick by the CMG-Pol ε complex be used as a primer chromatinization of the template could restrict the mobility of this complex. In future, rolling circle replication could provide an avenue to examine how CMG-Pol ε complex reaches the nick in the template.

We have shown previously that canonical origin sequences are not required for Mcm2-7 loading or origin activation *in vitro* (Gros et al., 2014; Gros et al., 2015; Remus et al., 2009). Nonetheless, we had found that ORC binding sites at ARS elements often exhibit the highest affinity for ORC within tested templates, resulting in the preferential loading of Mcm2-7 at these sites, and that mutation of the ORC binding site in ARS elements induced the redirection of Mcm2-7 loading to origin-distal sites, thus allowing the efficient replication of plasmids containing either mutant or wildtype origin sequences *in vitro* (Gros et al., 2014). In striking contrast, efficient plasmid replication is highly dependent on specific origin sequences in budding yeast cells (Marahrens and Stillman, 1992). Here we reconcile this discrepancy with the

finding that assembly of plasmids into chromatin establishes a dependency on specific origin sequences for efficient replication *in vitro*. We speculate that nucleosomes sequester lower-affinity non-canonical Mcm2-7 loading sites, while ORC bound at canonical origin sites may promote Mcm2-7 loading and replication initiation by establishing a permissive nucleosome-free region (Eaton et al., 2010).

Pol α synthesizes DNA with a high error rate due to its lack of proofreading activity (Kunkel, 2004), requiring that Pol α-synthesized DNA in the genome be kept at a minimum to ensure maintenance of the genetic information. Errors made by Pol α can be corrected by Pol δ during Okazaki fragment maturation (Pavlov et al., 2006). In addition, we find here that PCNA loading by RFC efficiently inhibits primer extension by pol α on both leading and lagging-strand template. These observations differ from earlier results obtained with the SV40 system, where it was found that RFC/PCNA inhibits primer extension by Pol α specifically on the leading strand, whereas Pol α was able to extend primers on the lagging strand even in the presence of RFC/PCNA (Tsurimoto et al., 1990; Waga and Stillman, 1994). The reasons for this difference between budding yeast and SV40 replication are unclear, but they may indicate a departure of Pol α regulation in SV40 replication from that during cellular chromosomal replication.

We show here that both Pol α and Pol ε can contribute under certain conditions to the synthesis of nascent lagging strands *in vitro*. However, Pol δ is essential for the synthesis of functional Okazaki fragments, as only Pol δ can perform the strand displacement required for primer removal by Fen1. Experiments that employed isolated recombinant CMG and synthetic fork substrates suggested that CMG does not support processive DNA synthesis

by Pol δ on the leading strand and that Pol ε moreover suppresses Pol δ activity on the leading strand (Georgescu et al., 2014; Georgescu et al., 2015). Contrary to these observations, we find here that in the absence of DNA synthesis by Polε, but in the presence of Pol ε^{pol-} complex, Pol δ can support efficient leading and lagging strand synthesis in conjunction with the CMG after regulated origin firing, as well as rolling circle replication when coupled to the CMG. These observations are consistent with the notion that Pol δ likely synthesizes both the leading and the lagging strand in cells depleted for Pol ε DNA polymerase activity (Dua et al., 1999; Kesti et al., 1999).

The system described here employs the proteins known to be essential for DNA replication in budding yeast cells. While efficient initiation and elongation of DNA replication are faithfully recapitulated by this system, termination of DNA replication appears to be inefficient. Future studies are, therefore, aimed at determining the conditions or identifying additional factors required for efficient termination. Moreover, it will be interesting to supplement the system with non-essential fork components such as Csm3-Tof1 and Mrc1, which are known to promote the rate of fork progression and fork stability *in vivo* (Bell and Labib, 2016).

Materials and methods

DNA templates

Plasmid pARS1 (4.8kb) was generated from pARS/WTA (Marahrens and Stillman, 1992) by excision of CEN4 with AfeI and PvuII. Plasmids pARS1-wt (5.9 kb), pARS1-A-B2- (5.9 kb), and pARS305 (9.8 kb) have been described previously (Gros et al.,2014).

The primer-template for DNA polymerase assays was generated by two-step PCR: In the first step, the 601 sequence was amplified with primers Fwd1 (5'-GATGCAGTAGCCTCGACTCGCATGACTCCGTCACGAGGGCGTTTTGGAG-3') and Rev1 (5'-ATCGAGAATCCCGGTGCC-3'). The PCR product was used as a template in a second PCR step, using the uracil-containing, and internally biotinylated, primer Fwd2 (5'-GTACC-bio-ATCTGCAGTGCTAATTGATGATCGAGGATCCGGAGGCTAGCGAAGAAGGGAGAUGCAGUAGCCUCGACUCGCAUGACUCCGUCA-3'), and 5'-biotinylated primer Rev2 (5'-bio-ATCGAGAATCCCGGTGCC 3'). The final PCR product was 5'-radiolabeled using [γ-32P]ATP and T4 polynucleotide kinase. USER (Uracil-Specific Excision Reagent, NEB) enzyme was used to remove uracils from the template, generating a single-stranded DNAgap in the substrate.

Protein purification

Human Topo II was purchased from Sigma. Human Fen1 was purchased from Syd Labs. E. coli SSB was a gift from Ken Marians (MSKCC). ORC, Cdc6, Cdt1·Mcm2-7, DDK, Mcm10, S. cerevisae histone octamers, and Nap1 were purified essentially as described (Gros et al., 2014; He et al., 1996; Kingston et al., 2011; McBryant et al., 2003).

Pol α

Strain YSD16 was grown at 30°C in YP-GL (YP + 2% glycerol / 2% lactic acid) to a density of 2 x10^7 cells / ml, and expression induced for 3 hours by addition of 2% galactose. Cells were harvested by centrifugation, washed once with 1M sorbitol/25 mM Hepes-KOH pH 7.6, once with buffer A (25 mM

Tris-HCl pH 7.5 / 10 % glycerol / 0.02 % NP-40) / 0.1 M NaCl, resuspended in 0.5 volumes of buffer A / 0.1 M NaCl / 1 mM DTT / protease inhibitors, and frozen dropwise in liquid nitrogen. The resulting popcorn was stored at -80°C until further processing. Cell lysate was prepared by crushing the frozen popcorn in a freezer mill (SPEX CertiPrep 6850 Freezer/Mill) for 6 cycles of 2 minutes at a rate of 15 impacts per second. Crushed cell powder was thawed on ice, resuspended with 1 volume of buffer A / 0.1 M NaCl / 1 mM DTT. The suspension was supplemented with an additional 0.3 M NaCl, and insoluble material pelleted by centrifugation in a T647.5 rotor (Thermo Scientific) for 30 minutes at 40,000 rpm. The clarified extract was supplemented with 2 mM $CaCl_2$ and incubated with calmodulin affinity beads for 2 hours at 4ºC. The calmodulin resin was washed with 10 CV of buffer A / 300 mM NaCl / 2 mM $CaCl_2$ / 1 mM DTT, and bound protein eluted with 8 CV of buffer A / 1 mM EDTA / 2 mM EGTA / 1 mM DTT. Peak fractions were pooled, dialyzed against buffer A / 120 mM NaCl / 1 mM DTT, and fractionated on a Mono Q column using an elution gradient of 0.12 – 1 M NaCl over 20 CV. Mono Q peak fractions were pooled and fractionated by gel-filtration on a Superdex 200 column equilibrated in buffer A / 150 mM NaCl / 1 mM DTT. Peak fractions were pooled and stored in aliquots of ~ 1 mM Pol α at -80ºC after snap freezing in liquid nitrogen. Protein yield was 1 – 2 mg per 12 L of culture.

Cdc45

Strain YSD15 was grown at 30°C in YP-GL to a density of 2 $x10^7$ cells / ml, arrested in G1 phase with 100 ng / ml a-factor, and expression induced for 3 hours by addition of 2% galactose. FLAG-tagged Cdc45 was purified from these cells essentially as described (Yeeles et al., 2015). Peak fractions were

pooled and stored in aliquots of ~ 2 mM Cdc45 at -80ºC after snap freezing in liquid nitrogen. Protein yield was 1 – 2 mg per 12 L of culture.

Sld2

Strain YSD13 was grown at 30°C in YP-GL (YP + 2% glycerol / 2% lactic acid) to a density of 2 x10^7 cells / ml, and expression induced for 2 hours by addition of 2% galactose. Cells were harvested by centrifugation, washed once with 1M sorbitol/25 mM Hepes-KOH pH 7.6, once with buffer B (25 mM Hepes-KOH pH 7.6 / 10 % glycerol / 0.02 % NP-40 / 1 mM EDTA) / 0.1 M KCl, resuspended in 0.5 volumes of buffer B / 0.1 M KCl / 1 mM DTT / protease inhibitors, and frozen dropwise in liquid nitrogen. The resulting popcorn was stored at -80°C until further processing. Cell lysate was prepared by crushing the frozen popcorn in a freezer mill (SPEX CertiPrep 6850 Freezer/Mill) for 6 cycles of 2 minutes at a rate of 15 impacts per second. Crushed cell powder was thawed on ice and resuspended with 1 volume of buffer B / 0.1 M KCl. The suspension was supplemented with an additional 0.4 M KCl, and insoluble material pelleted by centrifugation in a T647.5 rotor (Thermo Scientific) for 60 minutes at 40,000 rpm. FLAG- tagged Sld2 was subsequently isolated from the clarified extract as described (Yeeles et al., 2015). Peak fractions were pooled and stored in aliquots of ~ 1 mM Sld2 at -80ºC after snap freezing in liquid nitrogen. Protein yield was 1 – 2 mg per 12 L of culture.

Isw1a

Strain YSA10 was grown at 30°C in YP-GL to a density of 2 x10^7 cells / ml, arrested for 3 hours in G1 phase by addition of 100 ng / ml a-factor, and expression of Isw1-FLAG and Ioc3 induced for 4 hours by addition of 2%

galactose. Cells were harvested by centrifugation, washed twice with ice-cold H2O, once with buffer C (25 mM Hepes-KOH pH 7.6 / 0.1 mM EDTA / 0.5 mM EGTA / 2 mM $MgCl_2$ / 20 % glycerol / 0.02 % NP-40) / 0.3 M KCl / 1 mM DTT / protease inhibitor mix, resuspended in 1 volume of buffer C /0.3 M KCl / 1 mM DTT, and frozen dropwise in liquid nitrogen. The resulting popcorn was stored at -80°C until further processing.Cell lysate was prepared by crushing the frozen popcorn in a freezer mill (SPEX CertiPrep 6850 Freezer/Mill) for 6 cycles of 2 minutes at a rate of 15 impacts per second. Crushed cell powder was thawed on ice, resuspended with 1 volume of buffer C / 0.3 M KCl / 1 mM DTT, and soluble extract prepared by centrifugation of the suspension in a T647.5 rotor (Thermo Scientific) for 1 hour at45,000 rpm. The clarified supernatant was incubated for 3 hours with M2-agarose anti-FLAG beads (Sigma) at 4°C. Beads were recovered from the extract by centrifugation, washed three times with buffer C / 0.3 M KCl / 1 mM DTT, once with buffer C / 0.1 M KCl / 1 mM DTT, and bound proteins eluted with five resin volumes of buffer C / 0.1 M KCl / 1 mM DTT containing 0.25 mg/ml FLAG peptide. Peak fractions were pooled, applied to a Mono Q column, washed on the column with 10 CV of buffer C / 0.2 M KCl /1 mM DTT, and eluted in a gradient from 0.2 – 0.6 M KCl over 20 CV. Peak fractions were pooled, dialyzed against buffer C / 0.1 M KCl / 1 mM DTT, and stored in aliquots at -80°C after snap freezing in liquid nitrogen.

Sld3·Sld7

pET28b-His10-Smt3-Sld3 and pGEX-6P-1-Sld7 were co-transformed into BL21 DE3 Codon+ RIL cells. Cells were grown at 37 °C to a density of OD600 = 0.5-0.8, chilled on ice, supplemented with 2 % ethanol, and induced

with 1 mM IPTG over night at 18 °C. Cells were washed once in PBS, and the washed cell pellet stored at −80°C until further processing. Cells were resuspended in buffer D (50 mM Tris-HCl pH7.5 / 0.05 % NP-40 / 10 % glycerol) / 1 M NaCl / 2 mM β-mercaptoethanol / protease inhibitors (Roche, complete protease inhibitor cocktail), supplemented with 1 mg/mL lysozyme, and incubated for 30 minutes at 4°C with agitation. The cells were then lysed by sonication, and insoluble material was removed by centrifugation for 30 minutes at 15,000 rpm in an SS34 rotor. 0.25 g/ml solid ammonium sulfate was added to the supernatant, followed by gentle stirring, and centrifugation for 30 minutes at 15,000 rpm in an SS34 rotor. The protein pellet was resuspended in buffer D / 0.5 M NaCl / 2 mM β- mercaptoethanol and dialyzed against the same buffer for 2 hours at 4°C. After dialysis, the extract was incubated with glutathione sepharose for 3 hours at 4°C. The resin was washed with 10 CV of buffer A / 0.5 M NaCl / 2 mM β-mercaptoethanol, and bound protein eluted with 10 CV of buffer A / 0.5 M NaCl / 2 mM β-mercaptoethanol / 2 M glutathione. The eluates were pooled, dialyzed against buffer D / 0.3 M NaCl / 20 mM imidazole and incubated with PreScission protease (GE Healthcare) to remove the GST-tagfrom Sld7. The eluate was then incubated with Ni2+-NTA resin for 3 hours at 4°C. The resin was washed extensively with buffer D /0.3 M NaCl / 20 mM imidazole / 2 mM β-mercaptoethanol, and bound protein eluted with 10 CV of buffer D / 0.3 M NaCl / 200 mM imidazole / 2 mM β-mercaptoethanol. Peak fractions were pooled and separated on a Superose 6 column equilibrated in 25 mM Hepes-KOH pH 7.6 / 0.05 % NP-40 / 10% glycerol / 300 mM K-acetate / 2 mM β-mercaptoethanol. Peak fractions were pooled and stored in aliquots of ~ 1 mM

Sld3·Sld7 at -80ºC after snap freezing in liquid nitrogen. Protein yield was 1 – 2 mg per 6 L of culture.

Pol ε / Pol ε-D640A

Strain YDR116 was grown at 30°C in YP-GL to a density of 2 x10^7 cells / ml, arrested for 3 hours in G1 phase by addition of100 ng/ml a-factor, and protein expression induced for 4 hours by addition of 2% galactose. Cells were harvested by centrifugation, washed once with 1 M sorbitol / 25 mM Hepes-KOH pH 7.6 and once with buffer E (45 mM Hepes-KOH pH 7.6 / 10 % glycerol /0.02 % NP-40S) / 0.1 M NaCl / 1 mM DTT / protease inhibitors, resuspended in 0.5 volumes of buffer E / 0.1 M NaCl / 1 mM DTT, and frozen dropwise in liquid nitrogen. The resulting popcorn was stored at -80°C until further processing. Cell lysate was prepared by crushing the frozen popcorn in a freezer mill (SPEX CertiPrep 6850 Freezer/Mill) for 6 cycles of 2 minutes at a rate of 15 impacts per second. Crushed cell powder was thawed on ice, resuspended with 1 volume of buffer E / 0.1 M NaCl / 1 mM DTT. The salt concentration was adjusted to 0.3 M NaCl, and insoluble material pelleted by centrifugation of the suspension in a T647.5 rotor (Thermo Scientific) for 1 hour at 45,000 rpm. The clarified supernatant was supplemented with 2 mM $CaCl_2$ and incubated for 2 hours with calmodulin sepharose at 4°C. The resin was washed extensively with buffer E / 0.3 M NaCl / 2 mM $CaCl_2$, and bound protein eluted with 10 CV of buffer E / 0.3 M NaCl / 2 mM EGTA / 1 mM EDTA / 1 mM DTT. Peak fractions were pooled, applied to a Mono Q column, and eluted in a gradient from 0.15 – 0.5 M NaCl in buffer E / 1 mM DTT over 20 CV. Mono Q peak fractions were pooled and further fractionated by gel-filtration on a Superdex 200 column equilibrated in buffer E / 0.3 M K-acetate /

1 mM DTT. Peak fractions were pooled and stored in aliquots of ~ 2 mM Pol ε at -80ºC after snap freezing in liquid nitrogen. Protein yield was 2 – 4 mg per 12 L of culture. Polε-D640A was purified identically to Polε.

Clb5·Cdk1

Strain YDR105 was grown at 30°C in YP-GL to a density of 2 x10^7 cells / ml, and protein expression induced for 4 hours by addition of 2% galactose. Clb5·Cdk1 was subsequently purified using the procedure described for Polε. Final peak fractions were pooled and stored in aliquots of ~ 2 mM Clb5·Cdk1 at -80ºC after snap freezing in liquid nitrogen. Protein yield was 1 – 2 mg per 12L of culture.

GINS

GINS was purified from strain YDR109 using the procedure described for Pol ε. Final peak fractions were pooled and stored in aliquots of ~ 2 mM GINS at -80ºC after snap freezing in liquid nitrogen. Protein yield was 2 – 4 mg per 12 L of culture.

Dpb11

Strain YDR110 was grown at 30°C in YP-GL to a density of 2 x10^7 cells / ml, arrested for 3 hours in G1 phase by addition of100 ng/ml a-factor, and protein expression induced for 4 hours by addition of 2% galactose. Cells were harvested by centrifugation, washed once with 1 M sorbitol / 25 mM Hepes-KOH pH 7.6 and once with buffer E / 0.1 M KCl / 1 mM DTT / protease inhibitors, resuspended in 0.5 volumes of buffer E / 0.1 M KCl / 1 mM DTT, and frozen dropwise in liquid nitrogen. The resulting popcorn was stored at -

80°C until further processing. Cell lysate was prepared by crushing the frozen popcorn in a freezer mill (SPEX CertiPrep6850 Freezer/Mill) for 6 cycles of 2 minutes at a rate of 15 impacts per second. Crushed cell powder was thawed on ice, resuspended with 1 volume of buffer E / 0.1 M KCl / 1 mM DTT. The salt concentration was adjusted to 0.3 M KCl, and insoluble material pelleted by centrifugation of the suspension in a T647.5 rotor (Thermo Scientific) for 1 hour at 45,000 rpm. The clarified supernatant was supplemented with 2 mM $CaCl_2$ and incubated for 2 hours with calmodulin sepharose at 4°C. The resin was washed extensively with buffer E / 0.3 M KCl / 2 mM $CaCl_2$, and bound protein eluted with 10 CV of buffer E / 0.3 M KCl / 2mM EGTA / 1mM EDTA / 1 mM DTT. Peak fractions were pooled, applied to a Mono S column, and eluted in a gradient from 0.15 – 1 M KCl in buffer E / 1mM DTT over 20 CV. Peak fractions were pooled and dialyzed against buffer E / 0.3 M K-acetate / 1 mM DTT, and stored in aliquots of ~ 2 mM Dpb11 at -80ºC after snap freezing in liquid nitrogen. Protein yield was 2 – 4 mg per 12 L of culture.

Top2

Strain YSDR17 was grown at 30°C in YP-GL to a density of 2 x10^7 cells / ml, and protein expression induced for 6 hours byaddition of 2% galactose. Top2 was subsequently purified using the procedure described for Polε. Final peak fractions were pooled and stored in aliquots of ~ 1 mM Top2 at -80ºC after snap freezing in liquid nitrogen. Protein yield was 1 – 2 mg per 12 L of culture.

Top1

Top1 was purified from strain YDR 128. Cells were grown at 30°C in YP-GL to a density of 2 x10^7 cells / ml, and proteinexpression induced for 4

hours by addition of 2% galactose. Top1 was thereafter purified using the procedure described for Polε. Final peak fractions were pooled and stored in aliquots of ~ 1 mM Top1 at -80ºC after snap freezing in liquid nitrogen. Protein yield was 1 –2 mg per 12 L of culture.

RPA

RPA1, -2, and -3 were co-expressed in E. coli BL21 DE3 from plasmid pJM126 (He et al., 1996). Cells were grown at shaking condition to 37ºC in LB/ampicillin/chloramphenicol to OD600 = 0.2. Cultures were then shifted to 17ºC and grown until OD600 = 0.5. Expression was induced for 4 hours at 30ºC by addition of 0.4 mM IPTG. Cells were harvested by centrifugation and the cell pellet stored at -80ºC until further processing. Cell pellets were thawed on ice, resuspended in buffer F (25 mM Tris HCl pH 7.5 / 1 mM EDTA / 10 % glycerol) / 1 M NaCl / 1 mM DTT / protease inhibitors / 0.1 mg/ml lysozyme, and cells lyzed by sonication. The resulting extract was clarified by centrifugation in an SS34 rotor for 15 min at 12,000 rpm. Clarified extract was diluted 1:1 with cold buffer F / 1 mM DTT to reduce salt concentration to 0.5 M NaCl and applied to a HiTrap Blue HP column pre-equilibrated in buffer A / 0.5 M NaCl / 1 mM DTT. The column was washed sequentially with buffer F / 0.5 M NaCl / 1 mM DTT and buffer A / 0.8 M NaCl / 1 mM DTT, and bound protein eluted in buffer F / 2.5 M NaCl / 1 mM DTT / 40 % ethylene glycol. Peak fractions were pooled, diluted with buffer F /1 mM DTT to reduce the salt concentration to 0.5 M NaCl, and applied to ssDNA cellulose (Worthington). The ssDNA resin as washed with 2 CV buffer F / 0.5 M NaCl / 1 mM DTT, followed by 2 CV buffer F / 0.8 M NaCl / 1 mM DTT, and bound protein eluted with 5 CV buffer F / 1.5 M NaCl / 50 % ethylene glycol. Peak fractions were

pooled, dialyzed against buffer F / 0.15 M NaCl /1 mM DTT, and fractionated on a MonoQ column with a gradient of 0.15 M NaCl – 1 M NaCl in buffer F / 1 mM DTT over 20 CV. Peak fractions were pooled, dialyzed against buffer F / 0.1 M NaCl / 1 mM DTT, and stored in aliquots of 5 – 10 mM RPA at -80ºC after snap freezing in liquid nitrogen. Protein yield was ~ 2 mg per 1 L of culture.

Ctf4

A culture of E. coli BL21 DE3 RIL codon+ transformed with plasmid xxx was grown at 37°C in LB / ampicillin /chloramphenicol to an OD600 = 0.7, subjected to a cold shock in ice water for 20 minutes, and expression induced at 25°C over nightby addition of 1 mM IPTG and 2 % ethanol. The cells were harvested by centrifugation, washed twice with ice cold PBS, and stored at-80°C until further processing. The cell pellet was resuspended in buffer G (25 mM Hepes-KOH / 10 % glycerol / 0.05% NP40) / 1M NaCl / 2 mM b - mercaptoethanol / protease inhibitor cocktail, supplemented with 0.1 mg/ml lysozyme, and incubated for 20 minutes on ice. The cells were lysed by sonication, and insoluble material removed by centrifugation in an SS34 rotor for 30 minutes at 15,000 rpm. The clarified extract was incubated for 1 hour with Ni++-NTA agarose beads at 4°C. The beads were recovered by centrifugation, washed with 3 CV of buffer G / 0.5 M NaCl / 2 mM 2-mercaptoethanol, and bound protein eluted with 5 CV of buffer G / 0.5 M NaCl/ 100 mM imidazole / 2 mM 2-mercaptoethanol. Peak fractions were pooled, dialyzed against buffer G / 0.1 M NaCl / 2 mM b - mercaptoethanol, and fractionated on a Mono Q column using an elution gradient of 0.1 M – 1 M NaCl in buffer G / 2 mM b- mercaptoethanol over 30 CV. Peak fractions were

pooled and fractionated by gel-filtration on a Superdex 200 column equilibrated in45 mM Hepes-KOH pH 7.5 / 300 mM potassium acetate / 0.02 % NP-40 / 10 % glycerol / 2 mM b-mercaptoethanol. Peak fractions were pooled and stored in aliquots of ~ 3 mM at -80ºC after snap freezing in liquid nitrogen. Final peak fractions were pooled and stored in aliquots of ~ 3 mM Ctf4 at -80ºC after snap freezing in liquid nitrogen. Protein yield was ~ 1 mg per 1 L of culture.

RFC

Strain YIW389 was grown at 30°C in YP-GL to a density of 2 x10^7 cells / ml, after which protein overexpression was induced for 3 hours by addition of 2% galactose. Cells were harvested by centrifugation, washed sequentially once with buffer A (1M sorbitol / 25 mM Hepes-KOH pH 7.6) and with buffer H (25 mM Tris-HCl pH 7.5 / 10 % glycerol) / 100 mM NaCl, and finally resuspended in 0.5 volumes of buffer H / 100 mM NaCl / 1 mM DTT / protease inhibitor mix, and frozen dropwise in liquid nitrogen.Cell lysate was prepared by crushing the frozen popcorn in a freezer mill (SPEX CertiPrep 6850 Freezer/Mill) for 6 cycles of 2 minutes at a rate of 15 impacts per second. The resulting cell powder was thawed on ice, and resuspended in 1 volume of buffer H /0.02 % NP-40 / 100 mM NaCl / 1 mM DTT. The final NaCl concentration was adjusted to 0.4 M, and insoluble material pelleted by ultracentrifugation at 40,000 rpm for 30 minutes. Complexes were immuno-precipitated for 4 hours at 4°C from the clarified extract using M2 agarose anti-FLAG beads (Sigma). The resin was recovered from the extract, washed with 5 CV buffer H / 300 mM NaCl /1 mM DTT, and bound protein eluted with 4 CV buffer H / 300 mM NaCl / 0.5 mg ml-1 3xFLAG peptide. Peak fractions

from theFLAG pull-down were pooled and dialyzed against buffer H / 100 mM NaCl / 1 mM DTT and fractionated on a Mono Q column using gradient of 0.1 – 1 M NaCl in buffer H over 20 CV. Mono Q peak fractions were pooled and fractionated by gel-filtration on a Superdex 200 column equilibrated in 25 mM Hepes-KOH pH 7.6 / 300 mM K-acetate / 1 mM EDTA / 10 % glycerol / 1 mM DTT. Peak fractions were pooled and stored in aliquots of ~ 1 mM RFC at -80ºC after snap freezing in liquid nitrogen. Protein yield was ~ 2- 4 mg per 12 L of culture.

PCNA

PCNA was expressed as a His-tag fusion protein in E. coli BL21 DE3. Cells were grown at 37°C to OD600 = 0.5. After a 30 minute cold shock on ice, expression was induced at 20°C overnight by adding isopropyl-1-thio-β-D-galactopranoside (IPTG) to a final concentration of 0.5 mM. The cells were harvested by centrifugation and stored at -80ºC until further processing. The cell pellet was resuspended in 50 mM Na-phosphate pH 7.6 / 400 mM NaCl / 10 mM imidazole / 1 mM DTT / 0.1 mg/ml lysozyme, incubated for 15 minutes on ice, and cells lyzed by sonication. Cell debris was removed by centrifugation in an SS34 rotor at 14,000 rpm for 30 minutes. After incubation of the clarified extract with Ni++-NTA agarose beads for 2 hours at 4ºC, the resin was recovered by centrifugation, washed with 5 CV of 50 mM Na-phosphate pH 7.6 / 400 mM NaCl / 10 mM imidazole / 1 mM DTT, and bound protein eluted with 8 CV of 50 mM Na-phosphate pH 7.6 / 400 mM NaCl / 150 mM imidazole / 1 mM DTT. Peak fractions were pooled and dialyzed against buffer F / 0.1 M NaCl / 1 mM DTT, and fractionated on a Mono Q column using an elution gradient of0.1 – 1 M NaCl in buffer F over 20 CV, followed by

fractionation on a Superdex 200 gel-filtration column equilibrated in 25 mM Hepes-KOH pH 7.6 / 300 mM K-acetate / 1 mM EDTA / 10 % glycerol / 1 mM DTT. Peak fractions were pooled and stored in aliquots of ~ 5 mM PCNA at -80ºC after snap freezing in liquid nitrogen. Protein yield was ~ 5 mg per 1 L of culture.

Pol δ

Strain YDR131 was grown at 30°C in YP-GL to a density of 2 x10^7 cells/ml, after which protein overexpression wasinduced for 4 hours by addition of 2% galactose. Cells were harvested by centrifugation, washed sequentially once with 1M sorbitol /25 mM Hepes-KOH pH 7.6 and with buffer I (30 mM Hepes-KOH pH 7.6 / 2 mM EDTA / 1 mM EGTA / 0.02 % NP-40 / 10 %glycerol), and finally resuspended in 1 volume of buffer I / 1 mM DTT / protease inhibitor mix, and frozen dropwise in liquidnitrogen. Cell lysate was prepared by crushing the frozen popcorn in a freezer mill (SPEX CertiPrep 6850 Freezer/Mill) for 6 cycles of2 minutes at a rate of 15 impacts per second. The resulting cell powder was thawed on ice, and resuspended in 1 volume of buffer I / 1 mM DTT. 0.15 M ammonium sulfate and 0.45 % polymin P pH 7.3 were stirred into the cell lysate, and the suspension centrifuged for30 min at 40,000 rpm in a T647.5 rotor (Thermo Scientific). Proteins in the clarified extract were precipitated by addition of 0.3 g/mlof solid ammonium sulfate and centrifugation for 30 min at 40,000 rpm in a T647.5 rotor. The resulting protein pellet was resuspended in buffer I / 250 mM NaCl / 1 mM DTT, followed by two hours of dialysis against buffer I / 250 mM NaCl / 1 mM DTT. The extract was incubated for 2 hours with glutathione-sepharose at 4ºC. The resin was subsequently washed with 5 CV buffer I / 250 mM NaCl /1 mM DTT, 5 CV

buffer A / 250 mM NaCl / 5 mM Mg-acetate / 1 mM DTT, and 5 CV buffer I / 150 mM NaCl / 1 mM DTT. Bound protein was eluted with 6 CV buffer I / 150 mM NaCl / 20 mM glutathione / 1 mM DTT. Peak fractions were pooled and digested with TEV protease over night at 4ºC to remove the GST-tag from Pol3. The sample was diluted with 2 volumes of buffer K (25 mM Hepes-KOH pH 7.6 / 1 mM EDTA / 1 mM EGTA / 0.01 % NP-40 / 10 % glycerol) to reduce the NaCl concentration to 50 mM, and fractionated over a Mono S column, using an elution gradient of 0.05 – 1 M NaCl in buffer K. Peak fractions containing the full Polδ complex were pooled and fractionated by gel-filtration on a Superdex 200 column equilibrated in 25 mM Hepes-KOH pH 7.6 / 300 mM K-acetate / 1 mM EDTA / 10 % glycerol / 1 mM DTT. Peak fractions were pooled and stored in aliquots of ~ 1 mM Pol δ at -80ºC after snap freezing in liquid nitrogen. Protein yield was ~ 1 mg per 12 L of culture.

Fen1

A culture of E. coli BL21 DE3 transformed with plasmid pET28a-Fen1 was grown at 37°C to OD600 = 0.5, transferred to ice water for 30 minutes, and expression induced at 20°C over night by adding isopropyl-1-thio-β-D-galactopranoside (IPTG) to final concentration of 0.5 mM. The cells were harvested by centrifugation and stored at -80°C until further processing. The cell pellet wasresuspended in 50 mM sodium phosphate pH 7.6 / 400 mM NaCl / 10 mM imidazole / 1 mM DTT, followed by addition of 0.1 mg/mllysozyme and incubation for 15 minutes on ice. Cells were lysed by sonication, and insoluble material removed by centrifugation in an SS34 rotor for 30 minutes at 14,000 rpm. The clarified extract was rotated for 2 hours with

Ni++-NTA agarose at 4°C. The Ni++-resin was recovered by centrifugation, washed with 5 CV of 50 mM sodium phosphate pH 7.6 / 400 mM NaCl / 10 mM imidazole / 1 mM DTT, and bound protein eluted with 8 CV resin volumes of 50 mM sodium phosphate pH 7.6 / 400 mM NaCl / 150 mM imidazole / 1 mM DTT. Peak fractions were pooled, dialyzed against 25 mM Tris-HCl pH 7.5 / 0.1 M NaCl / 1 mM EDTA / 10 % glycerol / 1 mM DTT, and passed over a Mono Q column. The flow-through from the Mono Q column, which contains Fen1, was incubated with thrombin for 2 hours at 4ºC to remove the His-tag from Fen1, and further fractionated by gel-filtration on a Superdex 200 column equilibrated in 25 mM Hepes-KOH pH 7.6 / 300 mM KOAc / 1 mM EDTA / 10 % glycerol / 1 mM DTT. Peak fractions were pooled and stored in aliquots of ~ 2 mM Fen1 at -80°C after snap freezing in liquid nitrogen. Protein yield was ~ 1 mg per 1 L of culture.

Cdc9

A culture of E. coli BL21 DE3 transformed with plasmid pET15b-Cdc9 was grown at 37°C to OD600 = 0.5, transferred to ice water for 30 minutes, and expression induced at 20°C over night by adding isopropyl-1-thio-β-D-galactopranoside (IPTG) to final concentration of 0.5 mM. The cells were harvested by centrifugation and stored at -80°C until further processing. The cell pellet was resuspended in 50 mM Sodium phosphate pH 7.6 and was resuspended in 50 mM sodium phosphate pH 7.6 / 400 mM NaCl / 10 mM imidazole / 1 mM DTT, followed by addition of 0.1 mg/ml lysozyme and incubation for 15 minutes on ice. Cells were lysed by sonication, and insoluble material removed by centrifugation in an SS34 rotor for 30 minutes at 14,000 rpm. The clarified extract was rotated for 2 hours with Ni++-

NTA agarose at 4°C. The Ni++-resin was recovered by centrifugation, washed with 5 CV of 50 mM sodium phosphate pH 7.6 / 400 mM NaCl / 10 mM imidazole / 1 mM DTT, and bound protein eluted with 8 CV resin volumes of 50 mM sodium phosphate pH 7.6 / 400 mM NaCl / 150 mM imidazole / 1 mM DTT. Peak fractions were pooled, dialyzed against buffer F / 0.1 M NaCl / 1 mM DTT, and fractionated on a Mono Q column using an elution gradient of 0.1 – 1 M NaCl over 20 CV in buffer F / 1 mM DTT. Peak fractions were pooled and further fractionated by gel-filtration on a Superdex 200 column equilibrated in 25 mM Hepes-KOH pH 7.6 / 300 mM K-acetate / 1 mM EDTA / 10 % glycerol / 1 mM DTT. The purified protein was stored in aliquots of ~ 1 mM Cdc9 at -80°C after snap freezing in liquid nitrogen.
Protein yield was ~ 1 mg per 1 L of culture.

DNA replication assay

Reactions were performed at 30°C. Mcm2-7 loading was carried out for 20 minutes in a reaction volume of 20 ml containing 50 nM ORC, 50 nM Cdc6, 100 nM Cdt1·Mcm2-7, and 10 nM plasmid DNA template in 25mM Hepes-KOH pH 7.6 / 0.02 % NP-40 / 10 mM magnesium acetate / 5 % glycerol / 100 mM K-Acetate / 2 mM DTT / 5 mM ATP. DDK was then added to the loading reaction and incubation was continued for 20 minutes. Subsequently, BSA, Sld3·7 and Cdc45 were added to the mix and incubation continued for 5 minutes. Then CDK, GINS, Polε, Dpb11 and Sld2 were added to the reaction and incubated for 10min, followed by the addition of RPA, Ctf4, Polα, topoisomerase, RFC, PCNA, Cdc9, Fen1, Polδ, dNTP mix, CTP, GTP, UTP, and α^{32}P-dCTP. Mcm10 was added last into the reaction. The final volume was 50 ml and consisted of 1 mg/ml BSA, 60 nM DDK, 20 nM Sld3·7, 40 nM

Cdc45, 80 nM CDK, 80 nM GINS, 24 nM Polε, 40 nM Dpb11, 50 nM Sld2, 210 nM RPA, 30 nM Ctf4, 45 nM Polα, 80 mM dNTPs, 192 mM each CTP, GTP, and UTP, 66 nM α^{32}P-dCTP (3,000 Ci/mmol, Perkin-Elmer), 20 nM RFC, 70 nM PCNA, 20 nM Polδ, 20 nM Fen1, 36 nM Cdc9 and 20 nM Mcm10. Top1 or Top2 were included at 20 nM, while 2 U of hTopo II were included, as indicated. Reactions were terminated by incubation for 30 minutes at 37°C with 40 mM EDTA, 1.6 U Proteinase K, and 0.8% SDS. DNA was isolated by phenol/chloroform extraction and ethanol precipitation, and fractionated on native (1 × TAE) or alkaline (30 mM NaOH, 2 mM EDTA) 0.8% agarose gels. Gels were dried onto Whatman paper and analyzed by phosphor-imaging. For replication reactions on chromatin, nucleosomes were first assembled in a volume of 10 ml for one hour at 30ºC as described (Vary et al., 2004), using 3.1 mM Nap1, 350 nM histone octamer, 50 nM Isw1a, 20 nM plasmid template, and 100 nM ORC. The reaction was then continued as described above.

Primer-template extension assay

Nucleosome core particles were reconstituted at the 601 nucleosomal positioning sequence of the primer-template by salt dialysis as described previously (Luger et al., 1999). Biotinylated primer-template (5 fmol per reaction) was pre-incubated with streptavidin (500 fmol per reaction) on ice for 30 min. The streptavidin-bound primer-template was then incubated in a reaction volume of 34 µl with 25 fmol of RFC, and 25 fmol of PCNA for 10 min at 30°C, followed by the addition of 500 fmol of Pol δ and 25 pmol of human Fen1 for 30 min at 37°C. Reaction buffer contained 20 mM Tris-acetate, pH 7.8 / 1 mM DTT / 100µg/ml BSA / 2 mM $MgAc_2$ / 1 mM ATP / 100 µM dNTPs /

50mM NaCl. Reactions were terminated by freezing the samples in liquid N_2. DNA was purified from the reaction by phenol/chloroform and ethanol precipitation, and analyzed by 6% urea denaturing gel-electrophoresis and autoradiography

Okazaki fragment sequencing

DNA from a complete replication reaction on chromatinized pARS1 (4.8 Kb) in the absence of Cdc9 was purified as described (Smith and Whitehouse, 2012). Peak fractions from source 15Q elution containing short nascent fragments (150-500 bp) were pooled and ligated to adaptor primer pairs with single-stranded overhangs. Purified libraries were amplified (16 cycles) using Illumina TruSeq barcoded primers. Libraries were sequenced on an Illumina platform. After deep sequencing, the reads were mapped back to pARS1 (4.8 Kb) as described (Smith and Whitehouse, 2012). Briefly, Bowtie 2 was used to align the reads to pARS1 (4.8 Kb) sequence and Bedtools was used to isolate reads on Watson and Crick strands. A 500 bp average sliding window was used to smooth the data and the resulting Watson and Crick read values at every base were plotted.

Table 3.1 List of yeast strains used in chapter three

Strain	Genotype
YSA10	*MATa ade2-1 ura3-1 his3-11,15 trp1-1 leu2-3,112 can1-100 pep4::HIS3 P/Gal10 (ADE2) ISW1- FLAG-KanMX P/Gal1 (TRP1) IOC3*
YSD15	*MATa ade2-1 ura3-1 his3-11,15 trp1-1 leu2-3,112 can1-100 pep4::kanMX bar::hphNAT1 Gal- GAL4 (HIS3) Gal-CDC45-IF (TRP1)*
YDR105	*MATa ade2-1 ura3-1 his3-11,15 trp1-1 leu2-3,112 can1-100 pep4::kanMX bar::hphNAT1 Gal- GAL4 (HIS3) Gal-CDC28/CLB5-CBP (LEU2)*
YDR109	*MATa ade2-1 ura3-1 his3-11,15 trp1-1 leu2-3,112 can1-100 pep4::kanMX bar::hphNAT1 Gal- GAL4 (HIS3) Gal-SLD5/PSF1-CBP (LEU2) Gal-PSF2/PSF3 (URA3)*
YDR116	*MATa ade2-1 ura3-1 his3-11,15 trp1-1 leu2-3,112 can1-100 pep4::kanMX bar::hphNAT1 Gal- GAL4 (HIS3) Gal-DPB2/DPB3 (LEU2) Gal-CBP-POL2 /DPB4 (URA3)*
YDR110	*MATa ade2-1 ura3-1 his3-11,15 trp1-1 leu2-3,112 can1-100 pep4::kanMX bar::hphNAT1 Gal- GAL4 (HIS3) Gal-DPB11-CBP (URA3)*
YSD13	*MATa ade2-1 ura3-1 his3-11,15 trp1-1 leu2-3,112 can1-100 pep4::kanMX bar::hphNAT1 Gal- GAL4 (HIS3) Gal-SLD2-FLAG (URA3)*
YSD16	*MATa ade2-1 ura3-1 his3-11,15 trp1-1 leu2-3,112 can1-100 pep4::kanMX bar::hphNAT1 Gal- GAL4 (HIS3) GAL-POL1/POL12 (URA3) GAL-CBP-PRI1/PRI2 (LEU2)*
YIW389	*MATa ade2-1 ura3-1 his3-11,15 trp1-1 leu2-3,112 can1-100 pep4::kanMX bar::hphNAT1 GAL- RFC1-FLAG-HAT (HIS) GAL1-10-RFC2/RFC3 (TRP1) GAL-RFC4/RFC5 (URA3)*
YDR131	*MATa ade2-1 ura3-1 his3-11,15 trp1-1 leu2-3,112 can1-100 pep4::kanMX bar::hphNAT1 Gal- GAL4 / POL32 (HIS3) Gal-GST-POL3/POL31 (TRP1) Gal-POL32 (URA3)*
YDR128	*MATa ade2-1 ura3-1 his3-11,15 trp1-1 leu2-3,112 can1-100 pep4::kanMX bar::hphNAT1 Gal- GAL4 (HIS3) GAL-CBP-TOP1 (LEU2)*
YSD17	*MATa ade2-1 ura3-1 his3-11,15 trp1-1 leu2-3,112 can1-100 pep4::kanMX bar::hphNAT1 Gal- GAL4 (HIS3) Gal-CBP-TOP2(LEU2)*
YDR132	*MATa ade2-1 ura3-1 his3-11,15 trp1-1 leu2-3,112 can1-100 pep4::kanMX bar::hphNAT1 Gal- GAL4 (HIS3) Gal-DPB2/DPB3 (LEU2) Gal-CBP-POL2D640A /DPB4 (URA3)*

CHAPTER FOUR

DISCUSSION

Perspective on Reconstitution of Eukaryotic DNA replication

Previous studies in bacteriophages (reviewed in (Alberts, 1987)), bacteria (reviewed in ((Marians, 1992), and eukaryotic viruses (reviewed in (Kelly, 2017)), have illustrated the power of reconstituted systems for the detailed mechanistic analysis of the DNA replication reaction. The reconstitution of eukaryotic DNA replication has, therefore, been a long-standing endeavor in the field. Budding yeast has been a model for the study of eukaryotic DNA replication. In a major breakthrough, Bell and Stillman in 1992 identified ORC as a protein that binds *in vitro* to yeast origins in the presence of ATP (Bell and Stillman, 1992). The discovery of ORC as an initiator protein for eukaryotic DNA replication led to the characterization of early events in origin activation that paved the way to recapitulate this process, namely pre-RC formation, in a cell free extract-based system (Seki and Diffley, 2000). Reconstitution of pre-RC formation with purified proteins then followed, allowing the elucidation of the structure of the loaded Mcm2-7 helicase form (Evrin et al., 2009; Kawasaki et al., 2006; Remus et al., 2009). The complement of initiation factors necessary for replication initiation as evidenced by *in vivo* studies was then purified and shown to be sufficient for activation of Mcm2-7 DHs (Yeeles et al., 2015). The thesis work being presented here advances on the origin activation system by demonstrating that origin activation in the reconstituted system is bidirectional, supports coordinated leading and lagging strand synthesis by the three replicative DNA

polymerases, Pol α, Pol δ, and Pol ε, and recapitulates canonical Okazaki fragment maturation (Devbhandari et al., 2017).

Key conclusions from the thesis

In chapter two, I report a soluble, cell free DNA replication system and show that pre-RCs reconstituted with purified proteins can support DNA replication in S-phase extracts. DNA replication in the system is dependent cellular replication factors including pre-RC, DDK, CDK, DNA polymerases and Mcm10, thus exhibiting hallmarks of cellular DNA replication. All three stages of the DNA replication reaction - initiation, elongation, and termination - are supported by the reconstituted pre-RCs. Hence, the results from this chapter demonstrate that the Mcm2-7 double hexamer (DH) loaded around dsDNA during pre-RC formation (Evrin et al., 2009; Remus et al., 2009) is a true intermediate of eukaryotic DNA replication initiation.

In chapter three, I build on the system from the preceding chapter and report regulated replication of plasmid DNA by stepwise addition of purified proteins. The system displays the essential hallmarks of the eukaryotic DNA replication including the following: (1) Origin activation is bidirectional; (2) three replicative DNA polymerases, Pol α, Pol ε and Pol δ coordinately synthesize leading and lagging strands; (3) maturation of the Okazaki fragment occurs in a canonical fashion requiring the coordinated activities of Pol δ , Fen1 and Cdc9. Using this system, we uncover two regulatory roles for chromatin during DNA replication: (1) promoting origin-dependence during DNA replication; (2) determining Okazaki fragment length by restricting Pol δ. Initiation and elongation of DNA replication are efficiently recapitulated by the system. However, termination of DNA replication appears to be inefficient.

The system described in this thesis provides a functional platform for the detailed mechanistic analysis of events during eukaryotic chromosome replication. Below, I discuss a few of the outstanding questions in the field and how the system described here can provide insight into these questions.

Remodeling of Mcm2-7 hexamer during activation

During pre-RC formation Mcm2-7 exists as a stable head-to-head DH encircling dsDNA (Evrin et al., 2009; Remus et al., 2009). For activation of its DNA helicase activity Mcm2-7 requires association with the essential co-factors Cdc45 and GINS to form the CMG (Ilves et al., 2010). Once activated the Mcm2-7 helicase translocates on ssDNA moving 3′ to 5′ on the leading strand template while displacing the lagging strand template (Fu et al., 2011). RPC contains just one copy of Mcm4 (Gambus et al., 2006) and CMG complex purified from Drospohilla egg extract consist of just one Mcm2-7 hexamer (Moyer et al., 2006) suggesting separation of double hexamer during activation of helicase. Additionally, using a single molecule assay it has been shown that sister replisomes can progress independently of each other indicating that in its active form the replicative helicase comprises a single CMG (Yardimci et al., 2010). Hence, the activation of the Mcm2-7 helicase in S-phase after DH formation in G1 phase requires a remarkable and topologically complex molecular remodeling. In both of the systems described in chapter two and three of this thesis, reconstituted pre-RCs with purified proteins can initiate DNA replication. However, the exact mechanism of helicase activation remains far from clear.

Recent biochemical and structural studies have helped to delineate certain aspects of the Mcm2-7 helicase activation mechanism (Abid Ali et al.,

2017; Douglas et al., 2018; Noguchi et al., 2017). It has been reported that CMG assembly is accompanied by initial DNA untwisting and separation of the Mcm2-7 DH into discrete but inactive CMGs (Douglas et al., 2018). Activation of CMG requires Mcm10 and after activation sister CMGs have to pass each other as they translocate with the N-terminal tier leading in the direction of translocation (Douglas et al., 2018; Georgescu et al., 2017). Additionally, comparison of the structure of Mcm2-7 DH bound to DNA with CMG bound to replication fork substrate suggest how initial DNA melting might occur and how the lagging strand might be extruded during helicase activation. DH to CMG transition has been proposed to stretch the DNA promoting its initial unwinding (Abid Ali et al., 2017; Noguchi et al., 2017).

Despite these advancement major questions are still unanswered. For example, initial CMG formation prior to its activation requires several firing factors, such as Sld3, Sld2, Dpb11, Pol ε and the helicase co-factors Cdc45 and GINS (Douglas et al., 2018; Yeeles et al., 2015). However, it is currently not known how these non-enzymatic factors (as the non-catalytic activity of Pol ε is essential for CMG formation (Araki, 2010; Dua et al., 1999; Kesti et al., 1999)) structurally contribute towards CMG formation and separation. The DH is a very stable complex with the two hexamers making extensive inter-hexameric contacts at the NTD interface (Li et al., 2015; Noguchi et al., 2017). How are the contacts between two hexamers disrupted during DH separation to form single CMGs? To better understand this process, it will be crucial to determine the structure of the activation intermediates. We (in chapter two) and others have shown that reconstituted pre-RCs support the DDK- and CDK-regulated recruitment of initiation factors (Gros et al., 2014; Heller et al., 2011; Yeeles et al., 2015) suggesting an approach for the reconstitution of

DDK- and CDK-dependent sub-complexes with purified proteins that may shed light on the structural transitions occurring during pre-RC activation.

Recently, DDK-phosphorylated Mcm2-7 DHs have been imaged by negative stain and cryo-EM (Abid Ali et al., 2017; On et al., 2014). While significant conformational change was not detected upon DDK phosphorylation, symmetrical additional density was observed at the N-terminal dimerization interface of Mcm4 and Mcm6 (Abid Ali et al., 2017). Mcm4 and Mcm6 phosphorylation is required for Sld3 binding (Deegan et al., 2016) and the additional density observed has been proposed to serve as a binding surface for Sld3 and the recruitment of downstream replication factors. The reconstituted system reported in this thesis supports the regulated initiation of DNA replication dependent on each of the firing factors (Fig 3.1) and hence provides a platform for the systematic structural study of pre-IC intermediate complexes by the stepwise addition of initiation factors to the pre-RC.

Activation of the replicative helicase, Mcm2-7 also requires the extrusion of the lagging strand template from the central Mcm2-7 channel (Deegan and Diffley, 2016). Recent evidence suggests that CMG translocates on dsDNA prior to getting activated by Mcm10 (Douglas et al., 2018). How Mcm10 is involved in extruding the lagging strand is not clear. Initiation factors Sld2, Dpb11 and Sld3 are not thought to be part of replisome (Gambus et al., 2006; Tanaka and Araki, 2013) but it is unknown when these proteins are released. It remains unclear if these proteins are involved in extrusion of ssDNA during helicase activation or if they are no longer needed for CMG activation after CMG formation. One way to answer this question would be to assay for the generation of ssDNA using ssDNA-specific nucleases such as

P1 or S1 nuclease, as has been previously used for the study of origin unwinding in the *E. coli* system (Bramhill and Kornberg, 1988). Individual protein requirement for strand extrusion can then be tested by a series of protein dropout experiments.

Termination of DNA replication

Termination of DNA replication in eukaryotes is not as extensively studied as initiation and elongation (Dewar and Walter, 2017). The system reported herein can provide a platform for studying the mechanistic basis of termination of DNA replication. As can be seen in Fig 3.2A a significant fraction of replication products from the minimal origin activation reaction with purified proteins on a circular plasmid template culminated in the formation of decatenated monomer in the presence of Top2 indicating that termination of DNA replication is supported in these reaction conditions. In the presence of Top1, but not Top2, slow migrating replication products accumulated. It has been unclear if the slow migrating replication products result from the inability of Top1 to decatenate plasmid daughters or if they result from a defect in termination. To answer this, it would be necessary to differentiate if the slow migrating replication products obtained in presence of Top1 contain catenated dimers or incompletely replicated molecules.

Addition of the third replicative DNA polymerase, Pol δ, along with the clamp loading machinery (RFC and PCNA), Fen1, and the Cdc9 ligase, to the origin activation system resulted in a large fraction of replication products migrating as higher molecular weight products in a native agarose gel indicating that the daughter molecules were either incompletely replicated or had failed to be decatenate (Fig 3.9) . One possibility is that one or more of the

components added to the origin activation system inhibits the completion of replication and/or decatenation activity of Topo II. Additionally, as the experiment performed represents only one concentration of proteins being used it could also be that one or more proteins being used is limiting in the reaction or on the other hand masking the activity of other proteins.

An interesting observation from the comparison of the partially reconstituted replication system with S-phase extract (chapter two) with the fully reconstituted system (chapter three) is that termination appears to be more efficient in the presence of S-phase extract (Compare Fig 2.3 vs Fig 3.9). Similarly, Xenopus egg extract supports efficient termination of DNA replication (Dewar et al., 2015; Moreno et al., 2014). These observations may suggest that the reconstitution system described here might be missing proteins that promote termination. To test this hypothesis, the effect of S-phase extract addition to the efficieny of termination in the reconstituted system can be monitored. Furthermore, if S-phase extract indeed does promote replication termination, the activity responsible can be isolated and identified via fractionation of the extract.

Replication of Chromatin

DNA replication through chromatin poses a unique challenge to the replisome, as it must disassemble the nucleosomes in front of the fork as well as deposit nucleosomes behind the fork (Alabert et al., 2017; Bell and Labib, 2016). Nucleosome assembly behind the replication fork has been shown to be intrinsically coupled to lagging strand synthesis (Smith and Whitehouse, 2012). Consistent with this, we observe that nucleosome assembly limits Okazaki fragment length in our system (Fig 3.5) by inhibiting progression of

Pol δ (Fig 3.8). We also observed that daughter strands were indeed packaged into nucleosomes, as postulated by our model. This raises the question about how the nucleosomes are deposited into daughter strands in our system, since the canonical replication-coupled chromatin assembly machinery such as CAF-1 and Asf1 were not included here. Furthermore, how are the nucleosomes ahead of the fork being disassembled? We suspect that nucleosome assembly components Nap1 and Isw1 present in our reaction might promote both disassembly of nucleosomes ahead of the fork and the assembly of nucleosomes into daughters. Indeed, *in vitro* Nap1 has ability to assemble chromatin (Ito et al., 1996) as well as remove nucleosomes from DNA (Lorch et al., 2006).

Recently, it has been reported that Mcm2 as well as Dpb3-Dpb4 are involved in the symmetrical segregation of parental nucleosomes into daughter strands (Petryk et al., 2018; Yu et al., 2018). Further, Pol α binds to H2A-H2B and contributes to maintain repressive chromatin states in budding yeast, while RPA has also been shown to bind to H3-H4 and contribute to replication-coupled nucleosome assembly (Evrin et al., 2018; Liu et al., 2017). These observations suggest that these core replisome components present in our replication system could be involved in both assembly and disassembly of nucleosomes. The system reported here thus can be used to determine the specific contribution of these histone binding proteins in the replisome towards replication coupled nucleosome assembly and disassembly.

Nucleosome deposition in our replication system seems to be inefficient evidenced by the lack of extended nucleosomal arrays on nascent strands after Mnase digestion. The level of DNA synthesis in our system is reduced by around five-fold on chromatin relative to naked DNA. This indicates that

additional histone chaperones and chromatin remodelers most likely required for efficient chromatin replication *in vitro*. The system being reported here thus is poised for the identification of factors that promote efficient replication coupled chromatin assembly.

REFERENCES

Abid Ali, F., Douglas, M.E., Locke, J., Pye, V.E., Nans, A., Diffley, J.F.X., and Costa, A. (2017). Cryo-EM structure of a licensed DNA replication origin. Nat Commun *8*, 2241.

Adachi, Y., and Laemmli, U.K. (1994). Study of the cell cycle-dependent assembly of the DNA pre-replication centres in Xenopus egg extracts. EMBO J *13*, 4153-4164.

Alabert, C., and Groth, A. (2012). Chromatin replication and epigenome maintenance. Nat Rev Mol Cell Biol *13*, 153-167.

Alabert, C., Jasencakova, Z., and Groth, A. (2017). Chromatin Replication and Histone Dynamics. Adv Exp Med Biol *1042*, 311-333.

Alberts, B.M. (1987). Prokaryotic DNA replication mechanisms. Philos Trans R Soc Lond B Biol Sci *317*, 395-420.

Andrews, A.J., Chen, X., Zevin, A., Stargell, L.A., and Luger, K. (2010). The histone chaperone Nap1 promotes nucleosome assembly by eliminating nonnucleosomal histone DNA interactions. Mol Cell *37*, 834-842.

Aparicio, O.M., Weinstein, D.M., and Bell, S.P. (1997). Components and dynamics of DNA replication complexes in S. cerevisiae: redistribution of MCM proteins and Cdc45p during S phase. Cell *91*, 59-69.

Araki, H. (2010). Cyclin-dependent kinase-dependent initiation of chromosomal DNA replication. Curr Opin Cell Biol *22*, 766-771.

Araki, H., Leem, S.H., Phongdara, A., and Sugino, A. (1995). Dpb11, which interacts with DNA polymerase II(epsilon) in Saccharomyces cerevisiae, has a dual role in S-phase progression and at a cell cycle checkpoint. Proc Natl Acad Sci U S A *92*, 11791-11795.

Ayyagari, R., Gomes, X.V., Gordenin, D.A., and Burgers, P.M. (2003). Okazaki fragment maturation in yeast. I. Distribution of functions between FEN1 AND DNA2. J Biol Chem *278*, 1618-1625.

Bai, L., Yuan, Z., Sun, J., Georgescu, R., O'Donnell, M.E., and Li, H. (2017). Architecture of the Saccharomyces cerevisiae Replisome. Adv Exp Med Biol *1042*, 207-228.

Balakrishnan, L., and Bambara, R.A. (2013a). Flap endonuclease 1. Annu Rev Biochem *82*, 119-138.

Balakrishnan, L., and Bambara, R.A. (2013b). Okazaki fragment metabolism. Cold Spring Harb Perspect Biol *5*.

Barnes, D.E., Johnston, L.H., Kodama, K., Tomkinson, A.E., Lasko, D.D., and Lindahl, T. (1990). Human DNA ligase I cDNA: cloning and functional expression in Saccharomyces cerevisiae. Proc Natl Acad Sci U S A *87*, 6679-6683.

Barry, J., and Alberts, B. (1972). In vitro complementation as an assay for new proteins required for bacteriophage T4 DNA replication: purification of the complex specified by T4 genes 44 and 62. Proc Natl Acad Sci U S A *69*, 2717-2721.

Baxter, J., and Diffley, J.F. (2008). Topoisomerase II inactivation prevents the completion of DNA replication in budding yeast. Mol Cell *30*, 790-802.

Bell, S.P. (1995). Eukaryotic replicators and associated protein complexes. Curr Opin Genet Dev *5*, 162-167.

Bell, S.P., and Dutta, A. (2002). DNA replication in eukaryotic cells. Annu Rev Biochem *71*, 333-374.

Bell, S.P., Kobayashi, R., and Stillman, B. (1993). Yeast origin recognition complex functions in transcription silencing and DNA replication. Science *262*, 1844-1849.

Bell, S.P., and Labib, K. (2016). Chromosome Duplication in Saccharomyces cerevisiae. Genetics *203*, 1027-1067.

Bell, S.P., and Stillman, B. (1992). ATP-dependent recognition of eukaryotic origins of DNA replication by a multiprotein complex. Nature *357*, 128-134.

Belotserkovskaya, R., Oh, S., Bondarenko, V.A., Orphanides, G., Studitsky, V.M., and Reinberg, D. (2003). FACT facilitates transcription-dependent nucleosome alteration. Science *301*, 1090-1093.

Berbenetz, N.M., Nislow, C., and Brown, G.W. (2010). Diversity of eukaryotic DNA replication origins revealed by genome-wide analysis of chromatin structure. PLoS Genet *6*, e1001092.

Bermejo, R., Doksani, Y., Capra, T., Katou, Y.M., Tanaka, H., Shirahige, K., and Foiani, M. (2007). Top1- and Top2-mediated topological transitions at

replication forks ensure fork progression and stability and prevent DNA damage checkpoint activation. Genes Dev *21*, 1921-1936.

Bleichert, F., Botchan, M.R., and Berger, J.M. (2015). Crystal structure of the eukaryotic origin recognition complex. Nature *519*, 321-326.

Blow, J.J., and Gillespie, P.J. (2008). Replication licensing and cancer--a fatal entanglement? Nat Rev Cancer *8*, 799-806.

Blow, J.J., and Laskey, R.A. (1988). A role for the nuclear envelope in controlling DNA replication within the cell cycle. Nature *332*, 546-548.

Bochman, M.L., and Schwacha, A. (2008). The Mcm2-7 complex has in vitro helicase activity. Mol Cell *31*, 287-293.

Boos, D., Frigola, J., and Diffley, J.F. (2012). Activation of the replicative DNA helicase: breaking up is hard to do. Curr Opin Cell Biol *24*, 423-430.

Borowiec, J.A., and Hurwitz, J. (1988). Localized melting and structural changes in the SV40 origin of replication induced by T-antigen. EMBO J *7*, 3149-3158.

Bowers, J.L., Randell, J.C., Chen, S., and Bell, S.P. (2004). ATP hydrolysis by ORC catalyzes reiterative Mcm2-7 assembly at a defined origin of replication. Mol Cell *16*, 967-978.

Bramhill, D., and Kornberg, A. (1988). A model for initiation at origins of DNA replication. Cell *54*, 915-918.

Braun, K.A., Lao, Y., He, Z., Ingles, C.J., and Wold, M.S. (1997). Role of protein-protein interactions in the function of replication protein A (RPA): RPA modulates the activity of DNA polymerase alpha by multiple mechanisms. Biochemistry *36*, 8443-8454.

Breier, A.M., Chatterji, S., and Cozzarelli, N.R. (2004). Prediction of Saccharomyces cerevisiae replication origins. Genome Biol *5*, R22.

Brewer, B.J., and Fangman, W.L. (1987). The localization of replication origins on ARS plasmids in S. cerevisiae. Cell *51*, 463-471.

Broach, J.R., Li, Y.Y., Feldman, J., Jayaram, M., Abraham, J., Nasmyth, K.A., and Hicks, J.B. (1983). Localization and sequence analysis of yeast origins of DNA replication. Cold Spring Harb Symp Quant Biol *47 Pt 2*, 1165-1173.

Burgers, P.M. (1991). Saccharomyces cerevisiae replication factor C. II. Formation and activity of complexes with the proliferating cell nuclear antigen and with DNA polymerases delta and epsilon. J Biol Chem *266*, 22698-22706.

Burgers, P.M. (2009). Polymerase dynamics at the eukaryotic DNA replication fork. J Biol Chem *284*, 4041-4045.

Burgers, P.M.J., and Kunkel, T.A. (2017). Eukaryotic DNA Replication Fork. Annu Rev Biochem *86*, 417-438.

Burgess, R.J., Zhou, H., Han, J., and Zhang, Z. (2010). A role for Gcn5 in replication-coupled nucleosome assembly. Mol Cell *37*, 469-480.

Byun, T.S., Pacek, M., Yee, M.C., Walter, J.C., and Cimprich, K.A. (2005). Functional uncoupling of MCM helicase and DNA polymerase activities activates the ATR-dependent checkpoint. Genes Dev *19*, 1040-1052.

Cadoret, J.C., Meisch, F., Hassan-Zadeh, V., Luyten, I., Guillet, C., Duret, L., Quesneville, H., and Prioleau, M.N. (2008). Genome-wide studies highlight indirect links between human replication origins and gene regulation. Proc Natl Acad Sci U S A *105*, 15837-15842.

Callebaut, I., Courvalin, J.C., and Mornon, J.P. (1999). The BAH (bromo-adjacent homology) domain: a link between DNA methylation, replication and transcriptional regulation. FEBS Lett *446*, 189-193.

Carpenter, P.B., Mueller, P.R., and Dunphy, W.G. (1996). Role for a Xenopus Orc2-related protein in controlling DNA replication. Nature *379*, 357-360.

Chafin, D.R., Vitolo, J.M., Henricksen, L.A., Bambara, R.A., and Hayes, J.J. (2000). Human DNA ligase I efficiently seals nicks in nucleosomes. EMBO J *19*, 5492-5501.

Champoux, J.J. (2001). DNA topoisomerases: structure, function, and mechanism. Annu Rev Biochem *70*, 369-413.

Chen, S., de Vries, M.A., and Bell, S.P. (2007). Orc6 is required for dynamic recruitment of Cdt1 during repeated Mcm2-7 loading. Genes Dev *21*, 2897-2907.

Chen, Z., Speck, C., Wendel, P., Tang, C., Stillman, B., and Li, H. (2008). The architecture of the DNA replication origin recognition complex in Saccharomyces cerevisiae. Proc Natl Acad Sci U S A *105*, 10326-10331.

Cheng, L., Collyer, T., and Hardy, C.F. (1999). Cell cycle regulation of DNA replication initiator factor Dbf4p. Mol Cell Biol *19*, 4270-4278.

Chesnokov, I., Gossen, M., Remus, D., and Botchan, M. (1999). Assembly of functionally active Drosophila origin recognition complex from recombinant proteins. Genes Dev *13*, 1289-1296.

Chilkova, O., Jonsson, B.H., and Johansson, E. (2003). The quaternary structure of DNA polymerase epsilon from Saccharomyces cerevisiae. J Biol Chem *278*, 14082-14086.

Chilkova, O., Stenlund, P., Isoz, I., Stith, C.M., Grabowski, P., Lundstrom, E.B., Burgers, P.M., and Johansson, E. (2007). The eukaryotic leading and lagging strand DNA polymerases are loaded onto primer-ends via separate mechanisms but have comparable processivity in the presence of PCNA. Nucleic Acids Res *35*, 6588-6597.

Clarey, M.G., Erzberger, J.P., Grob, P., Leschziner, A.E., Berger, J.M., Nogales, E., and Botchan, M. (2006). Nucleotide-dependent conformational changes in the DnaA-like core of the origin recognition complex. Nat Struct Mol Biol *13*, 684-690.

Clausen, A.R., Lujan, S.A., Burkholder, A.B., Orebaugh, C.D., Williams, J.S., Clausen, M.F., Malc, E.P., Mieczkowski, P.A., Fargo, D.C., Smith, D.J.*, et al.* (2015). Tracking replication enzymology in vivo by genome-wide mapping of ribonucleotide incorporation. Nat Struct Mol Biol *22*, 185-191.

Clement, C., and Almouzni, G. (2015). MCM2 binding to histones H3-H4 and ASF1 supports a tetramer-to-dimer model for histone inheritance at the replication fork. Nat Struct Mol Biol *22*, 587-589.

Clemente-Ruiz, M., Gonzalez-Prieto, R., and Prado, F. (2011). Histone H3K56 acetylation, CAF1, and Rtt106 coordinate nucleosome assembly and stability of advancing replication forks. PLoS Genet *7*, e1002376.

Clemente-Ruiz, M., and Prado, F. (2009). Chromatin assembly controls replication fork stability. EMBO Rep *10*, 790-796.

Cocker, J.H., Piatti, S., Santocanale, C., Nasmyth, K., and Diffley, J.F. (1996). An essential role for the Cdc6 protein in forming the pre-replicative complexes of budding yeast. Nature *379*, 180-182.

Coleman, T.R., Carpenter, P.B., and Dunphy, W.G. (1996). The Xenopus Cdc6 protein is essential for the initiation of a single round of DNA replication in cell-free extracts. Cell *87*, 53-63.

Collins, N., Poot, R.A., Kukimoto, I., Garcia-Jimenez, C., Dellaire, G., and Varga-Weisz, P.D. (2002). An ACF1-ISWI chromatin-remodeling complex is required for DNA replication through heterochromatin. Nat Genet *32*, 627-632.

Corbett, K.D., and Berger, J.M. (2004). Structure, molecular mechanisms, and evolutionary relationships in DNA topoisomerases. Annu Rev Biophys Biomol Struct *33*, 95-118.

Costa, A., Ilves, I., Tamberg, N., Petojevic, T., Nogales, E., Botchan, M.R., and Berger, J.M. (2011). The structural basis for MCM2-7 helicase activation by GINS and Cdc45. Nat Struct Mol Biol *18*, 471-477.

Coster, G., Frigola, J., Beuron, F., Morris, E.P., and Diffley, J.F. (2014). Origin licensing requires ATP binding and hydrolysis by the MCM replicative helicase. Mol Cell *55*, 666-677.

Coverley, D., Kenny, M.K., Lane, D.P., and Wood, R.D. (1992). A role for the human single-stranded DNA binding protein HSSB/RPA in an early stage of nucleotide excision repair. Nucleic Acids Res *20*, 3873-3880.

Coverley, D., Kenny, M.K., Munn, M., Rupp, W.D., Lane, D.P., and Wood, R.D. (1991). Requirement for the replication protein SSB in human DNA excision repair. Nature *349*, 538-541.

Cuvier, O., Stanojcic, S., Lemaitre, J.M., and Mechali, M. (2008). A topoisomerase II-dependent mechanism for resetting replicons at the S-M-phase transition. Genes Dev *22*, 860-865.

D'Arcy, S., Martin, K.W., Panchenko, T., Chen, X., Bergeron, S., Stargell, L.A., Black, B.E., and Luger, K. (2013). Chaperone Nap1 shields histone surfaces used in a nucleosome and can put H2A-H2B in an unconventional tetrameric form. Mol Cell *51*, 662-677.

Daigaku, Y., Keszthelyi, A., Muller, C.A., Miyabe, I., Brooks, T., Retkute, R., Hubank, M., Nieduszynski, C.A., and Carr, A.M. (2015). A global profile of replicative polymerase usage. Nat Struct Mol Biol *22*, 192-198.

Davey, M.J., Indiani, C., and O'Donnell, M. (2003). Reconstitution of the Mcm2-7p heterohexamer, subunit arrangement, and ATP site architecture. J Biol Chem *278*, 4491-4499.

Deegan, T.D., Yeeles, J.T., and Diffley, J.F. (2016). Phosphopeptide binding by Sld3 links Dbf4-dependent kinase to MCM replicative helicase activation. EMBO J *35*, 961-973.

Delgado, S., Gomez, M., Bird, A., and Antequera, F. (1998). Initiation of DNA replication at CpG islands in mammalian chromosomes. EMBO J *17*, 2426-2435.

Devbhandari, S., Jiang, J., Kumar, C., Whitehouse, I., and Remus, D. (2017). Chromatin Constrains the Initiation and Elongation of DNA Replication. Mol Cell *65*, 131-141.

Dewar, J.M., Budzowska, M., and Walter, J.C. (2015). The mechanism of DNA replication termination in vertebrates. Nature *525*, 345-350.

Dewar, J.M., Low, E., Mann, M., Raschle, M., and Walter, J.C. (2017). CRL2(Lrr1) promotes unloading of the vertebrate replisome from chromatin during replication termination. Genes Dev *31*, 275-290.

Dewar, J.M., and Walter, J.C. (2017). Mechanisms of DNA replication termination. Nat Rev Mol Cell Biol *18*, 507-516.

Diffley, J.F. (2004). Regulation of early events in chromosome replication. Curr Biol *14*, R778-786.

Diffley, J.F. (2011). Quality control in the initiation of eukaryotic DNA replication. Philos Trans R Soc Lond B Biol Sci *366*, 3545-3553.

Diffley, J.F., and Cocker, J.H. (1992). Protein-DNA interactions at a yeast replication origin. Nature *357*, 169-172.

Diffley, J.F., Cocker, J.H., Dowell, S.J., and Rowley, A. (1994). Two steps in the assembly of complexes at yeast replication origins in vivo. Cell *78*, 303-316.

DiNardo, S., Voelkel, K., and Sternglanz, R. (1984). DNA topoisomerase II mutant of Saccharomyces cerevisiae: topoisomerase II is required for segregation of daughter molecules at the termination of DNA replication. Proc Natl Acad Sci U S A *81*, 2616-2620.

Dodson, M., Dean, F.B., Bullock, P., Echols, H., and Hurwitz, J. (1987). Unwinding of duplex DNA from the SV40 origin of replication by T antigen. Science *238*, 964-967.

Douglas, M.E., Ali, F.A., Costa, A., and Diffley, J.F.X. (2018). The mechanism of eukaryotic CMG helicase activation. Nature *555*, 265-268.

Dowell, S.J., Romanowski, P., and Diffley, J.F. (1994). Interaction of Dbf4, the Cdc7 protein kinase regulatory subunit, with yeast replication origins in vivo. Science *265*, 1243-1246.

Driscoll, R., Hudson, A., and Jackson, S.P. (2007). Yeast Rtt109 promotes genome stability by acetylating histone H3 on lysine 56. Science *315*, 649-652.

Dua, R., Levy, D.L., and Campbell, J.L. (1999). Analysis of the essential functions of the C-terminal protein/protein interaction domain of Saccharomyces cerevisiae pol epsilon and its unexpected ability to support growth in the absence of the DNA polymerase domain. J Biol Chem *274*, 22283-22288.

Eaton, M.L., Galani, K., Kang, S., Bell, S.P., and MacAlpine, D.M. (2010). Conserved nucleosome positioning defines replication origins. Genes Dev *24*, 748-753.

English, C.M., Adkins, M.W., Carson, J.J., Churchill, M.E., and Tyler, J.K. (2006). Structural basis for the histone chaperone activity of Asf1. Cell *127*, 495-508.

Erzberger, J.P., and Berger, J.M. (2006). Evolutionary relationships and structural mechanisms of AAA+ proteins. Annu Rev Biophys Biomol Struct *35*, 93-114.

Evrin, C., Clarke, P., Zech, J., Lurz, R., Sun, J., Uhle, S., Li, H., Stillman, B., and Speck, C. (2009). A double-hexameric MCM2-7 complex is loaded onto origin DNA during licensing of eukaryotic DNA replication. Proc Natl Acad Sci U S A *106*, 20240-20245.

Evrin, C., Maman, J.D., Diamante, A., Pellegrini, L., and Labib, K. (2018). Histone H2A-H2B binding by Pol alpha in the eukaryotic replisome contributes to the maintenance of repressive chromatin. EMBO J.

Fachinetti, D., Bermejo, R., Cocito, A., Minardi, S., Katou, Y., Kanoh, Y., Shirahige, K., Azvolinsky, A., Zakian, V.A., and Foiani, M. (2010). Replication termination at eukaryotic chromosomes is mediated by Top2 and occurs at genomic loci containing pausing elements. Mol Cell *39*, 595-605.

Fairman, M.P., and Stillman, B. (1988). Cellular factors required for multiple stages of SV40 DNA replication in vitro. EMBO J *7*, 1211-1218.

Fiorani, P., and Bjornsti, M.A. (2000). Mechanisms of DNA topoisomerase I-induced cell killing in the yeast Saccharomyces cerevisiae. Ann N Y Acad Sci *922*, 65-75.

Franz, A., Orth, M., Pirson, P.A., Sonneville, R., Blow, J.J., Gartner, A., Stemmann, O., and Hoppe, T. (2011). CDC-48/p97 coordinates CDT-1 degradation with GINS chromatin dissociation to ensure faithful DNA replication. Mol Cell *44*, 85-96.

Frigola, J., Remus, D., Mehanna, A., and Diffley, J.F. (2013). ATPase-dependent quality control of DNA replication origin licensing. Nature *495*, 339-343.

Fu, Y.V., Yardimci, H., Long, D.T., Ho, T.V., Guainazzi, A., Bermudez, V.P., Hurwitz, J., van Oijen, A., Scharer, O.D., and Walter, J.C. (2011). Selective bypass of a lagging strand roadblock by the eukaryotic replicative DNA helicase. Cell *146*, 931-941.

Funnell, B.E., Baker, T.A., and Kornberg, A. (1986). Complete enzymatic replication of plasmids containing the origin of the Escherichia coli chromosome. J Biol Chem *261*, 5616-5624.

Gambus, A., Jones, R.C., Sanchez-Diaz, A., Kanemaki, M., van Deursen, F., Edmondson, R.D., and Labib, K. (2006). GINS maintains association of Cdc45 with MCM in replisome progression complexes at eukaryotic DNA replication forks. Nat Cell Biol *8*, 358-366.

Gambus, A., Khoudoli, G.A., Jones, R.C., and Blow, J.J. (2011). MCM2-7 form double hexamers at licensed origins in Xenopus egg extract. J Biol Chem *286*, 11855-11864.

Gambus, A., van Deursen, F., Polychronopoulos, D., Foltman, M., Jones, R.C., Edmondson, R.D., Calzada, A., and Labib, K. (2009). A key role for Ctf4 in coupling the MCM2-7 helicase to DNA polymerase alpha within the eukaryotic replisome. EMBO J *28*, 2992-3004.

Garbacz, M.A., Lujan, S.A., Burkholder, A.B., Cox, P.B., Wu, Q., Zhou, Z.X., Haber, J.E., and Kunkel, T.A. (2018). Evidence that DNA polymerase delta contributes to initiating leading strand DNA replication in Saccharomyces cerevisiae. Nat Commun *9*, 858.

Garcia, V., Furuya, K., and Carr, A.M. (2005). Identification and functional analysis of TopBP1 and its homologs. DNA Repair (Amst) *4*, 1227-1239.

Garg, P., Stith, C.M., Sabouri, N., Johansson, E., and Burgers, P.M. (2004). Idling by DNA polymerase delta maintains a ligatable nick during lagging-strand DNA replication. Genes Dev *18*, 2764-2773.

Gavin, K.A., Hidaka, M., and Stillman, B. (1995). Conserved initiator proteins in eukaryotes. Science *270*, 1667-1671.

Georgescu, R., Yuan, Z., Bai, L., de Luna Almeida Santos, R., Sun, J., Zhang, D., Yurieva, O., Li, H., and O'Donnell, M.E. (2017). Structure of eukaryotic CMG helicase at a replication fork and implications to replisome architecture and origin initiation. Proc Natl Acad Sci U S A *114*, E697-E706.

Georgescu, R.E., Langston, L., Yao, N.Y., Yurieva, O., Zhang, D., Finkelstein, J., Agarwal, T., and O'Donnell, M.E. (2014). Mechanism of asymmetric polymerase assembly at the eukaryotic replication fork. Nat Struct Mol Biol *21*, 664-670.

Georgescu, R.E., Schauer, G.D., Yao, N.Y., Langston, L.D., Yurieva, O., Zhang, D., Finkelstein, J., and O'Donnell, M.E. (2015). Reconstitution of a eukaryotic replisome reveals suppression mechanisms that define leading/lagging strand operation. Elife *4*, e04988.

Gerik, K.J., Li, X., Pautz, A., and Burgers, P.M. (1998). Characterization of the two small subunits of Saccharomyces cerevisiae DNA polymerase delta. J Biol Chem *273*, 19747-19755.

Gomes, X.V., Henricksen, L.A., and Wold, M.S. (1996). Proteolytic mapping of human replication protein A: evidence for multiple structural domains and a conformational change upon interaction with single-stranded DNA. Biochemistry *35*, 5586-5595.

Grallert, B., and Nurse, P. (1996). The ORC1 homolog orp1 in fission yeast plays a key role in regulating onset of S phase. Genes Dev *10*, 2644-2654.

Grasby, J.A., Finger, L.D., Tsutakawa, S.E., Atack, J.M., and Tainer, J.A. (2012). Unpairing and gating: sequence-independent substrate recognition by FEN superfamily nucleases. Trends Biochem Sci *37*, 74-84.

Gregan, J., Lindner, K., Brimage, L., Franklin, R., Namdar, M., Hart, E.A., Aves, S.J., and Kearsey, S.E. (2003). Fission yeast Cdc23/Mcm10 functions after pre-replicative complex formation to promote Cdc45 chromatin binding. Mol Biol Cell *14*, 3876-3887.

Gros, J., Devbhandari, S., and Remus, D. (2014). Origin plasticity during budding yeast DNA replication in vitro. EMBO J *33*, 621-636.

Gros, J., Kumar, C., Lynch, G., Yadav, T., Whitehouse, I., and Remus, D. (2015). Post-licensing Specification of Eukaryotic Replication Origins by Facilitated Mcm2-7 Sliding along DNA. Mol Cell *60*, 797-807.

Groth, A., Corpet, A., Cook, A.J., Roche, D., Bartek, J., Lukas, J., and Almouzni, G. (2007). Regulation of replication fork progression through histone supply and demand. Science *318*, 1928-1931.

Hamatake, R.K., Hasegawa, H., Clark, A.B., Bebenek, K., Kunkel, T.A., and Sugino, A. (1990). Purification and characterization of DNA polymerase II from the yeast Saccharomyces cerevisiae. Identification of the catalytic core and a possible holoenzyme form of the enzyme. J Biol Chem *265*, 4072-4083.

Han, J., Zhou, H., Horazdovsky, B., Zhang, K., Xu, R.M., and Zhang, Z. (2007). Rtt109 acetylates histone H3 lysine 56 and functions in DNA replication. Science *315*, 653-655.

Hardy, C.F., Dryga, O., Seematter, S., Pahl, P.M., and Sclafani, R.A. (1997). mcm5/cdc46-bob1 bypasses the requirement for the S phase activator Cdc7p. Proc Natl Acad Sci U S A *94*, 3151-3155.

Harland, R.M., and Laskey, R.A. (1980). Regulated replication of DNA microinjected into eggs of Xenopus laevis. Cell *21*, 761-771.

Hartwell, L.H. (1973). Three additional genes required for deoxyribonucleic acid synthesis in Saccharomyces cerevisiae. J Bacteriol *115*, 966-974.

Hartwell, L.H. (1976). Sequential function of gene products relative to DNA synthesis in the yeast cell cycle. J Mol Biol *104*, 803-817.

Hawkins, M., Retkute, R., Muller, C.A., Saner, N., Tanaka, T.U., de Moura, A.P., and Nieduszynski, C.A. (2013). High-resolution replication profiles define the stochastic nature of genome replication initiation and termination. Cell Rep *5*, 1132-1141.

He, Z., Wong, J.M., Maniar, H.S., Brill, S.J., and Ingles, C.J. (1996). Assessing the requirements for nucleotide excision repair proteins of Saccharomyces cerevisiae in an in vitro system. J Biol Chem *271*, 28243-28249.

Heinzel, S.S., Krysan, P.J., Tran, C.T., and Calos, M.P. (1991). Autonomous DNA replication in human cells is affected by the size and the source of the DNA. Mol Cell Biol *11*, 2263-2272.

Heller, R.C., Kang, S., Lam, W.M., Chen, S., Chan, C.S., and Bell, S.P. (2011). Eukaryotic origin-dependent DNA replication in vitro reveals sequential action of DDK and S-CDK kinases. Cell *146*, 80-91.

Hinkle, D.C., and Richardson, C.C. (1975). Bacteriophage T7 deoxyribonucleic acid replication in vitro. Purification and properties of the gene 4 protein of bacteriophage T7. J Biol Chem *250*, 5523-5529.

Hoek, M., and Stillman, B. (2003). Chromatin assembly factor 1 is essential and couples chromatin assembly to DNA replication in vivo. Proc Natl Acad Sci U S A *100*, 12183-12188.

Hofmann, J.F., and Beach, D. (1994). cdt1 is an essential target of the Cdc10/Sct1 transcription factor: requirement for DNA replication and inhibition of mitosis. EMBO J *13*, 425-434.

Hogan, E., and Koshland, D. (1992). Addition of extra origins of replication to a minichromosome suppresses its mitotic loss in cdc6 and cdc14 mutants of Saccharomyces cerevisiae. Proc Natl Acad Sci U S A *89*, 3098-3102.

Hogg, M., Osterman, P., Bylund, G.O., Ganai, R.A., Lundstrom, E.B., Sauer-Eriksson, A.E., and Johansson, E. (2014). Structural basis for processive DNA synthesis by yeast DNA polymerase varepsilon. Nat Struct Mol Biol *21*, 49-55.

Howes, T.R., and Tomkinson, A.E. (2012). DNA ligase I, the replicative DNA ligase. Subcell Biochem *62*, 327-341.

Hua, X.H., and Newport, J. (1998). Identification of a preinitiation step in DNA replication that is independent of origin recognition complex and cdc6, but dependent on cdk2. J Cell Biol *140*, 271-281.

Huang, H., Stromme, C.B., Saredi, G., Hodl, M., Strandsby, A., Gonzalez-Aguilera, C., Chen, S., Groth, A., and Patel, D.J. (2015). A unique binding mode enables MCM2 to chaperone histones H3-H4 at replication forks. Nat Struct Mol Biol *22*, 618-626.

Huberman, J.A., Zhu, J.G., Davis, L.R., and Newlon, C.S. (1988). Close association of a DNA replication origin and an ARS element on chromosome III of the yeast, Saccharomyces cerevisiae. Nucleic Acids Res *16*, 6373-6384.

Huggins, C.F., Chafin, D.R., Aoyagi, S., Henricksen, L.A., Bambara, R.A., and Hayes, J.J. (2002). Flap endonuclease 1 efficiently cleaves base excision repair and DNA replication intermediates assembled into nucleosomes. Mol Cell *10*, 1201-1211.

Hyrien, O., and Mechali, M. (1993). Chromosomal replication initiates and terminates at random sequences but at regular intervals in the ribosomal DNA of Xenopus early embryos. EMBO J *12*, 4511-4520.

Iida, T., and Araki, H. (2004). Noncompetitive counteractions of DNA polymerase epsilon and ISW2/yCHRAC for epigenetic inheritance of telomere position effect in Saccharomyces cerevisiae. Mol Cell Biol *24*, 217-227.

Ilves, I., Petojevic, T., Pesavento, J.J., and Botchan, M.R. (2010). Activation of the MCM2-7 helicase by association with Cdc45 and GINS proteins. Mol Cell *37*, 247-258.

Ishimi, Y., Ishida, R., and Andoh, T. (1992). Effect of ICRF-193, a novel DNA topoisomerase II inhibitor, on simian virus 40 DNA and chromosome replication in vitro. Mol Cell Biol *12*, 4007-4014.

Ishimi, Y., Komamura-Kohno, Y., Arai, K., and Masai, H. (2001). Biochemical activities associated with mouse Mcm2 protein. J Biol Chem *276*, 42744-42752.

Ito, T., Bulger, M., Kobayashi, R., and Kadonaga, J.T. (1996). Drosophila NAP-1 is a core histone chaperone that functions in ATP-facilitated assembly of regularly spaced nucleosomal arrays. Mol Cell Biol *16*, 3112-3124.

Jackson, A.L., Pahl, P.M., Harrison, K., Rosamond, J., and Sclafani, R.A. (1993). Cell cycle regulation of the yeast Cdc7 protein kinase by association with the Dbf4 protein. Mol Cell Biol *13*, 2899-2908.

Jacob, F., Brenner, S., and Cuzin, F. (1963). On the regulation of DNA replication in bacteria: Cold Spring Harbor Symp Quant Biol *28*, 329-348.

Jamai, A., Puglisi, A., and Strubin, M. (2009). Histone chaperone spt16 promotes redeposition of the original h3-h4 histones evicted by elongating RNA polymerase. Mol Cell *35*, 377-383.

Johnson, R.E., Klassen, R., Prakash, L., and Prakash, S. (2015). A Major Role of DNA Polymerase delta in Replication of Both the Leading and Lagging DNA Strands. Mol Cell *59*, 163-175.

Johnson, R.E., Klassen, R., Prakash, L., and Prakash, S. (2016). Response to Burgers et al. Mol Cell *61*, 494-495.

Johnston, L.H., and Nasmyth, K.A. (1978). Saccharomyces cerevisiae cell cycle mutant cdc9 is defective in DNA ligase. Nature *274*, 891-893.

Kamimura, Y., Masumoto, H., Sugino, A., and Araki, H. (1998). Sld2, which interacts with Dpb11 in Saccharomyces cerevisiae, is required for chromosomal DNA replication. Mol Cell Biol *18*, 6102-6109.

Kamimura, Y., Tak, Y.S., Sugino, A., and Araki, H. (2001). Sld3, which interacts with Cdc45 (Sld4), functions for chromosomal DNA replication in Saccharomyces cerevisiae. EMBO J *20*, 2097-2107.

Kanemaki, M., and Labib, K. (2006). Distinct roles for Sld3 and GINS during establishment and progression of eukaryotic DNA replication forks. EMBO J *25*, 1753-1763.

Kang, S., Warner, M.D., and Bell, S.P. (2014). Multiple functions for Mcm2-7 ATPase motifs during replication initiation. Mol Cell *55*, 655-665.

Kanke, M., Kodama, Y., Takahashi, T.S., Nakagawa, T., and Masukata, H. (2012). Mcm10 plays an essential role in origin DNA unwinding after loading of the CMG components. EMBO J *31*, 2182-2194.

Karnani, N., Taylor, C.M., Malhotra, A., and Dutta, A. (2010). Genomic study of replication initiation in human chromosomes reveals the influence of transcription regulation and chromatin structure on origin selection. Mol Biol Cell *21*, 393-404.

Katan-Khaykovich, Y., and Struhl, K. (2011). Splitting of H3-H4 tetramers at transcriptionally active genes undergoing dynamic histone exchange. Proc Natl Acad Sci U S A *108*, 1296-1301.

Kawasaki, Y., Kim, H.D., Kojima, A., Seki, T., and Sugino, A. (2006). Reconstitution of Saccharomyces cerevisiae prereplicative complex assembly in vitro. Genes Cells *11*, 745-756.

Kelch, B.A., Makino, D.L., O'Donnell, M., and Kuriyan, J. (2012). Clamp loader ATPases and the evolution of DNA replication machinery. BMC Biol *10*, 34.

Kelly, T. (2017). Historical Perspective of Eukaryotic DNA Replication. Adv Exp Med Biol *1042*, 1-41.

Kelly, T.J., Martin, G.S., Forsburg, S.L., Stephen, R.J., Russo, A., and Nurse, P. (1993). The fission yeast cdc18+ gene product couples S phase to START and mitosis. Cell *74*, 371-382.

Kesti, T., Flick, K., Keranen, S., Syvaoja, J.E., and Wittenberg, C. (1999). DNA polymerase epsilon catalytic domains are dispensable for DNA replication, DNA repair, and cell viability. Mol Cell *3*, 679-685.

Kilkenny, M.L., Simon, A.C., Mainwaring, J., Wirthensohn, D., Holzer, S., and Pellegrini, L. (2017). The human CTF4-orthologue AND-1 interacts with DNA polymerase alpha/primase via its unique C-terminal HMG box. Open Biol *7*.

Kim, C., Paulus, B.F., and Wold, M.S. (1994). Interactions of human replication protein A with oligonucleotides. Biochemistry *33*, 14197-14206.

Kingston, I.J., Yung, J.S., and Singleton, M.R. (2011). Biophysical characterization of the centromere-specific nucleosome from budding yeast. J Biol Chem *286*, 4021-4026.

Kitada, K., Johnston, L.H., Sugino, T., and Sugino, A. (1992). Temperature-sensitive cdc7 mutations of Saccharomyces cerevisiae are suppressed by the DBF4 gene, which is required for the G1/S cell cycle transition. Genetics *131*, 21-29.

Klemm, R.D., Austin, R.J., and Bell, S.P. (1997). Coordinate binding of ATP and origin DNA regulates the ATPase activity of the origin recognition complex. Cell *88*, 493-502.

Kneissl, M., Putter, V., Szalay, A.A., and Grummt, F. (2003). Interaction and assembly of murine pre-replicative complex proteins in yeast and mouse cells. J Mol Biol *327*, 111-128.

Koh, K.D., Balachander, S., Hesselberth, J.R., and Storici, F. (2015). Ribose-seq: global mapping of ribonucleotides embedded in genomic DNA. Nat Methods *12*, 251-257, 253 p following 257.

Kornberg, R.D. (1977). Structure of chromatin. Annu Rev Biochem *46*, 931-954.

Kunkel, T.A. (2004). DNA replication fidelity. J Biol Chem *279*, 16895-16898.
Kunkel, T.A., and Burgers, P.M. (2008). Dividing the workload at a eukaryotic replication fork. Trends Cell Biol *18*, 521-527.

Kurat, C.F., Yeeles, J.T.P., Patel, H., Early, A., and Diffley, J.F.X. (2017). Chromatin Controls DNA Replication Origin Selection, Lagging-Strand Synthesis, and Replication Fork Rates. Mol Cell *65*, 117-130.

Labib, K. (2010). How do Cdc7 and cyclin-dependent kinases trigger the initiation of chromosome replication in eukaryotic cells? Genes Dev *24*, 1208-1219.

Labib, K., Kearsey, S.E., and Diffley, J.F. (2001). MCM2-7 proteins are essential components of prereplicative complexes that accumulate cooperatively in the nucleus during G1-phase and are required to establish, but not maintain, the S-phase checkpoint. Mol Biol Cell *12*, 3658-3667.

Labib, K., Tercero, J.A., and Diffley, J.F. (2000). Uninterrupted MCM2-7 function required for DNA replication fork progression. Science *288*, 1643-1647.

Langston, L.D., and O'Donnell, M. (2008). DNA polymerase delta is highly processive with proliferating cell nuclear antigen and undergoes collision release upon completing DNA. J Biol Chem *283*, 29522-29531.

Langston, L.D., Zhang, D., Yurieva, O., Georgescu, R.E., Finkelstein, J., Yao, N.Y., Indiani, C., and O'Donnell, M.E. (2014). CMG helicase and DNA polymerase epsilon form a functional 15-subunit holoenzyme for eukaryotic leading-strand DNA replication. Proc Natl Acad Sci U S A *111*, 15390-15395.

Laskey, R.A., Honda, B.M., Mills, A.D., and Finch, J.T. (1978). Nucleosomes are assembled by an acidic protein which binds histones and transfers them to DNA. Nature *275*, 416-420.

Lee, C., Hong, B., Choi, J.M., Kim, Y., Watanabe, S., Ishimi, Y., Enomoto, T., Tada, S., Kim, Y., and Cho, Y. (2004). Structural basis for inhibition of the replication licensing factor Cdt1 by geminin. Nature *430*, 913-917.

Lee, D.G., and Bell, S.P. (1997). Architecture of the yeast origin recognition complex bound to origins of DNA replication. Mol Cell Biol *17*, 7159-7168.

Lee, H.S., Lee, S.A., Hur, S.K., Seo, J.W., and Kwon, J. (2014). Stabilization and targeting of INO80 to replication forks by BAP1 during normal DNA synthesis. Nat Commun *5*, 5128.

Lee, S.H., Pan, Z.Q., Kwong, A.D., Burgers, P.M., and Hurwitz, J. (1991). Synthesis of DNA by DNA polymerase epsilon in vitro. J Biol Chem *266*, 22707-22717.

Lei, M., Kawasaki, Y., Young, M.R., Kihara, M., Sugino, A., and Tye, B.K. (1997). Mcm2 is a target of regulation by Cdc7-Dbf4 during the initiation of DNA synthesis. Genes Dev *11*, 3365-3374.

Leonard, A.C., and Mechali, M. (2013). DNA replication origins. Cold Spring Harb Perspect Biol *5*, a010116.

Levin, D.S., McKenna, A.E., Motycka, T.A., Matsumoto, Y., and Tomkinson, A.E. (2000). Interaction between PCNA and DNA ligase I is critical for joining of Okazaki fragments and long-patch base-excision repair. Curr Biol *10*, 919-922.

Li, H., and Stillman, B. (2012). The origin recognition complex: a biochemical and structural view. Subcell Biochem *62*, 37-58.

Li, J.J., and Kelly, T.J. (1984). Simian virus 40 DNA replication in vitro. Proc Natl Acad Sci U S A *81*, 6973-6977.

Li, N., Lam, W.H., Zhai, Y., Cheng, J., Cheng, E., Zhao, Y., Gao, N., and Tye, B.K. (2018). Structure of the origin recognition complex bound to DNA replication origin. Nature *559*, 217-222.

Li, N., Zhai, Y., Zhang, Y., Li, W., Yang, M., Lei, J., Tye, B.K., and Gao, N. (2015). Structure of the eukaryotic MCM complex at 3.8 A. Nature *524*, 186-191.

Li, Q., Zhou, H., Wurtele, H., Davies, B., Horazdovsky, B., Verreault, A., and Zhang, Z. (2008). Acetylation of histone H3 lysine 56 regulates replication-coupled nucleosome assembly. Cell *134*, 244-255.

Li, X., Li, J., Harrington, J., Lieber, M.R., and Burgers, P.M. (1995). Lagging strand DNA synthesis at the eukaryotic replication fork involves binding and stimulation of FEN-1 by proliferating cell nuclear antigen. J Biol Chem *270*, 22109-22112.

Liang, C., Weinreich, M., and Stillman, B. (1995). ORC and Cdc6p interact and determine the frequency of initiation of DNA replication in the genome. Cell *81*, 667-676.

Liu, A.P., and Fletcher, D.A. (2009). Biology under construction: in vitro reconstitution of cellular function. Nat Rev Mol Cell Biol *10*, 644-650.

Liu, J., Smith, C.L., DeRyckere, D., DeAngelis, K., Martin, G.S., and Berger, J.M. (2000). Structure and function of Cdc6/Cdc18: implications for origin recognition and checkpoint control. Mol Cell *6*, 637-648.

Liu, S., Balasov, M., Wang, H., Wu, L., Chesnokov, I.N., and Liu, Y. (2011). Structural analysis of human Orc6 protein reveals a homology with transcription factor TFIIB. Proc Natl Acad Sci U S A *108*, 7373-7378.

Liu, S., Xu, Z., Leng, H., Zheng, P., Yang, J., Chen, K., Feng, J., and Li, Q. (2017). RPA binds histone H3-H4 and functions in DNA replication-coupled nucleosome assembly. Science *355*, 415-420.

Lorch, Y., Maier-Davis, B., and Kornberg, R.D. (2006). Chromatin remodeling by nucleosome disassembly in vitro. Proc Natl Acad Sci U S A *103*, 3090-3093.

Lowary, P.T., and Widom, J. (1998). New DNA sequence rules for high affinity binding to histone octamer and sequence-directed nucleosome positioning. J Mol Biol *276*, 19-42.

Lucchini, R., and Sogo, J.M. (1995). Replication of transcriptionally active chromatin. Nature *374*, 276-280.

Luger, K., Mader, A.W., Richmond, R.K., Sargent, D.F., and Richmond, T.J. (1997). Crystal structure of the nucleosome core particle at 2.8 A resolution. Nature *389*, 251-260.

Luger, K., Rechsteiner, T.J., and Richmond, T.J. (1999). Preparation of nucleosome core particle from recombinant histones. Methods Enzymol *304*, 3-19.

MacAlpine, D.M., and Almouzni, G. (2013). Chromatin and DNA replication. Cold Spring Harb Perspect Biol *5*, a010207.

MacAlpine, D.M., and Bell, S.P. (2005). A genomic view of eukaryotic DNA replication. Chromosome Res *13*, 309-326.

MacAlpine, H.K., Gordan, R., Powell, S.K., Hartemink, A.J., and MacAlpine, D.M. (2010). Drosophila ORC localizes to open chromatin and marks sites of cohesin complex loading. Genome Res *20*, 201-211.

Madine, M.A., Khoo, C.Y., Mills, A.D., and Laskey, R.A. (1995). MCM3 complex required for cell cycle regulation of DNA replication in vertebrate cells. Nature *375*, 421-424.

Maine, G.T., Sinha, P., and Tye, B.K. (1984). Mutants of S. cerevisiae defective in the maintenance of minichromosomes. Genetics *106*, 365-385.

Maiorano, D., Moreau, J., and Mechali, M. (2000). XCDT1 is required for the assembly of pre-replicative complexes in Xenopus laevis. Nature *404*, 622-625.

Majka, J., and Burgers, P.M. (2004). The PCNA-RFC families of DNA clamps and clamp loaders. Prog Nucleic Acid Res Mol Biol *78*, 227-260.

Manke, I.A., Lowery, D.M., Nguyen, A., and Yaffe, M.B. (2003). BRCT repeats as phosphopeptide-binding modules involved in protein targeting. Science *302*, 636-639.

Mantiero, D., Mackenzie, A., Donaldson, A., and Zegerman, P. (2011). Limiting replication initiation factors execute the temporal programme of origin firing in budding yeast. EMBO J *30*, 4805-4814.

Marahrens, Y., and Stillman, B. (1992). A yeast chromosomal origin of DNA replication defined by multiple functional elements. Science *255*, 817-823.
Marians, K.J. (1992). Prokaryotic DNA replication. Annu Rev Biochem *61*, 673-719.

Maric, M., Maculins, T., De Piccoli, G., and Labib, K. (2014). Cdc48 and a ubiquitin ligase drive disassembly of the CMG helicase at the end of DNA replication. Science *346*, 1253596.

Marino, F., Vindigni, A., and Onesti, S. (2013). Bioinformatic analysis of RecQ4 helicases reveals the presence of a RQC domain and a Zn knuckle. Biophys Chem *177-178*, 34-39.

Masai, H., Matsumoto, S., You, Z., Yoshizawa-Sugata, N., and Oda, M. (2010). Eukaryotic chromosome DNA replication: where, when, and how? Annu Rev Biochem *79*, 89-130.

Masai, H., Taniyama, C., Ogino, K., Matsui, E., Kakusho, N., Matsumoto, S., Kim, J.M., Ishii, A., Tanaka, T., Kobayashi, T.*, et al.* (2006). Phosphorylation of MCM4 by Cdc7 kinase facilitates its interaction with Cdc45 on the chromatin. J Biol Chem *281*, 39249-39261.

Masumoto, H., Muramatsu, S., Kamimura, Y., and Araki, H. (2002). S-Cdk-dependent phosphorylation of Sld2 essential for chromosomal DNA replication in budding yeast. Nature *415*, 651-655.

Masumoto, H., Sugino, A., and Araki, H. (2000). Dpb11 controls the association between DNA polymerases alpha and epsilon and the autonomously replicating sequence region of budding yeast. Mol Cell Biol *20*, 2809-2817.

Mattiroli, F., Gu, Y., Yadav, T., Balsbaugh, J.L., Harris, M.R., Findlay, E.S., Liu, Y., Radebaugh, C.A., Stargell, L.A., Ahn, N.G.*, et al.* (2017). DNA-mediated association of two histone-bound complexes of yeast Chromatin

Assembly Factor-1 (CAF-1) drives tetrasome assembly in the wake of DNA replication. Elife *6*.

McBryant, S.J., Park, Y.J., Abernathy, S.M., Laybourn, P.J., Nyborg, J.K., and Luger, K. (2003). Preferential binding of the histone (H3-H4)2 tetramer by NAP1 is mediated by the amino-terminal histone tails. J Biol Chem *278*, 44574-44583.

McGuffee, S.R., Smith, D.J., and Whitehouse, I. (2013). Quantitative, genome-wide analysis of eukaryotic replication initiation and termination. Mol Cell *50*, 123-135.

McKnight, S.L., and Miller, O.L., Jr. (1977). Electron microscopic analysis of chromatin replication in the cellular blastoderm Drosophila melanogaster embryo. Cell *12*, 795-804.

Mechali, M., and Kearsey, S. (1984). Lack of specific sequence requirement for DNA replication in Xenopus eggs compared with high sequence specificity in yeast. Cell *38*, 55-64.

Mejlvang, J., Feng, Y., Alabert, C., Neelsen, K.J., Jasencakova, Z., Zhao, X., Lees, M., Sandelin, A., Pasero, P., Lopes, M.*, et al.* (2014). New histone supply regulates replication fork speed and PCNA unloading. J Cell Biol *204*, 29-43.

Merchant, A.M., Kawasaki, Y., Chen, Y., Lei, M., and Tye, B.K. (1997). A lesion in the DNA replication initiation factor Mcm10 induces pausing of elongation forks through chromosomal replication origins in Saccharomyces cerevisiae. Mol Cell Biol *17*, 3261-3271.

Moir, D., Stewart, S.E., Osmond, B.C., and Botstein, D. (1982). Cold-sensitive cell-division-cycle mutants of yeast: isolation, properties, and pseudoreversion studies. Genetics *100*, 547-563.

Moore, S.P., Erdile, L., Kelly, T., and Fishel, R. (1991). The human homologous pairing protein HPP-1 is specifically stimulated by the cognate single-stranded binding protein hRP-A. Proc Natl Acad Sci U S A *88*, 9067-9071.

Moreno, S.P., Bailey, R., Campion, N., Herron, S., and Gambus, A. (2014). Polyubiquitylation drives replisome disassembly at the termination of DNA replication. Science *346*, 477-481.

Morrison, A., Araki, H., Clark, A.B., Hamatake, R.K., and Sugino, A. (1990). A third essential DNA polymerase in S. cerevisiae. Cell *62*, 1143-1151.

Morrison, A., Bell, J.B., Kunkel, T.A., and Sugino, A. (1991). Eukaryotic DNA polymerase amino acid sequence required for 3'----5' exonuclease activity. Proc Natl Acad Sci U S A *88*, 9473-9477.

Morrison, A., and Sugino, A. (1994). The 3'-->5' exonucleases of both DNA polymerases delta and epsilon participate in correcting errors of DNA replication in Saccharomyces cerevisiae. Mol Gen Genet *242*, 289-296.

Mossi, R., Keller, R.C., Ferrari, E., and Hubscher, U. (2000). DNA polymerase switching: II. Replication factor C abrogates primer synthesis by DNA polymerase alpha at a critical length. J Mol Biol *295*, 803-814.

Moyer, S.E., Lewis, P.W., and Botchan, M.R. (2006). Isolation of the Cdc45/Mcm2-7/GINS (CMG) complex, a candidate for the eukaryotic DNA replication fork helicase. Proc Natl Acad Sci U S A *103*, 10236-10241.

Muramatsu, S., Hirai, K., Tak, Y.S., Kamimura, Y., and Araki, H. (2010). CDK-dependent complex formation between replication proteins Dpb11, Sld2, Pol (epsilon}, and GINS in budding yeast. Genes Dev *24*, 602-612.

Muzi-Falconi, M., Giannattasio, M., Foiani, M., and Plevani, P. (2003). The DNA polymerase alpha-primase complex: multiple functions and interactions. ScientificWorldJournal *3*, 21-33.

Myung, K., Pennaneach, V., Kats, E.S., and Kolodner, R.D. (2003). Saccharomyces cerevisiae chromatin-assembly factors that act during DNA replication function in the maintenance of genome stability. Proc Natl Acad Sci U S A *100*, 6640-6645.

Natsume, R., Eitoku, M., Akai, Y., Sano, N., Horikoshi, M., and Senda, T. (2007). Structure and function of the histone chaperone CIA/ASF1 complexed with histones H3 and H4. Nature *446*, 338-341.

Neuwald, A.F., Aravind, L., Spouge, J.L., and Koonin, E.V. (1999). AAA+: A class of chaperone-like ATPases associated with the assembly, operation, and disassembly of protein complexes. Genome Res *9*, 27-43.

Nick McElhinny, S.A., Gordenin, D.A., Stith, C.M., Burgers, P.M., and Kunkel, T.A. (2008). Division of labor at the eukaryotic replication fork. Mol Cell *30*, 137-144.

Nishitani, H., Lygerou, Z., Nishimoto, T., and Nurse, P. (2000). The Cdt1 protein is required to license DNA for replication in fission yeast. Nature *404*, 625-628.

Noguchi, Y., Yuan, Z., Bai, L., Schneider, S., Zhao, G., Stillman, B., Speck, C., and Li, H. (2017). Cryo-EM structure of Mcm2-7 double hexamer on DNA suggests a lagging-strand DNA extrusion model. Proc Natl Acad Sci U S A *114*, E9529-E9538.

Nunez-Ramirez, R., Klinge, S., Sauguet, L., Melero, R., Recuero-Checa, M.A., Kilkenny, M., Perera, R.L., Garcia-Alvarez, B., Hall, R.J., Nogales, E.*, et al.* (2011). Flexible tethering of primase and DNA Pol alpha in the eukaryotic primosome. Nucleic Acids Res *39*, 8187-8199.

Nurse, P., and Bissett, Y. (1981). Gene required in G1 for commitment to cell cycle and in G2 for control of mitosis in fission yeast. Nature *292*, 558-560.

Oakley, G.G., and Patrick, S.M. (2010). Replication protein A: directing traffic at the intersection of replication and repair. Front Biosci (Landmark Ed) *15*, 883-900.

Okazaki, R., Okazaki, T., Sakabe, K., Sugimoto, K., and Sugino, A. (1968). Mechanism of DNA chain growth. I. Possible discontinuity and unusual secondary structure of newly synthesized chains. Proc Natl Acad Sci U S A *59*, 598-605.

On, K.F., Beuron, F., Frith, D., Snijders, A.P., Morris, E.P., and Diffley, J.F. (2014). Prereplicative complexes assembled in vitro support origin-dependent and independent DNA replication. EMBO J *33*, 605-620.

Orphanides, G., Wu, W.H., Lane, W.S., Hampsey, M., and Reinberg, D. (1999). The chromatin-specific transcription elongation factor FACT comprises human SPT16 and SSRP1 proteins. Nature *400*, 284-288.

Oshiro, G., Owens, J.C., Shellman, Y., Sclafani, R.A., and Li, J.J. (1999). Cell cycle control of Cdc7p kinase activity through regulation of Dbf4p stability. Mol Cell Biol *19*, 4888-4896.

Pacek, M., Tutter, A.V., Kubota, Y., Takisawa, H., and Walter, J.C. (2006). Localization of MCM2-7, Cdc45, and GINS to the site of DNA unwinding during eukaryotic DNA replication. Mol Cell *21*, 581-587.

Pacek, M., and Walter, J.C. (2004). A requirement for MCM7 and Cdc45 in chromosome unwinding during eukaryotic DNA replication. EMBO J *23*, 3667-3676.

Palmer, R.E., Hogan, E., and Koshland, D. (1990). Mitotic transmission of artificial chromosomes in cdc mutants of the yeast, Saccharomyces cerevisiae. Genetics *125*, 763-774.

Pavlov, Y.I., Frahm, C., Nick McElhinny, S.A., Niimi, A., Suzuki, M., and Kunkel, T.A. (2006). Evidence that errors made by DNA polymerase alpha are corrected by DNA polymerase delta. Curr Biol *16*, 202-207.

Pellegrini, L. (2012). The Pol alpha-primase complex. Subcell Biochem *62*, 157-169.

Perera, R.L., Torella, R., Klinge, S., Kilkenny, M.L., Maman, J.D., and Pellegrini, L. (2013). Mechanism for priming DNA synthesis by yeast DNA polymerase alpha. Elife *2*, e00482.

Perkins, G., and Diffley, J.F. (1998). Nucleotide-dependent prereplicative complex assembly by Cdc6p, a homolog of eukaryotic and prokaryotic clamp-loaders. Mol Cell *2*, 23-32.

Peter, B.J., Ullsperger, C., Hiasa, H., Marians, K.J., and Cozzarelli, N.R. (1998). The structure of supercoiled intermediates in DNA replication. Cell *94*, 819-827.

Petryk, N., Dalby, M., Wenger, A., Stromme, C.B., Strandsby, A., Andersson, R., and Groth, A. (2018). MCM2 promotes symmetric inheritance of modified histones during DNA replication. Science *361*, 1389-1392.

Petryk, N., Kahli, M., d'Aubenton-Carafa, Y., Jaszczyszyn, Y., Shen, Y., Silvain, M., Thermes, C., Chen, C.L., and Hyrien, O. (2016). Replication landscape of the human genome. Nat Commun *7*, 10208.

Podust, L.M., Podust, V.N., Sogo, J.M., and Hubscher, U. (1995). Mammalian DNA polymerase auxiliary proteins: analysis of replication factor C-catalyzed proliferating cell nuclear antigen loading onto circular double-stranded DNA. Mol Cell Biol *15*, 3072-3081.

Poot, R.A., Bozhenok, L., van den Berg, D.L., Steffensen, S., Ferreira, F., Grimaldi, M., Gilbert, N., Ferreira, J., and Varga-Weisz, P.D. (2004). The Williams syndrome transcription factor interacts with PCNA to target chromatin remodelling by ISWI to replication foci. Nat Cell Biol *6*, 1236-1244.

Prakash, A., and Borgstahl, G.E. (2012). The structure and function of replication protein A in DNA replication. Subcell Biochem *62*, 171-196.

Prelich, G., Tan, C.K., Kostura, M., Mathews, M.B., So, A.G., Downey, K.M., and Stillman, B. (1987). Functional identity of proliferating cell nuclear antigen and a DNA polymerase-delta auxiliary protein. Nature *326*, 517-520.

Prior, C.P., Cantor, C.R., Johnson, E.M., and Allfrey, V.G. (1980). Incorporation of exogenous pyrene-labeled histone into Physarum chromatin: a system for studying changes in nucleosomes assembled in vivo. Cell *20*, 597-608.

Pursell, Z.F., Isoz, I., Lundstrom, E.B., Johansson, E., and Kunkel, T.A. (2007). Yeast DNA polymerase epsilon participates in leading-strand DNA replication. Science *317*, 127-130.

Radman-Livaja, M., Verzijlbergen, K.F., Weiner, A., van Welsem, T., Friedman, N., Rando, O.J., and van Leeuwen, F. (2011). Patterns and mechanisms of ancestral histone protein inheritance in budding yeast. PLoS Biol *9*, e1001075.

Randell, J.C., Bowers, J.L., Rodriguez, H.K., and Bell, S.P. (2006). Sequential ATP hydrolysis by Cdc6 and ORC directs loading of the Mcm2-7 helicase. Mol Cell *21*, 29-39.

Ransom, M., Dennehey, B.K., and Tyler, J.K. (2010). Chaperoning histones during DNA replication and repair. Cell *140*, 183-195.

Rao, H., and Stillman, B. (1995). The origin recognition complex interacts with a bipartite DNA binding site within yeast replicators. Proc Natl Acad Sci U S A *92*, 2224-2228.

Remus, D., Beuron, F., Tolun, G., Griffith, J.D., Morris, E.P., and Diffley, J.F. (2009). Concerted loading of Mcm2-7 double hexamers around DNA during DNA replication origin licensing. Cell *139*, 719-730.

Remus, D., and Diffley, J.F. (2009). Eukaryotic DNA replication control: lock and load, then fire. Curr Opin Cell Biol *21*, 771-777.

Ricke, R.M., and Bielinsky, A.K. (2004). Mcm10 regulates the stability and chromatin association of DNA polymerase-alpha. Mol Cell *16*, 173-185.

Romanowski, P., Madine, M.A., Rowles, A., Blow, J.J., and Laskey, R.A. (1996). The Xenopus origin recognition complex is essential for DNA replication and MCM binding to chromatin. Curr Biol *6*, 1416-1425.

Rossi, M.L., and Bambara, R.A. (2006). Reconstituted Okazaki fragment processing indicates two pathways of primer removal. J Biol Chem *281*, 26051-26061.

Rowles, A., Chong, J.P., Brown, L., Howell, M., Evan, G.I., and Blow, J.J. (1996). Interaction between the origin recognition complex and the replication licensing system in Xenopus. Cell *87*, 287-296.

Rowles, A., Tada, S., and Blow, J.J. (1999). Changes in association of the Xenopus origin recognition complex with chromatin on licensing of replication origins. J Cell Sci *112 (Pt 12)*, 2011-2018.

Rowley, A., Cocker, J.H., Harwood, J., and Diffley, J.F. (1995). Initiation complex assembly at budding yeast replication origins begins with the recognition of a bipartite sequence by limiting amounts of the initiator, ORC. EMBO J *14*, 2631-2641.

Sanchez-Pulido, L., Diffley, J.F., and Ponting, C.P. (2010). Homology explains the functional similarities of Treslin/Ticrr and Sld3. Curr Biol *20*, R509-510.

Santocanale, C., and Diffley, J.F. (1996). ORC- and Cdc6-dependent complexes at active and inactive chromosomal replication origins in Saccharomyces cerevisiae. EMBO J *15*, 6671-6679.

Sauer, P.V., Timm, J., Liu, D., Sitbon, D., Boeri-Erba, E., Velours, C., Mucke, N., Langowski, J., Ochsenbein, F., Almouzni, G.*, et al.* (2017). Insights into the molecular architecture and histone H3-H4 deposition mechanism of yeast Chromatin assembly factor 1. Elife *6*.

Schauer, G.D., and O'Donnell, M.E. (2017). Quality control mechanisms exclude incorrect polymerases from the eukaryotic replication fork. Proc Natl Acad Sci U S A *114*, 675-680.

Schekman, R., Weiner, J.H., Weiner, A., and Kornberg, A. (1975). Ten proteins required for conversion of phiX174 single-stranded DNA to duplex form in vitro. Resolution and reconstitution. J Biol Chem *250*, 5859-5865.

Schvartzman, J.B., and Stasiak, A. (2004). A topological view of the replicon. EMBO Rep *5*, 256-261.

Schwob, E., and Nasmyth, K. (1993). CLB5 and CLB6, a new pair of B cyclins involved in DNA replication in Saccharomyces cerevisiae. Genes Dev *7*, 1160-1175.

Seale, R.L., and Simpson, R.T. (1975). Effects of cycloheximide on chromatin biosynthesis. J Mol Biol *94*, 479-501.

Segal, E., and Widom, J. (2009). Poly(dA:dT) tracts: major determinants of nucleosome organization. Curr Opin Struct Biol *19*, 65-71.

Seki, T., and Diffley, J.F. (2000). Stepwise assembly of initiation proteins at budding yeast replication origins in vitro. Proc Natl Acad Sci U S A *97*, 14115-14120.

Sengupta, S., van Deursen, F., de Piccoli, G., and Labib, K. (2013). Dpb2 integrates the leading-strand DNA polymerase into the eukaryotic replisome. Curr Biol *23*, 543-552.

Shcherbakova, P.V., and Pavlov, Y.I. (1996). 3'-->5' exonucleases of DNA polymerases epsilon and delta correct base analog induced DNA replication errors on opposite DNA strands in Saccharomyces cerevisiae. Genetics *142*, 717-726.

Sheu, Y.J., and Stillman, B. (2006). Cdc7-Dbf4 phosphorylates MCM proteins via a docking site-mediated mechanism to promote S phase progression. Mol Cell *24*, 101-113.

Sheu, Y.J., and Stillman, B. (2010). The Dbf4-Cdc7 kinase promotes S phase by alleviating an inhibitory activity in Mcm4. Nature *463*, 113-117.

Siddiqui, K., On, K.F., and Diffley, J.F. (2013). Regulating DNA replication in eukarya. Cold Spring Harb Perspect Biol *5*.

Simpson, R.T. (1990). Nucleosome positioning can affect the function of a cis-acting DNA element in vivo. Nature *343*, 387-389.

Smith, D.J., and Whitehouse, I. (2012). Intrinsic coupling of lagging-strand synthesis to chromatin assembly. Nature *483*, 434-438.

Smith, S., and Stillman, B. (1989). Purification and characterization of CAF-I, a human cell factor required for chromatin assembly during DNA replication in vitro. Cell *58*, 15-25.

Sogo, J.M., Lopes, M., and Foiani, M. (2002). Fork reversal and ssDNA accumulation at stalled replication forks owing to checkpoint defects. Science *297*, 599-602.

Speck, C., Chen, Z., Li, H., and Stillman, B. (2005). ATPase-dependent cooperative binding of ORC and Cdc6 to origin DNA. Nat Struct Mol Biol *12*, 965-971.

Stillman, B. (2015). Reconsidering DNA Polymerases at the Replication Fork in Eukaryotes. Mol Cell *59*, 139-141.

Stinchcomb, D.T., Struhl, K., and Davis, R.W. (1979). Isolation and characterisation of a yeast chromosomal replicator. Nature *282*, 39-43.

Stodola, J.L., and Burgers, P.M. (2016). Resolving individual steps of Okazaki-fragment maturation at a millisecond timescale. Nat Struct Mol Biol *23*, 402-408.

Stodola, J.L., and Burgers, P.M. (2017). Mechanism of Lagging-Strand DNA Replication in Eukaryotes. Adv Exp Med Biol *1042*, 117-133.

Straube, K., Blackwell, J.S., Jr., and Pemberton, L.F. (2010). Nap1 and Chz1 have separate Htz1 nuclear import and assembly functions. Traffic *11*, 185-197.

Sugino, A. (1995). Yeast DNA polymerases and their role at the replication fork. Trends Biochem Sci *20*, 319-323.

Sun, J., Evrin, C., Samel, S.A., Fernandez-Cid, A., Riera, A., Kawakami, H., Stillman, B., Speck, C., and Li, H. (2013). Cryo-EM structure of a helicase loading intermediate containing ORC-Cdc6-Cdt1-MCM2-7 bound to DNA. Nat Struct Mol Biol *20*, 944-951.

Sun, J., Shi, Y., Georgescu, R.E., Yuan, Z., Chait, B.T., Li, H., and O'Donnell, M.E. (2015). The architecture of a eukaryotic replisome. Nat Struct Mol Biol *22*, 976-982.

Tak, Y.S., Tanaka, Y., Endo, S., Kamimura, Y., and Araki, H. (2006). A CDK-catalysed regulatory phosphorylation for formation of the DNA replication complex Sld2-Dpb11. EMBO J *25*, 1987-1996.

Takayama, Y., Kamimura, Y., Okawa, M., Muramatsu, S., Sugino, A., and Araki, H. (2003). GINS, a novel multiprotein complex required for chromosomal DNA replication in budding yeast. Genes Dev *17*, 1153-1165.

Tan, B.C., Chien, C.T., Hirose, S., and Lee, S.C. (2006). Functional cooperation between FACT and MCM helicase facilitates initiation of chromatin DNA replication. EMBO J *25*, 3975-3985.

Tanaka, S., and Araki, H. (2013). Helicase activation and establishment of replication forks at chromosomal origins of replication. Cold Spring Harb Perspect Biol *5*, a010371.

Tanaka, S., and Diffley, J.F. (2002). Interdependent nuclear accumulation of budding yeast Cdt1 and Mcm2-7 during G1 phase. Nat Cell Biol *4*, 198-207.

Tanaka, S., Nakato, R., Katou, Y., Shirahige, K., and Araki, H. (2011). Origin association of Sld3, Sld7, and Cdc45 proteins is a key step for determination of origin-firing timing. Curr Biol *21*, 2055-2063.

Tanaka, S., Umemori, T., Hirai, K., Muramatsu, S., Kamimura, Y., and Araki, H. (2007). CDK-dependent phosphorylation of Sld2 and Sld3 initiates DNA replication in budding yeast. Nature *445*, 328-332.

Ticau, S., Friedman, L.J., Champasa, K., Correa, I.R., Jr., Gelles, J., and Bell, S.P. (2017). Mechanism and timing of Mcm2-7 ring closure during DNA replication origin licensing. Nat Struct Mol Biol *24*, 309-315.

Ticau, S., Friedman, L.J., Ivica, N.A., Gelles, J., and Bell, S.P. (2015). Single-molecule studies of origin licensing reveal mechanisms ensuring bidirectional helicase loading. Cell *161*, 513-525.

Tocilj, A., On, K.F., Yuan, Z., Sun, J., Elkayam, E., Li, H., Stillman, B., and Joshua-Tor, L. (2017). Structure of the active form of human origin recognition complex and its ATPase motor module. Elife *6*.

Todorov, I.T., Attaran, A., and Kearsey, S.E. (1995). BM28, a human member of the MCM2-3-5 family, is displaced from chromatin during DNA replication. J Cell Biol *129*, 1433-1445.

Treisman, J.E., Follette, P.J., O'Farrell, P.H., and Rubin, G.M. (1995). Cell proliferation and DNA replication defects in a Drosophila MCM2 mutant. Genes Dev *9*, 1709-1715.

Tsubota, T., Berndsen, C.E., Erkmann, J.A., Smith, C.L., Yang, L., Freitas, M.A., Denu, J.M., and Kaufman, P.D. (2007). Histone H3-K56 acetylation is catalyzed by histone chaperone-dependent complexes. Mol Cell *25*, 703-712.

Tsunaka, Y., Fujiwara, Y., Oyama, T., Hirose, S., and Morikawa, K. (2016). Integrated molecular mechanism directing nucleosome reorganization by human FACT. Genes Dev *30*, 673-686.

Tsurimoto, T., Melendy, T., and Stillman, B. (1990). Sequential initiation of lagging and leading strand synthesis by two different polymerase complexes at the SV40 DNA replication origin. Nature *346*, 534-539.

Tsurimoto, T., and Stillman, B. (1989). Purification of a cellular replication factor, RF-C, that is required for coordinated synthesis of leading and lagging strands during simian virus 40 DNA replication in vitro. Mol Cell Biol *9*, 609-619.

Tsurimoto, T., and Stillman, B. (1991). Replication factors required for SV40 DNA replication in vitro. II. Switching of DNA polymerase alpha and delta during initiation of leading and lagging strand synthesis. J Biol Chem *266*, 1961-1968.

van Deursen, F., Sengupta, S., De Piccoli, G., Sanchez-Diaz, A., and Labib, K. (2012). Mcm10 associates with the loaded DNA helicase at replication origins and defines a novel step in its activation. EMBO J *31*, 2195-2206.

Vary, J.C., Jr., Fazzio, T.G., and Tsukiyama, T. (2004). Assembly of yeast chromatin using ISWI complexes. Methods Enzymol *375*, 88-102.

Vashee, S., Cvetic, C., Lu, W., Simancek, P., Kelly, T.J., and Walter, J.C. (2003). Sequence-independent DNA binding and replication initiation by the human origin recognition complex. Genes Dev *17*, 1894-1908.

Vassilev, A., and DePamphilis, M.L. (2017). Links between DNA Replication, Stem Cells and Cancer. Genes (Basel) *8*.

Vestner, B., Waldmann, T., and Gruss, C. (2000). Histone octamer dissociation is not required for in vitro replication of simian virus 40 minichromosomes. J Biol Chem *275*, 8190-8195.

Vijayakumar, S., Chapados, B.R., Schmidt, K.H., Kolodner, R.D., Tainer, J.A., and Tomkinson, A.E. (2007). The C-terminal domain of yeast PCNA is required for physical and functional interactions with Cdc9 DNA ligase. Nucleic Acids Res *35*, 1624-1637.

Vincent, J.A., Kwong, T.J., and Tsukiyama, T. (2008). ATP-dependent chromatin remodeling shapes the DNA replication landscape. Nat Struct Mol Biol *15*, 477-484.

Vos, S.M., Tretter, E.M., Schmidt, B.H., and Berger, J.M. (2011). All tangled up: how cells direct, manage and exploit topoisomerase function. Nat Rev Mol Cell Biol *12*, 827-841.

Voth, W.P., Takahata, S., Nishikawa, J.L., Metcalfe, B.M., Naar, A.M., and Stillman, D.J. (2014). A role for FACT in repopulation of nucleosomes at inducible genes. PLoS One *9*, e84092.

Waga, S., Bauer, G., and Stillman, B. (1994). Reconstitution of complete SV40 DNA replication with purified replication factors. J Biol Chem *269*, 10923-10934.

Waga, S., and Stillman, B. (1994). Anatomy of a DNA replication fork revealed by reconstitution of SV40 DNA replication in vitro. Nature *369*, 207-212.

Walter, J., and Newport, J. (2000). Initiation of eukaryotic DNA replication: origin unwinding and sequential chromatin association of Cdc45, RPA, and DNA polymerase alpha. Mol Cell *5*, 617-627.

Wang, J.C. (2002). Cellular roles of DNA topoisomerases: a molecular perspective. Nat Rev Mol Cell Biol *3*, 430-440.

Watase, G., Takisawa, H., and Kanemaki, M.T. (2012). Mcm10 plays a role in functioning of the eukaryotic replicative DNA helicase, Cdc45-Mcm-GINS. Curr Biol *22*, 343-349.

Weintraub, H. (1972). A possible role for histone in the synthesis of DNA. Nature *240*, 449-453.

Whitehouse, I., and Smith, D.J. (2013). Chromatin dynamics at the replication fork: there's more to life than histones. Curr Opin Genet Dev *23*, 140-146.

Whittaker, A.J., Royzman, I., and Orr-Weaver, T.L. (2000). Drosophila double parked: a conserved, essential replication protein that colocalizes with the origin recognition complex and links DNA replication with mitosis and the down-regulation of S phase transcripts. Genes Dev *14*, 1765-1776.

Wickner, S., and Hurwitz, J. (1974). Conversion of phiX174 viral DNA to double-stranded form by purified Escherichia coli proteins. Proc Natl Acad Sci U S A *71*, 4120-4124.

Wobbe, C.R., Weissbach, L., Borowiec, J.A., Dean, F.B., Murakami, Y., Bullock, P., and Hurwitz, J. (1987). Replication of simian virus 40 origin-containing DNA in vitro with purified proteins. Proc Natl Acad Sci U S A *84*, 1834-1838.

Wohlschlegel, J.A., Dhar, S.K., Prokhorova, T.A., Dutta, A., and Walter, J.C. (2002). Xenopus Mcm10 binds to origins of DNA replication after Mcm2-7 and stimulates origin binding of Cdc45. Mol Cell *9*, 233-240.

Wohlschlegel, J.A., Dwyer, B.T., Dhar, S.K., Cvetic, C., Walter, J.C., and Dutta, A. (2000). Inhibition of eukaryotic DNA replication by geminin binding to Cdt1. Science *290*, 2309-2312.

Wold, M.S. (1997). Replication protein A: a heterotrimeric, single-stranded DNA-binding protein required for eukaryotic DNA metabolism. Annu Rev Biochem *66*, 61-92.

Wold, M.S., and Kelly, T. (1988). Purification and characterization of replication protein A, a cellular protein required for in vitro replication of simian virus 40 DNA. Proc Natl Acad Sci U S A *85*, 2523-2527.

Wold, M.S., Weinberg, D.H., Virshup, D.M., Li, J.J., and Kelly, T.J. (1989). Identification of cellular proteins required for simian virus 40 DNA replication. J Biol Chem *264*, 2801-2809.

Wu, R., Wang, J., and Liang, C. (2012). Cdt1p, through its interaction with Mcm6p, is required for the formation, nuclear accumulation and chromatin loading of the MCM complex. J Cell Sci *125*, 209-219.

Yabuuchi, H., Yamada, Y., Uchida, T., Sunathvanichkul, T., Nakagawa, T., and Masukata, H. (2006). Ordered assembly of Sld3, GINS and Cdc45 is distinctly regulated by DDK and CDK for activation of replication origins. EMBO J *25*, 4663-4674.

Yadav, T., and Whitehouse, I. (2016). Replication-Coupled Nucleosome Assembly and Positioning by ATP-Dependent Chromatin-Remodeling Enzymes. Cell Rep *15*, 715-723.

Yamasu, K., and Senshu, T. (1990). Conservative segregation of tetrameric units of H3 and H4 histones during nucleosome replication. J Biochem *107*, 15-20.

Yao, N.Y., and O'Donnell, M. (2012). The RFC clamp loader: structure and function. Subcell Biochem *62*, 259-279.

Yardimci, H., Loveland, A.B., Habuchi, S., van Oijen, A.M., and Walter, J.C. (2010). Uncoupling of sister replisomes during eukaryotic DNA replication. Mol Cell *40*, 834-840.

Yeeles, J.T., Deegan, T.D., Janska, A., Early, A., and Diffley, J.F. (2015). Regulated eukaryotic DNA replication origin firing with purified proteins. Nature *519*, 431-435.

Yeeles, J.T.P., Janska, A., Early, A., and Diffley, J.F.X. (2017). How the Eukaryotic Replisome Achieves Rapid and Efficient DNA Replication. Mol Cell *65*, 105-116.

Yu, C., Gan, H., Serra-Cardona, A., Zhang, L., Gan, S., Sharma, S., Johansson, E., Chabes, A., Xu, R.M., and Zhang, Z. (2018). A mechanism for preventing asymmetric histone segregation onto replicating DNA strands. Science *361*, 1386-1389.

Yu, X., Chini, C.C., He, M., Mer, G., and Chen, J. (2003). The BRCT domain is a phospho-protein binding domain. Science *302*, 639-642.

Yuan, Z., Riera, A., Bai, L., Sun, J., Nandi, S., Spanos, C., Chen, Z.A., Barbon, M., Rappsilber, J., Stillman, B.*, et al.* (2017). Structural basis of Mcm2-7 replicative helicase loading by ORC-Cdc6 and Cdt1. Nat Struct Mol Biol *24*, 316-324.

Yuzhakov, A., Kelman, Z., Hurwitz, J., and O'Donnell, M. (1999). Multiple competition reactions for RPA order the assembly of the DNA polymerase delta holoenzyme. EMBO J *18*, 6189-6199.

Zegerman, P., and Diffley, J.F. (2007). Phosphorylation of Sld2 and Sld3 by cyclin-dependent kinases promotes DNA replication in budding yeast. Nature *445*, 281-285.

Zhang, Z., Shibahara, K., and Stillman, B. (2000). PCNA connects DNA replication to epigenetic inheritance in yeast. Nature *408*, 221-225.

Zhou, J.C., Janska, A., Goswami, P., Renault, L., Abid Ali, F., Kotecha, A., Diffley, J.F.X., and Costa, A. (2017). CMG-Pol epsilon dynamics suggests a mechanism for the establishment of leading-strand synthesis in the eukaryotic replisome. Proc Natl Acad Sci U S A *114*, 4141-4146.

Zhu, W., Ukomadu, C., Jha, S., Senga, T., Dhar, S.K., Wohlschlegel, J.A., Nutt, L.K., Kornbluth, S., and Dutta, A. (2007). Mcm10 and And-1/CTF4 recruit DNA polymerase alpha to chromatin for initiation of DNA replication. Genes Dev *21*, 2288-2299.

Zou, L., Mitchell, J., and Stillman, B. (1997). CDC45, a novel yeast gene that functions with the origin recognition complex and Mcm proteins in initiation of DNA replication. Mol Cell Biol *17*, 553-563.